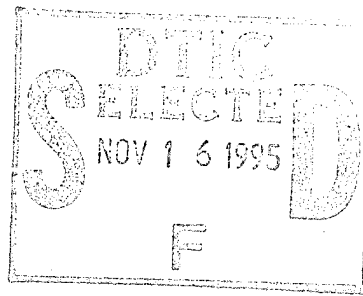


D120113



CML-80-1

NASA CR 159884

CONTACT LAW AND IMPACT
RESPONSES OF LAMINATED COMPOSITES

C.T. Sun
S.H. Yang

February 1980

DTIC-AI <i>thi</i>	
Distribution / 11-2-95	
Availability Codes	
Dist	Avail and/or Special
A-1	

19951114 098

Approved for public release
Distribution Unlimited

1. Report No. NASA CR 159884		2. Government Accession No.		3. Recipient's Catalog No.	
4. Title and Subtitle Contact Law and Impact Responses of Laminated Composites				5. Report Date February 1980	
				6. Performing Organization Code	
7. Author(s) C. T. Sun and S. H. Yang				8. Performing Organization Report No.	
9. Performing Organization Name and Address Purdue University School of Aeronautics and Astronautics West Lafayette, IN 47907				10. Work Unit No.	
				11. Contract or Grant No. NSG3185	
12. Sponsoring Agency Name and Address National Aeronautics and Space Administration Washington DC 20546				13. Type of Report and Period Covered Interim Report	
				14. Sponsoring Agency Code	
15. Supplementary Notes Project Manager: C. C. Chamis Structures & Mechanical Technologies Division NASA-Lewis Research Center 21000 Brookpark Road, Mail Stop 49-3; Cleveland, OH 44135					
16. Abstract Static indentation tests were performed to determine the law of contact between a steel ball and glass/epoxy and graphite/epoxy laminated composites. For both composites the power law with an index of 1.5 was found to be adequate for the loading curve. Substantial permanent deformations were noted after the unloading. A high order beam finite element was used to compute the dynamic contact force and response of the laminated composite subjected to the impact of an elastic sphere. This program can be used with either the classical Hertzian contact law or the measured contact law. A simple method has been introduced for estimating the contact force and contact duration in elastic impacts.					
17. Key Words (Suggested by Author(s)) Indentation law, impact response; contact force, contact duration, permanent deformation, finite element, transient response, composite beams, composite plates, structural mechanics				18. Distribution Statement Unclassified, Unlimited	
19. Security Classif. (of this report) Unclassified		20. Security Classif. (of this page) Unclassified		21. No. of Pages 103	22. Price*

* For sale by the National Technical Information Service, Springfield, Virginia 22161

TABLE OF CONTENTS

	Page
Table of Contents	iii
List of Tables	iv
List of Figures	v
Nomenclature	vii
1. Introduction	1
2. Indentation Law for Hard Object Impact of Composites	3
2.1 Hertzian Law of Contact	3
2.2 Indentation Law for Laminated Composites	4
3. Impact Responses by Finite Element Analysis	28
3.1 The Finite Element	28
3.2 Impact Response	29
4. A Simple Method for Computing Contact Force and Duration in Elastic Impact	38
4.1 Impact of an Elastic Sphere on a Mass with a Flat Surface	38
4.2 Equivalent Mass Model	40
4.3 Simply-Supported Beam	42
4.4 Simply-Supported Rectangular Plate	45
5. Conclusions	62
6. References	63
Appendix A: A Computer Program for Finite Element Analysis of the Transverse Impact of a Beam	64
Appendix B: A Computer Program for Estimating the Contact Force History by Using the Equivalent Mass Model	98

LIST OF TABLES

Table		Page
1	Indentation law $F = k \alpha^n$	8
2	Indentation law $F = k^* \beta^n$	9

LIST OF FIGURES

Figure	Page
2.1 Indentation test set-up	10
2.2 Least-square fit of the contact force-indentation relation for glass/epoxy with 2-inch span	11
2.3 Least-square fit of the contact force-indentation relation for glass/epoxy with 4-inch span	12
2.4 Least-square fit of the contact force-indentation relation for glass/epoxy with 6-inch span	13
2.5 Least-square fit with $n = 1.5$ for glass/epoxy with 2-inch span	14
2.6 Least-square fit with $n = 1.5$ for glass/epoxy with 4-inch span	15
2.7 Least-square fit with $n = 1.5$ for glass/epoxy with 6-inch span	16
2.8 Least-square fit of the contact force-indentation relation for graphite/epoxy with 2-inch span	17
2.9 Least-square fit of the contact force-indentation relation for graphite/epoxy with 4-inch span	18
2.10 Least-square fit with $n = 1.5$ for graphite/epoxy with 4-inch span	19
2.11 Unloading curves for glass/epoxy with 2-inch span	20
2.12 Unloading curves for glass/epoxy with 4-inch span	21
2.13 Unloading curves for glass/epoxy with 6-inch span	22
2.14 Unloading curves for graphite/epoxy with 2-inch span	23
2.15 Unloading curves for glass/epoxy with 2-inch span	24
2.16 Unloading curves for glass/epoxy with 4-inch span	25
2.17 Unloading curves for glass/epoxy with 6-inch span	26
2.18 Unloading curves for graphite/epoxy with 2-inch span	27
3.1 Response of simply-supported steel beam (0.5"W x 0.5"D x 30"L) subjected to impact of a steel ball with initial velocity 12 in/sec.	32
3.2 Response of a simply-supported steel beam (0.5"W x 3"D x 30"L) subjected to impact of a steel ball with initial velocity 1200 in/sec.	33

	Page
3.3 Response of a simply-supported steel beam (0.5"W x 3.0"D x 30"L) subjected to impact of a steel ball with initial velocity 12 in/sec.	34
3.4 Response of a simply-supported steel beam (0.5"W x 0.5"D x 30"L) subjected to impact of a steel ball with initial velocity 1200 in/sec.	35
3.5 Contact forces with elastic and plastic unloadings in a simply-supported glass/epoxy laminated beam (1"W x 0.19"D x 7.5"L) subjected to impact of a steel ball at $v_i = 1000$ in/sec.	36
3.6 Contact forces with elastic and plastic unloadings in a simply-supported glass/epoxy laminated beam (1"W x 0.19"D x 7.5"L) subjected to impact of a steel ball at $v_i = 1500$ in/sec.	37
4.1 Contact force history for the Timoshenko problem	54
4.2 Simply-supported steel beam (0.5"W x 0.5"D x 30"L) subjected to impact of a steel ball at 12 in/sec.	55
4.3 Simply-supported steel beam (0.5"W x 0.5"D x 30"L) subjected to impact of a steel ball at 1200 in/sec.	56
4.4 Simply-supported steel beam (0.5"W x 3"D x 30"L) subjected to impact of a steel at 12 in/sec.	57
4.5 Simply-supported steel beam (0.5"W x 3"D x 30"L) subjected to a steel ball at 1200 in/sec.	58
4.6 Simply-supported steel beam (0.5"W x 0.08"D x 15"L) subjected to impact of a steel ball at 100 in/sec.	59
4.7 Simply-supported graphite/epoxy beam (0.5"W x 0.08"D x 15"L) subjected to impact of a steel ball at 100 in/sec.	60
4.8 Contact force history for a simply-supported steel plate (20 cm x 20 cm x 0.8 cm) subjected to impact of a steel ball (2 cm diameter) at 100 cm/sec.	61
A-1 Deck set-up	69
A-2 Response of a cantilever steel beam (0.5"W x 0.08"D x 15"L) subjected to impact of a steel ball at 100 in/sec.	80
A-3 Displacement profiles at various times after impact of the steel beam	81
A-4 Response of cantilever graphite/epoxy beam (0.5"W x 0.08"D x 15"L) subjected to impact of a steel ball at 100 in/sec.	82
A-5 Displacement profiles at various times after impact of the composite beam	83

NOMENCLATURE

A	Cross-sectional area of beam
A_{ij}, B_{ij}, D_{ij}	Laminate stiffness
D	Depth of beam or bending rigidity of beam
E	Young's Modulus
E_b	Young's Modulus of beam
E_L	Young's Modulus in the fiber direction
E_s	Young's Modulus of isotropic sphere
E_T	Young's Modulus in the transverse direction
F	Contact force
F_{max}	Maximum contact force
G_{LT}	Shear Modulus
I	Moment of inertia
K	Kinetic energy
K_t	Total kinetic energy
K^*	K/F_{max}^2
K_{mn}	Eigen value of the (m,n) mode
L	Span or length of beam
L_1	Linear operator (bending)
L_2	Linear operator (shear)
Q_{mn}	Generalized force
\bar{Q}_{ij}	Reduced stiffness of composite material
R_s	Radius of sphere
T	Impact duration
T_n	Period of the nth mode
U	Potential or strain energy
U^*	U/F_{max}^2
$W(x,t)$	Deflection of beam or plate
$W_n(x)$	Eigen function of the nth mode

a	Dimension of plate
a_i	Constant coefficients ($i=1,6$)
b	Dimension of plate
f_1	Strain energy function for simply-supported beam
f_3	Strain energy function for simply-supported plate
g_1	Kinetic energy function for simply-supported beam
g_3	Kinetic energy function for simply-supported plate
h	Depth of beam or plate
k	Contact Modulus
k^*	Contact force per unit indentation depth
[k]	Stiffness matrix
m_s	Mass of sphere
m_t	Mass of target or equivalent mass at time t
[m]	Mass matrix
n	Index of indentation power law (loading)
q	Index of indentation power law (unloading)
$q(x,t)$	Forcing function
s	Laplace transformation parameter
t	time
v_s	Velocity of sphere
v_t	Velocity of target
w_b	Bending displacement
$\overline{w_b}$	Laplace transformed function of w_b
w_s	Transverse shear deformation
$\overline{w_s}$	Laplace transformed function of w_s
α	Indentation depth
α_0	Permanent indentation
α_m	Maximum indentation
β	α/R_s , nondimensional indentation
ρ	Mass density of beam
κ	Curvature, or shear correction factor
ξ	1/reduced mass
η	α/α_{max} , relative indentation
ω_n	Natural frequency of the nth mode of beam
ω_{mn}	Natural frequency of the (m,n) mode of plate
∇^2	Laplacian operator
ψ_x, ψ_y	Rotations of plane sections of plate

1. Introduction

It has been a known fact that laminated fiber composites currently in use are relatively weak in resisting impact loads. Great attention has been given to modeling the dynamic behavior of composites subjected to foreign object impacts and to the search for new forms of composites that are capable of improving the impact-resistant property.

Failure modes in composites resulting from the impacts of a hard object and a soft object are, in general, quite different. If the object is relatively rigid and small, then the contact time is short and extensive damage is usually confined to the neighborhood of the contact region. How to quantify the amount of damage received by the composite in the impact zone becomes the central question in the hard-object impact problem.

There are several major factors which could affect the amount of damage in a laminated composite due to the impact of a hard object. Among them are the mass and approach velocity of the object, the bending rigidity of the laminate, and the contact behavior (or the contact law). Many researchers have correlated the impact velocity with the damage for a given mass. Such relationship between the damage and impact velocity becomes invalid if the mass of the striker or the bending property of the laminate is changed. The use of a single parameter which could account for the combined effect of the above mentioned variables is highly desirable.

Energy dissipation takes place in the process of impact that results in damage. It is thus reasonable to use this amount of energy consumed in the impact zone to measure the degree of damage in the target composite beam. There could be various damage modes such as breakage of

fibers, cracking in the matrix, delamination, and plastic deformations, which could all contribute to the energy dissipation in the impact zone. It is conceivable that analytical estimates of the energies associated with these damage modes are prohibitive. A static indentation test which produces the loading-unloading curve may prove to be a simple means for determining such damage energy, since the energy dissipated during the loading and unloading cycle is simply the area enclosed by the curve.

In this report, results of the indentation tests on glass/epoxy and graphite/epoxy laminated composites are presented. The results show that the loading curve follow the power law with a power index 1.5, which is identical to the classical Hertzian contact law. Substantial permanent deformations are observed even when loaded at very low load levels. The unloading curves also follow a power law.

A high order beam finite element is used for computing the dynamic response of laminated composite beams subjected to the impact of an elastic sphere. This finite element includes the classical elastic Hertzian law of contact as well as the measured contact law. The computer program developed for this beam finite element is listed as Appendix A. A simple method has been developed for computing the contact force and contact duration. An estimate of the contact duration is needed in the finite element program in selecting a proper time increment in the time integration procedure. This method is found to be quite accurate except for very thin beams.

2. Indentation Law for Hard Object Impact of Composites

2.1 Hertzian Law of Contact

When two solid bodies are in contact, deformation takes place in the contact zone and the contact force results. Once the contact force is obtained, conventional methods for stress analysis can be used to find the stress distribution in the bodies. To determine the contact force - indentation relationship often becomes the most important step in analyzing the contact problem.

The most famous elastic contact law was developed by Hertz [1] for the contact of two spheres of elastic isotropic materials. The problem was solved based on the theory of elasticity. A special case is that if the radius of one of the spheres becomes infinite, then the problem becomes the contact of an elastic sphere and an elastic half space. The contact force F and the indentation depth α were found to have the relation

$$F = k \alpha^{3/2} \quad (2-1)$$

where

$$k = \frac{4}{3} R_s^{1/2} \left[\frac{1-\nu_1^2}{E_1} + \frac{1-\nu_2^2}{E_2} \right]^{-1} \quad (2-2)$$

In Eq. (2-2), R_s is the radius of the sphere, ν is the Poisson's ratio, E is the Young's modulus, and the subscripts 1 and 2 indicate the two bodies. Equation (2-1) is usually called the Hertzian law of contact for a sphere on half space.

The 3/2 power law given by Eq. (2-1) was found to be valid by Willis [2] for a rigid sphere pressed on a transversely isotropic half space. A modified contact law with

$$k = \frac{4}{3} R_s^{1/2} \left[\frac{1-\nu_s^2}{E_s} + \frac{1}{E_T} \right]^{-1} \quad (2-3)$$

was employed by Sun [3] for a study on impact of laminated composites. In Eq. (2-3), R_s , ν_s and E_s are the radius, the Poisson's ratio and the Young's modulus of the isotropic sphere, respectively, and E_T is the Young's modulus of the fiber-reinforced composite normal to the impact plane.

In applying the classical Hertzian contact law to the impact of laminated fibrous composites we face several uncertainties. First, the half space assumption is not valid since the laminates in use are of finite thickness. Second, the anisotropic and nonhomogeneous property of laminated composites may alter the form of the law. Third, the strain rate effect which is not accounted for by the Hertzian law may have significant effect on the $F-\alpha$ relation. Except for the strain rate effect, the first two uncertainties are solvable by analyzing the exact contact problem of a sphere pressed into a laminated composite using three-dimensional elasticity. However, experience tells us that analytical solutions for such contact problems are extremely difficult to obtain especially if permanent deformations are to be accounted for during unloadings. Since unloading paths are particularly important in our study, the experimental approach is taken to determine the law of contact for composites. However, in this study, the strain rate effect is still neglected.

2.2 Indentation Law for Laminated Composites

2.2.1 Theoretical Model

In this study the general form for the indentation law for laminated composites is extended from the classical Hertzian Law. We assume that for loading

$$F = k \alpha^n \quad (2-4)$$

where k and n will be determined experimentally. It is obvious that when $n = 3/2$ and k is given by Eq. (2-2), this relation becomes the Hertzian law for isotropic bodies. It is noted that the constant k has a very strange unit if n is not an integer. Also, the value of k depends on the unit used for α . A more physically meaningful expression may be derived by using a nondimensional indentation depth

$$\beta = \alpha/R_s \quad (2-5)$$

with which the indentation can be written as

$$F = k^* \beta^n \quad (2-6)$$

In Eq. (2-6), k^* has the unit of force. For the Hertzian law,

$$k^* = \frac{4}{3} R_s^2 \left[\frac{1-\nu_1^2}{E_1} + \frac{1-\nu_2^2}{E_2} \right]^{-1} \quad (2-7)$$

Permanent indentations in composite targets are usually generated even at relatively low projectile impact speeds. The permanent indentation accounts for the major part of the energy loss of the projectile. Some energy imparted from the projectile to the target can be stored in the form of vibrational energy in the target. As far as the local damage at the impact zone is concerned, the permanent indentation is of more interest to us. For this reason, the force-indentation law for the recovery process must be established. In this study, we assume, in the recovery process,

$$F = F_m \left[\frac{\alpha - \alpha_0}{\alpha_m - \alpha_0} \right]^q \quad (2-8)$$

where F_m is the maximum contact force just before unloading takes place, α_m is the indentation corresponding to F_m , and α_o is the permanent indentation. This recovery law was proposed by Barnhart and Goldsmith [4] for impact of a steel ball onto an armor plate.

2.2.2 Experimental Results

The experimental set-up is depicted by the sketch in Fig. 2.1. The indentation was measured by a dial gage that permits reading up to 1/5000 in. The dial gage was mounted on the loading piston so that only the relative displacement between the indenter and the beam was recorded. The indenter was a steel ball of $\frac{1}{4}$ in. diameter. The beam was clamped at both ends with various spans.

Two types of laminated composites have been tested, namely glass/epoxy and graphite/epoxy. The glass/epoxy was Scotch Ply 1002 by the 3M Company. It contained 10 0^0 -plies and 9 90^0 -plies which alternate in the layup with one 0^0 -ply on top and one at the bottom. The thickness of the beam was 0.19 in. and the width was 1.5 in. The graphite/epoxy specimens were $[0/(\pm 45)_2/0_2/\pm 45]_s$ laminates. Three different spans, 2 in., 4 in. and 6 in., were used for the glass/epoxy laminates and two spans, 2 in. and 4 in., were used for the graphite/epoxy laminates.

The Loading Curve

For the glass/epoxy laminate, three sets of loading data were obtained for each span. These data were used to determine the best fit for the power law, Eq. (2-4), using the least squares method. The results were presented in Figs. 2.2-2.4. The power indices for the three cases appear to be rather close to that of the classical Hertzian law for isotropic media,

i.e., $n = 1.5$. The small deviation from $n = 1.5$ could be due to measurement errors. For this reason, we set $n = 1.5$ and then determined k by using the least square fit. The resulting curves are shown in Figs. 2.5-2.7. These curves seem to fit the data very well also.

The results of the indentation test on the graphite/epoxy laminated beams are presented in Figs. 2.8-2.10. For the 2-inch span, the best least square fit is $n = 1.5$; and for the 4-inch span as shown in Fig. 2.10, $n = 1.5$ also yields a very good fit.

Table 1 summarizes the indentation laws (the loading portion) obtained from the experimental results for a glass/epoxy composite and a graphite/epoxy composite. It is interesting to note that with $n = 1.5$, the values of k for different spans are almost a constant. This indicates that the indentation law is independent of span. In other words, the bending stress does not influence the "contact rigidity".

Table 2 presents the indentation laws in terms of β and k^* with $n = 1.5$ (see Eq. (2-6)).

The Unloading Curve

From the test results we have observed that permanent deformation would occur after an indentation test no matter how small the load was. The unloading paths are very different from the loading path as can be seen from Figs. 2.11-2.14 for both glass/epoxy and graphite/epoxy. The unloading curve is modeled by using Eq. (2-8) in which q and α_0 have to be determined. Since the permanent indentation depth α_0 is difficult to measure, the whole data for each unloading path were taken to determine the two parameters q and α_0 . The value $q = 2.5$ seems to yield the best overall fit as shown in Figs. 2.11-2.14. For $q = 3.0$ (see Figs. 2.15-2.18) α_0 becomes negative in some cases.

Table 1. Indentation law $F = k \alpha^n$ (α in inches).

	Glass/Epoxy [[0/90) ₄ /0/90/0/(90/0) ₄]			Graphite/Epoxy [0/(+45) ₂ /0 ₂ /+45] _s	
	Span	2" n	4" k	6" n	4" k
Least Squares		1.54	1.54	1.66	1.63
Fit		5.569×10^5	5.603×10^5	9.655×10^5	9.99×10^5
1.5 Power		1.5	1.5	1.5	1.5
Fit		4.617×10^5	4.633×10^5	4.592×10^5	5.126×10^5
Modified Hertzian Law Eq.(2-3)		$F = 5.461 \times 10^5 \alpha^{1.5}$ $R_s = 0.125"$, $\nu_s = 0.3$, $E_s = 30 \times 10^6$ psi. $E_T = 1.2 \times 10^6$ psi.			
		$F = 5.24 \times 10^5 \alpha^{1.5}$ $E_T = 1.15 \times 10^6$ psi.			

Table 2. Indentation law $F = k^* \beta^n$

	Glass/Epoxy [[0/90) ₄ /0/90/0/(90/0) ₄]			Graphite/Epoxy [0/(+45) ₂ /0 ₂ /+45] _s		
Span	2"	4"	6"	2"	4"	
1.5 Power	1.5	1.5	1.5	1.5	1.5	
Fit	2.0405×10^4	2.0475×10^4	2.0294×10^4	2.6357×10^4	2.2654×10^4	
Modified Hertzian Law Eq. (2-6)	$F = 2.4134 \times 10^4 \beta^{1.5}$			$F = 2.32 \times 10^4 \beta^{1.5}$		

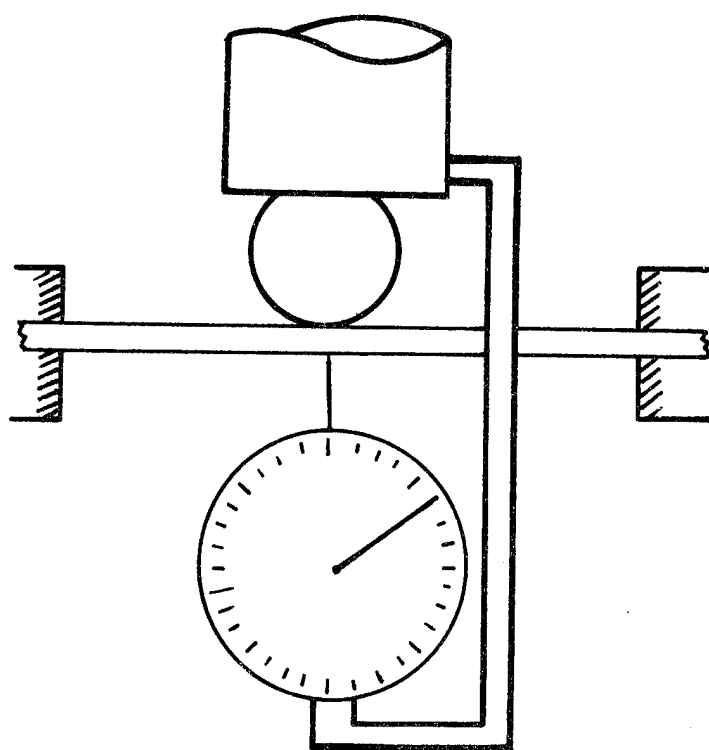


Fig. 2.1 Indentation test setup

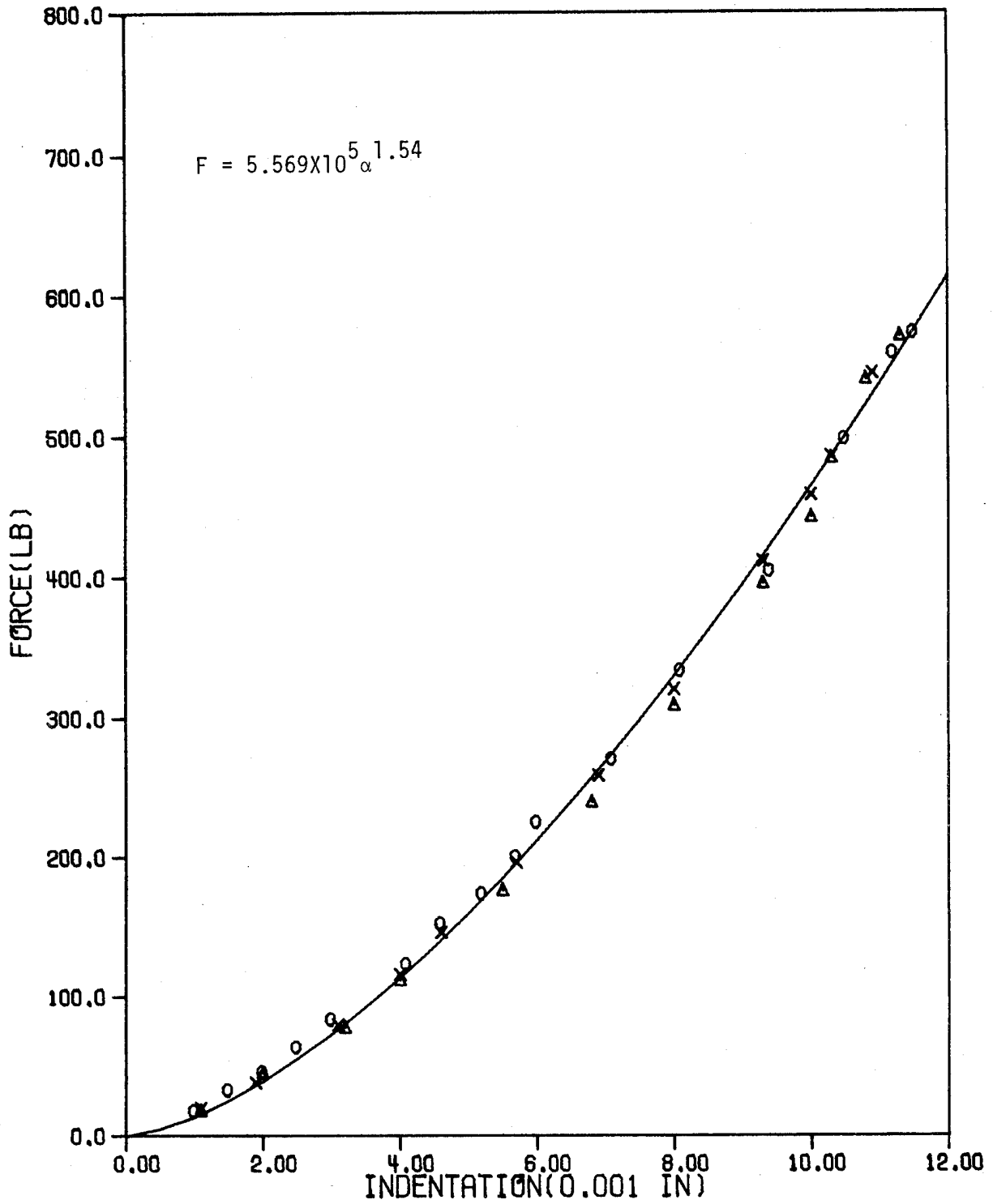


Fig. 2.2. Least-square fit of the contact force - indentation relation for glass/epoxy with 2-inch span.

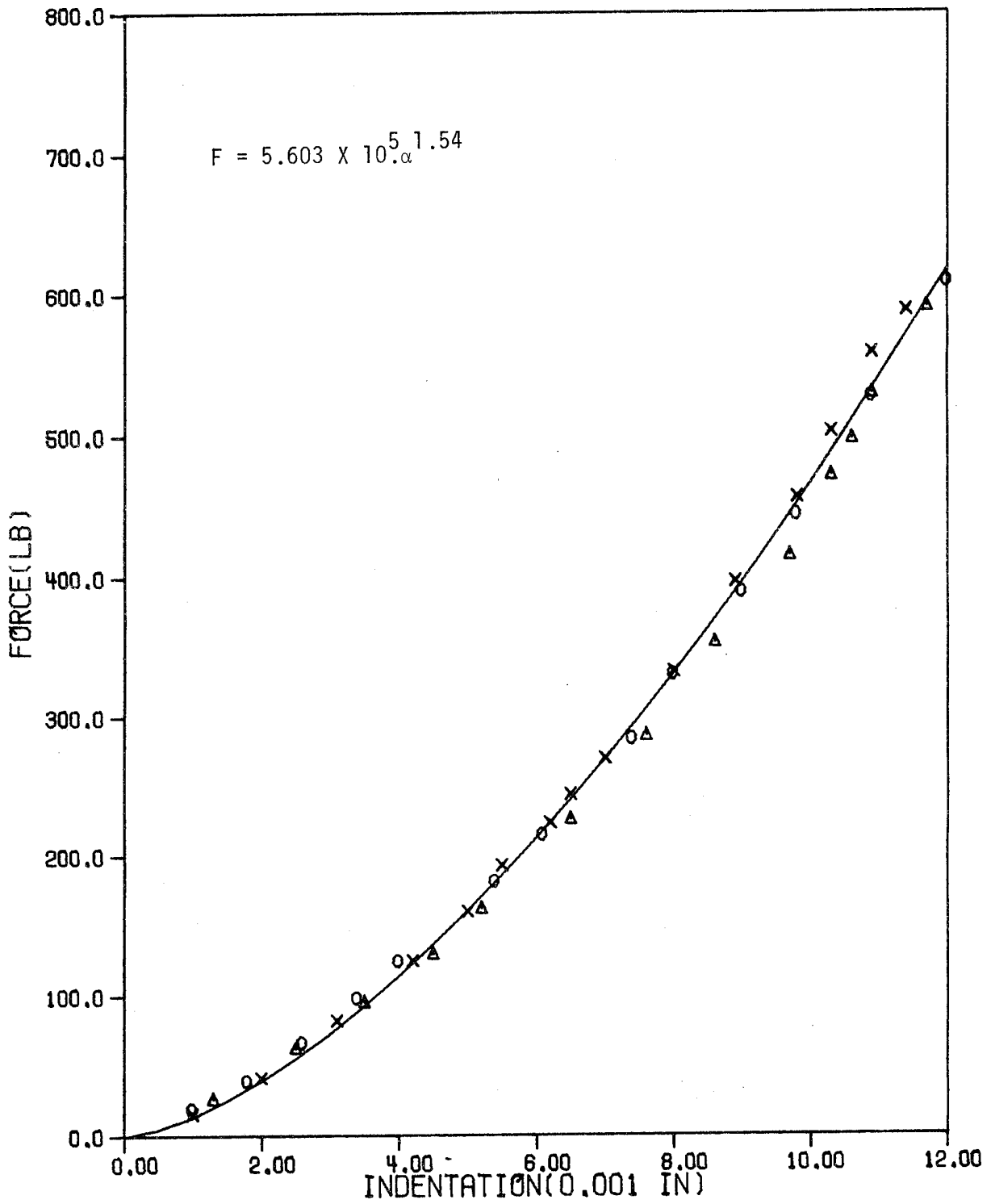


Fig. 2.3. Least-square fit of the contact force-indentation relation for glass/epoxy with 4-inch span.

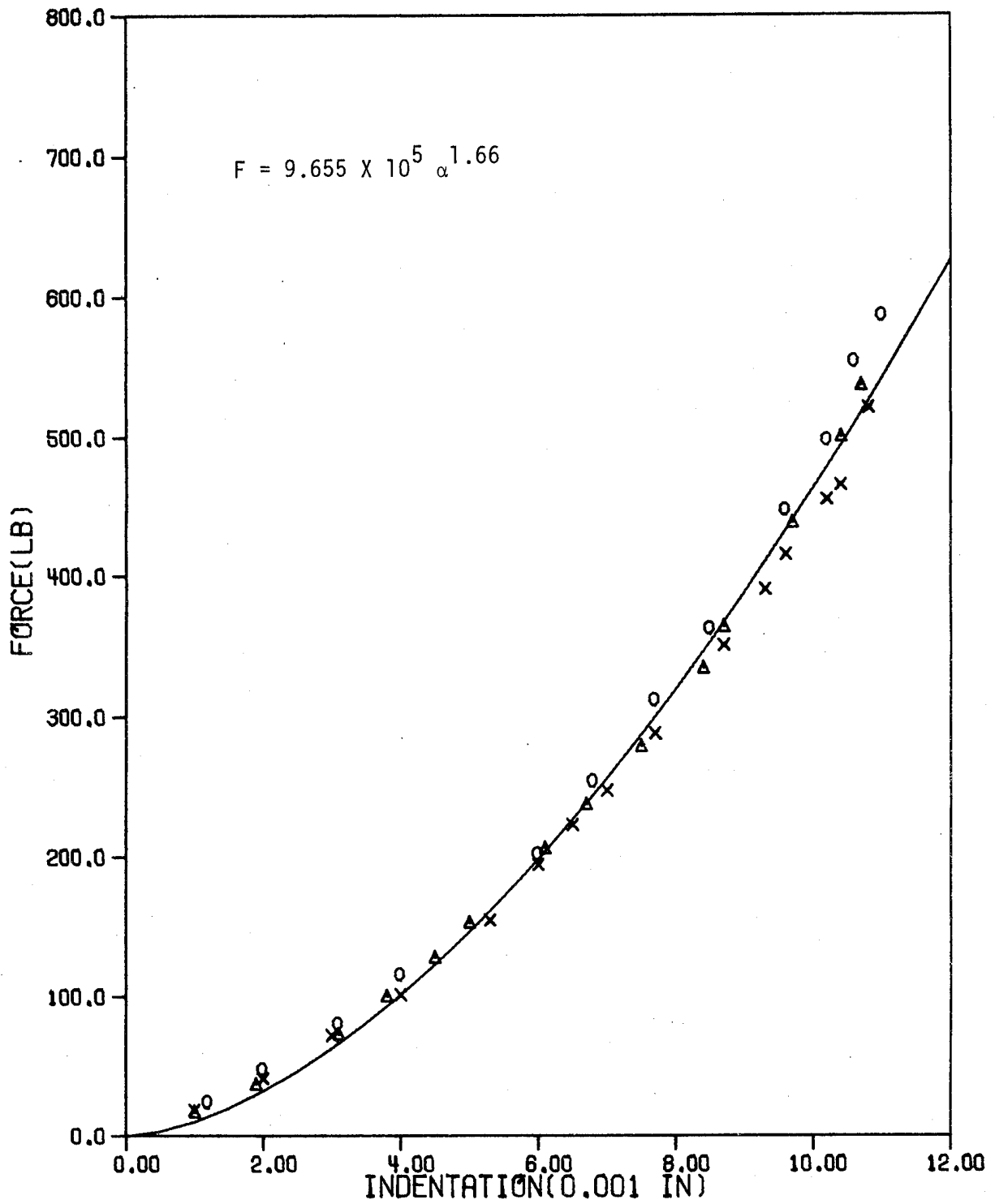


Fig. 2.4. Least-square fit of the contact force - indentation relation for glass/epoxy with 6-inch span.

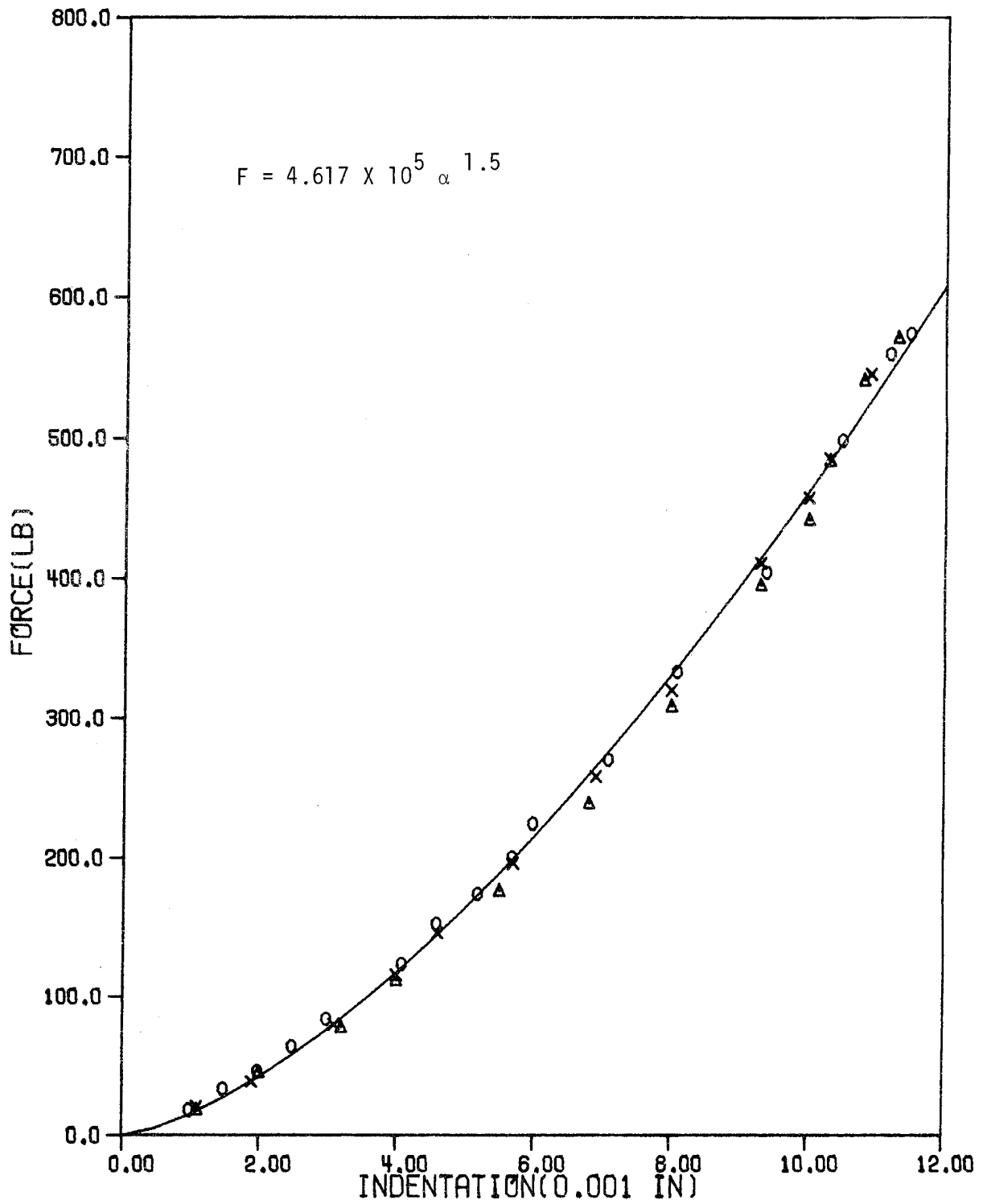


Fig. 2.5. Least-square fit with $n = 1.5$ for glass/epoxy with 2-inch span.

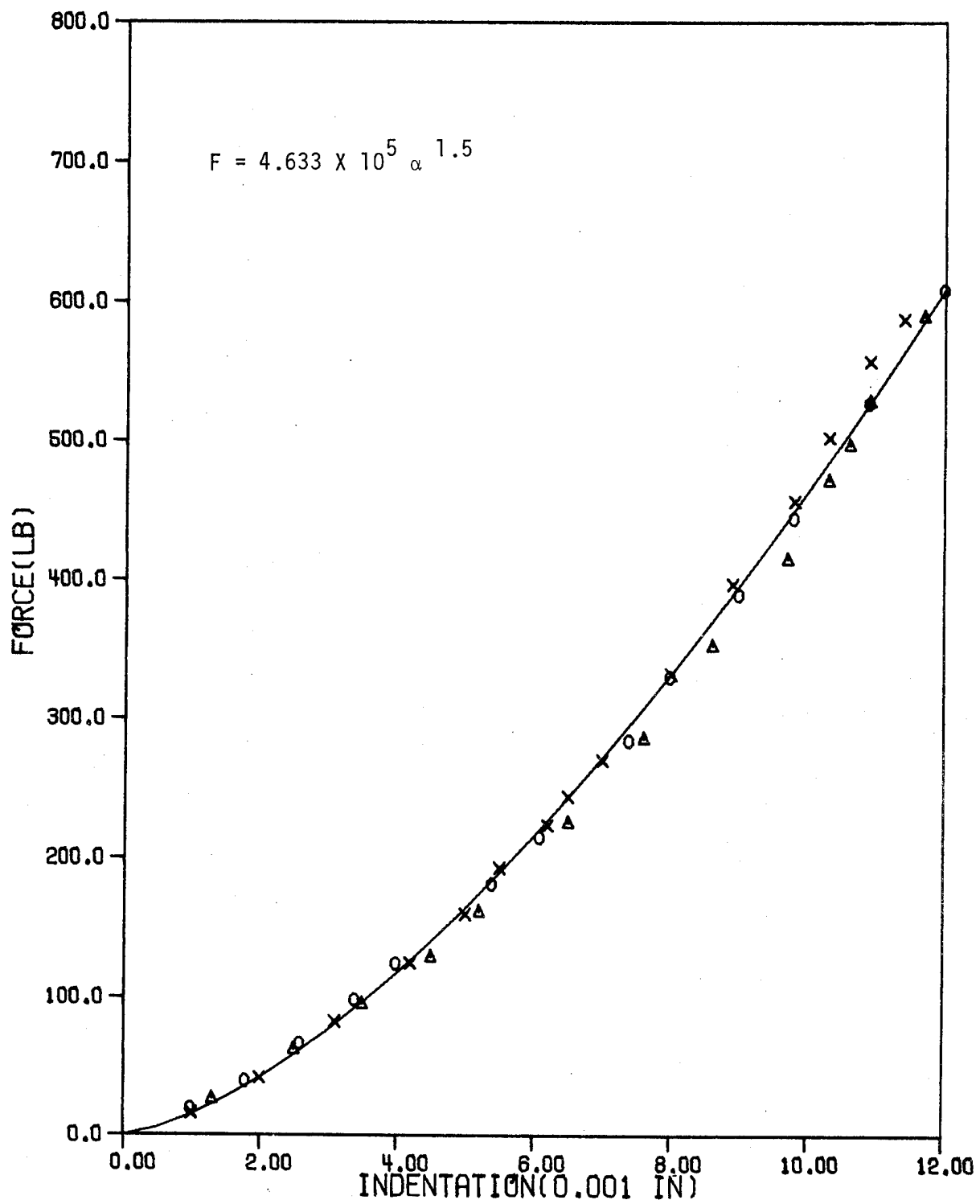


Fig. 2.6. Least-square fit with $n = 1.5$ for glass/epoxy with 4-inch span.

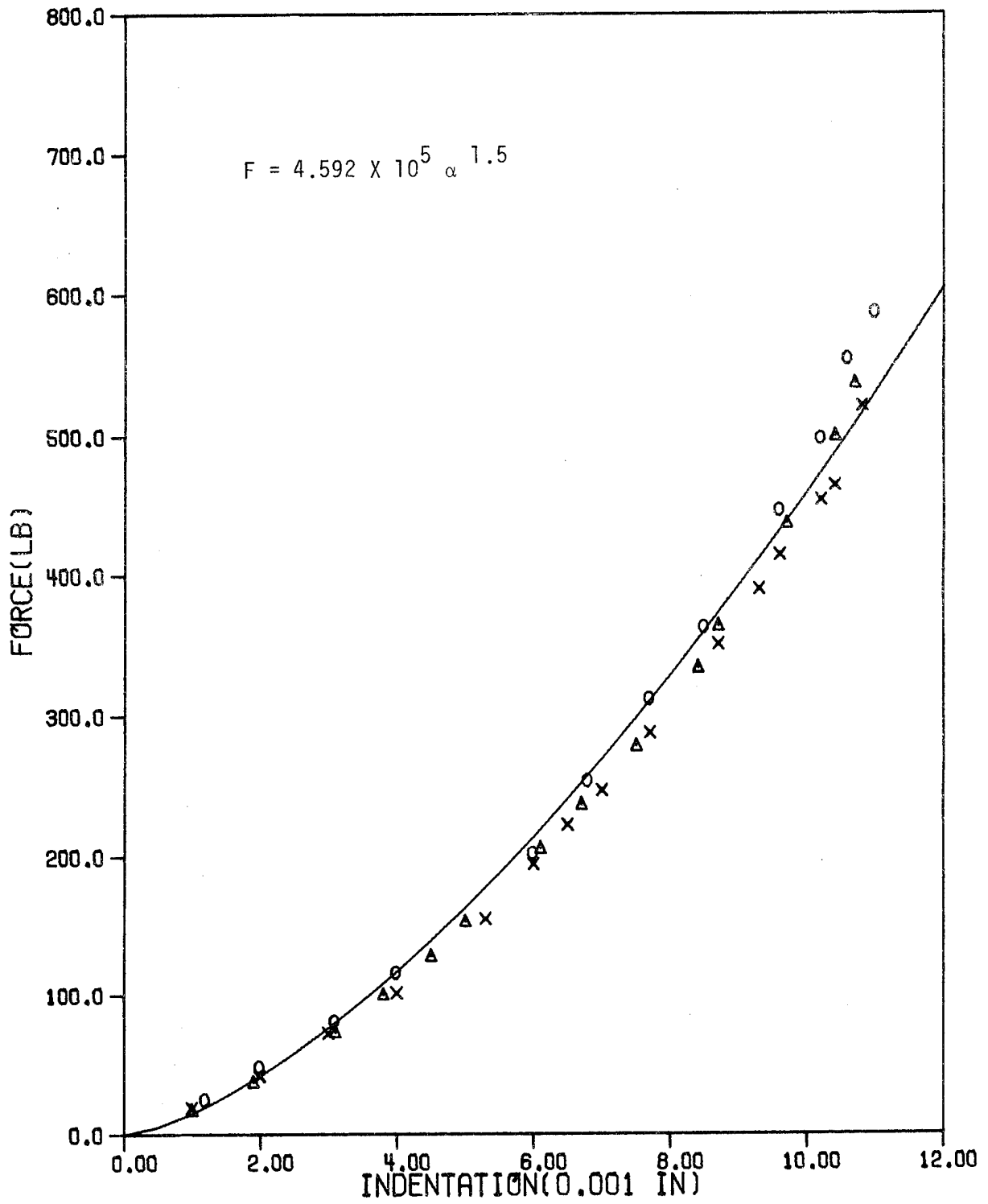


Fig. 2.7. Least-square fit with $n = 1.5$ for glass/epoxy with 6-inch span.

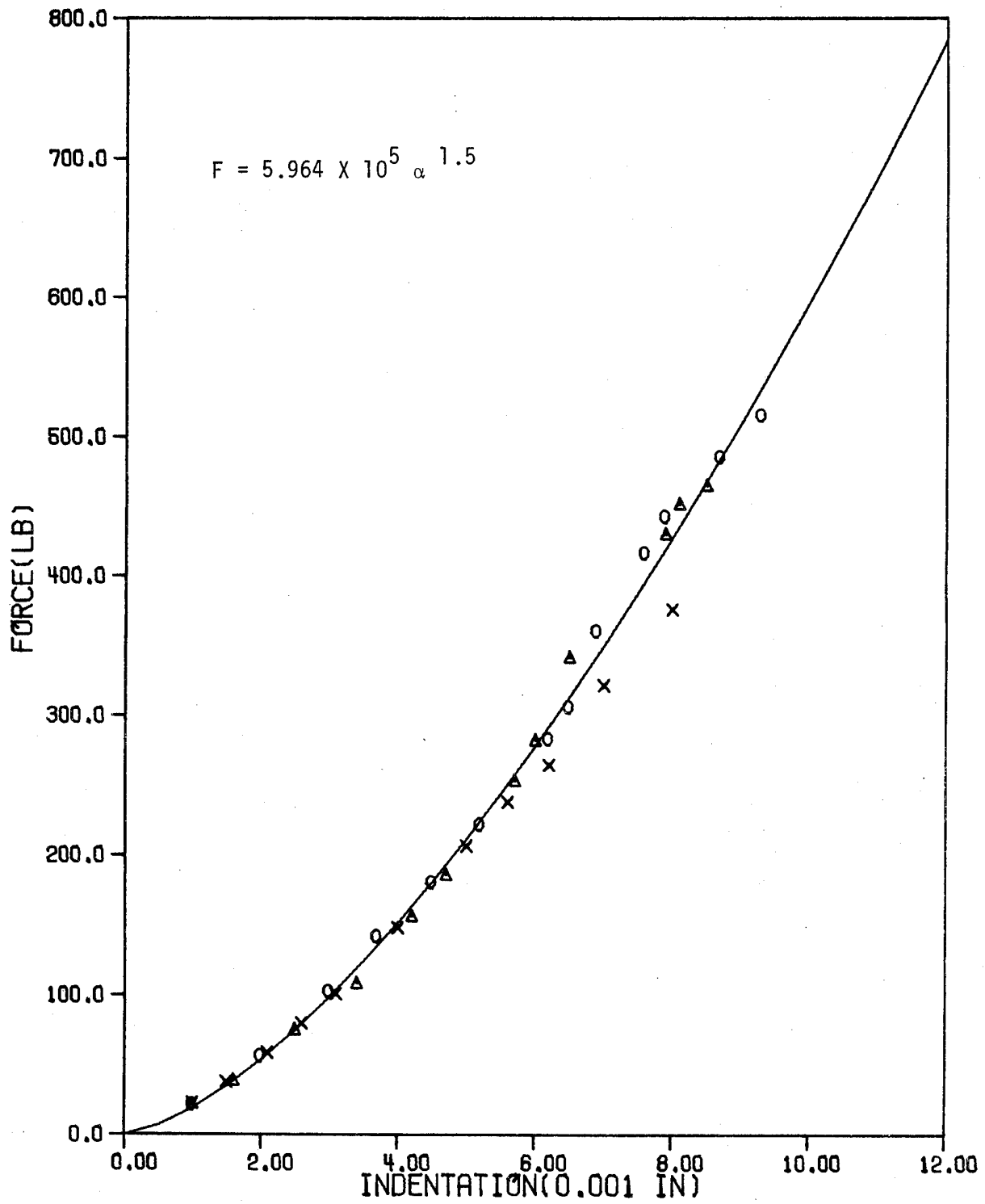


Fig. 2.8. Least-square fit of the contact force - indentation relation for graphite/epoxy with 2-inch span.

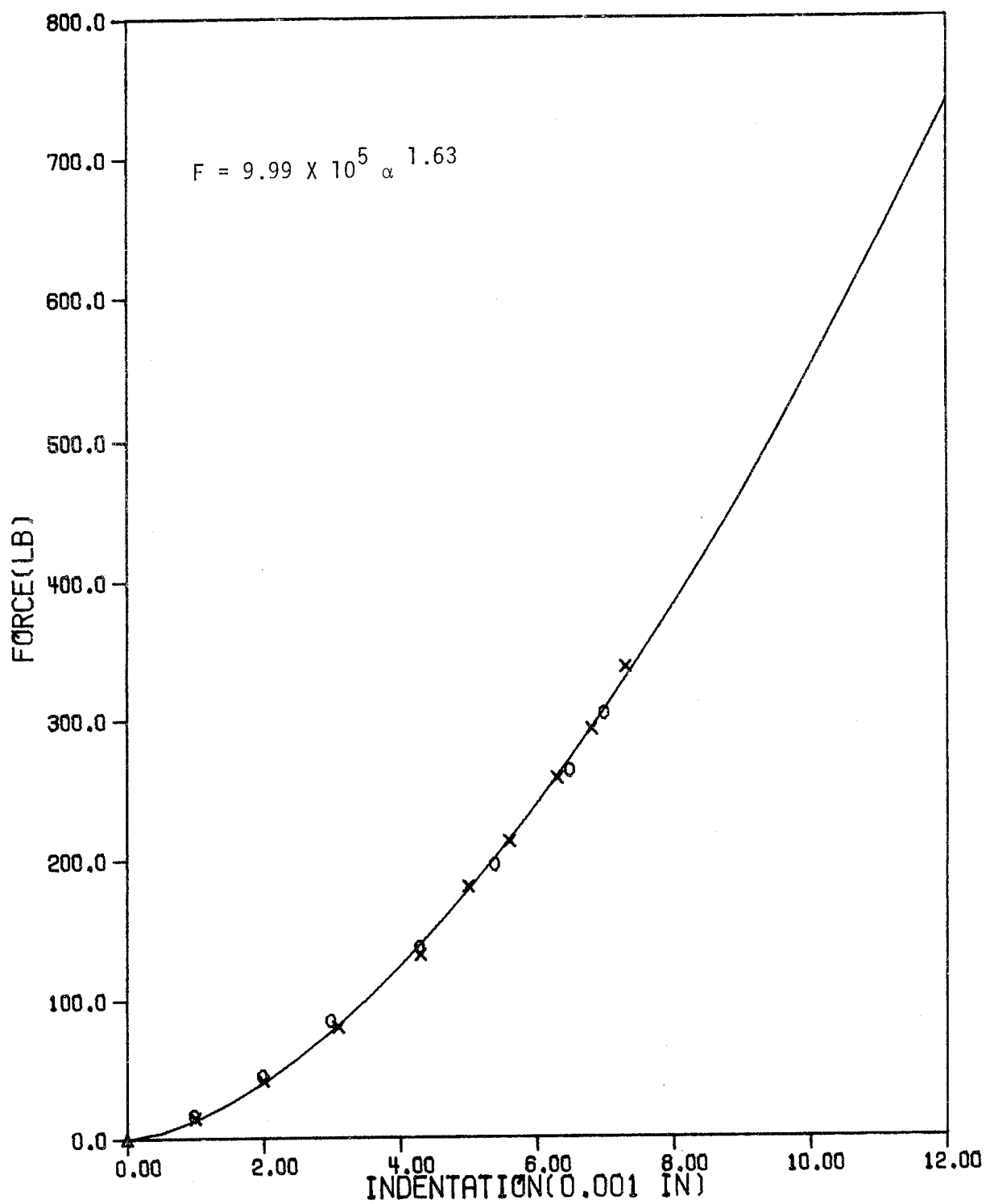


Fig. 2.9. Least-square fit of the contact force - indentation relation for graphite/epoxy with 4-inch span.

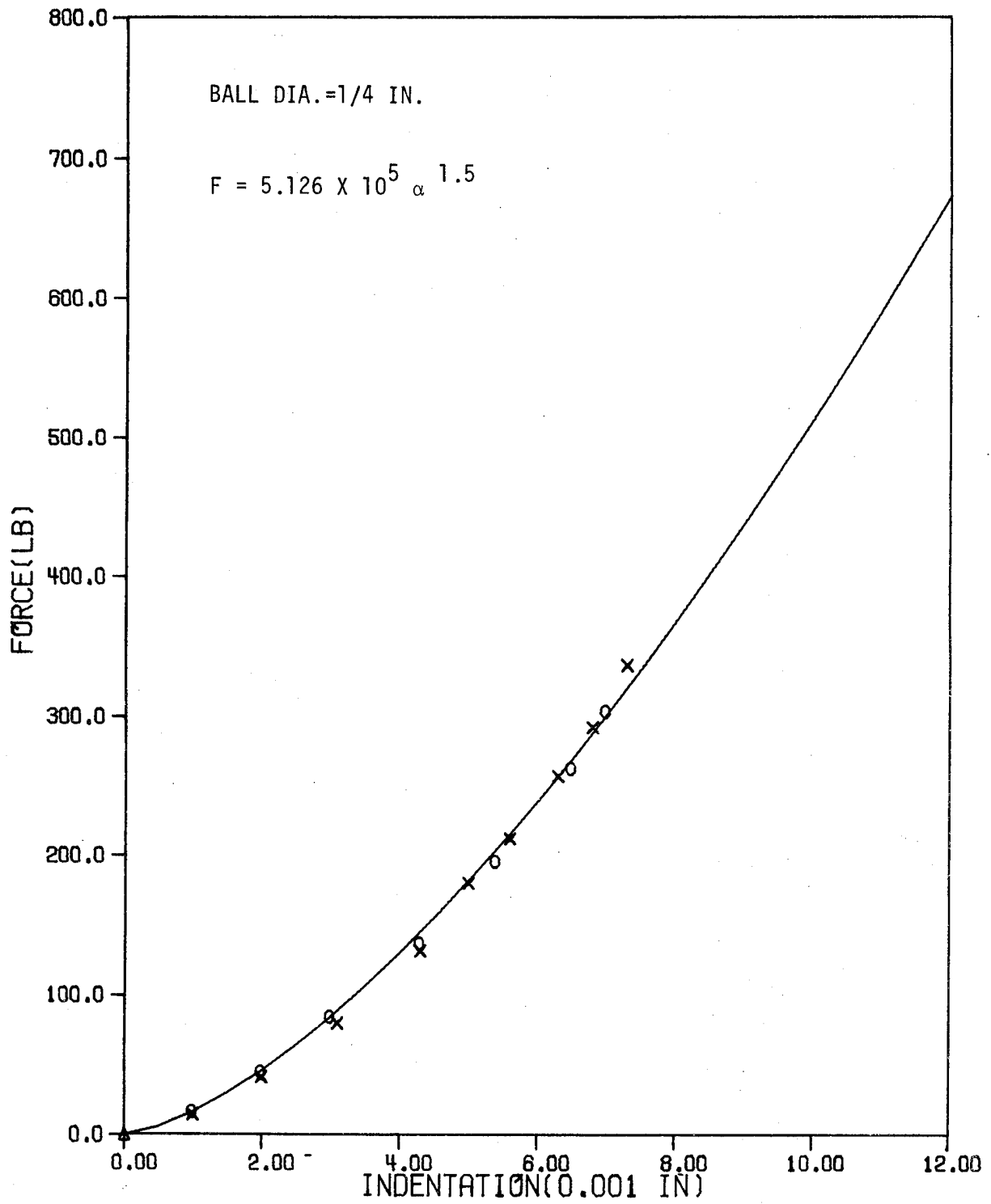


Fig. 2.10. Least-square fit with $n = 1.5$ for graphite/epoxy with 4-inch span.

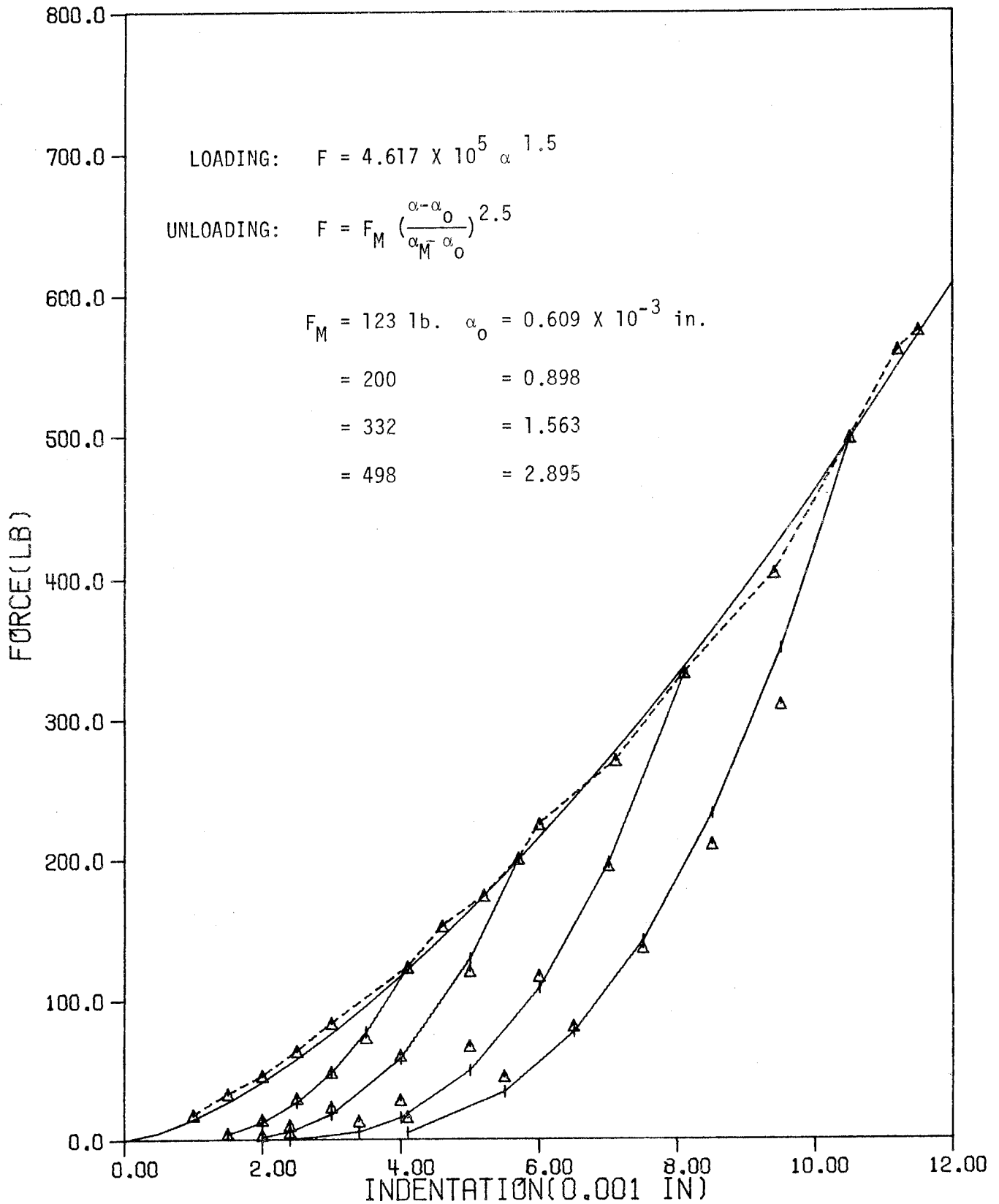


Fig. 2.11. Unloading curves for glass/epoxy with 2-inch span.

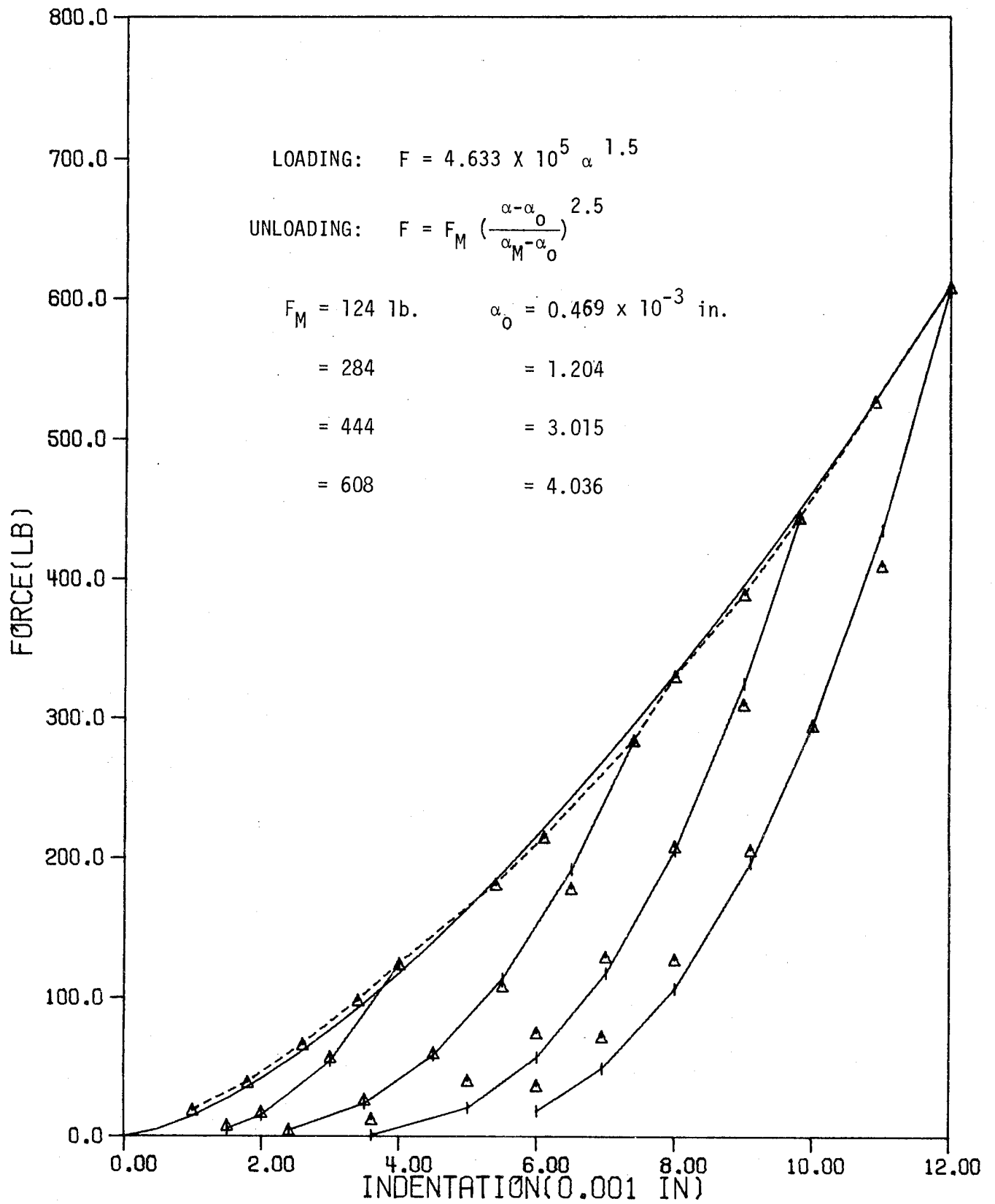


Fig. 2.12. Unloading curves for glass/epoxy with 4-inch span.

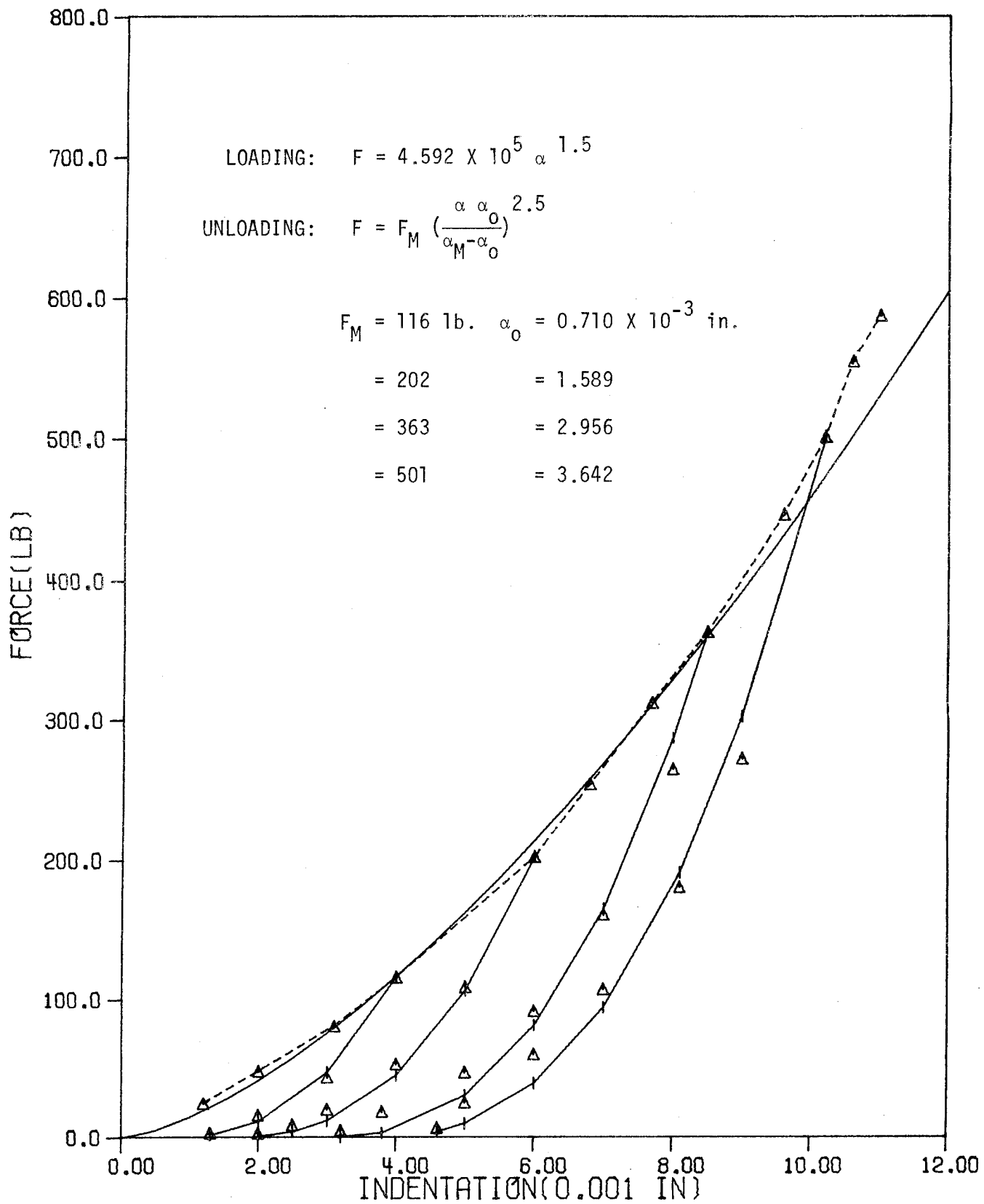


Fig. 2.13. Unloading curves for glass/epoxy with 6-inch span.

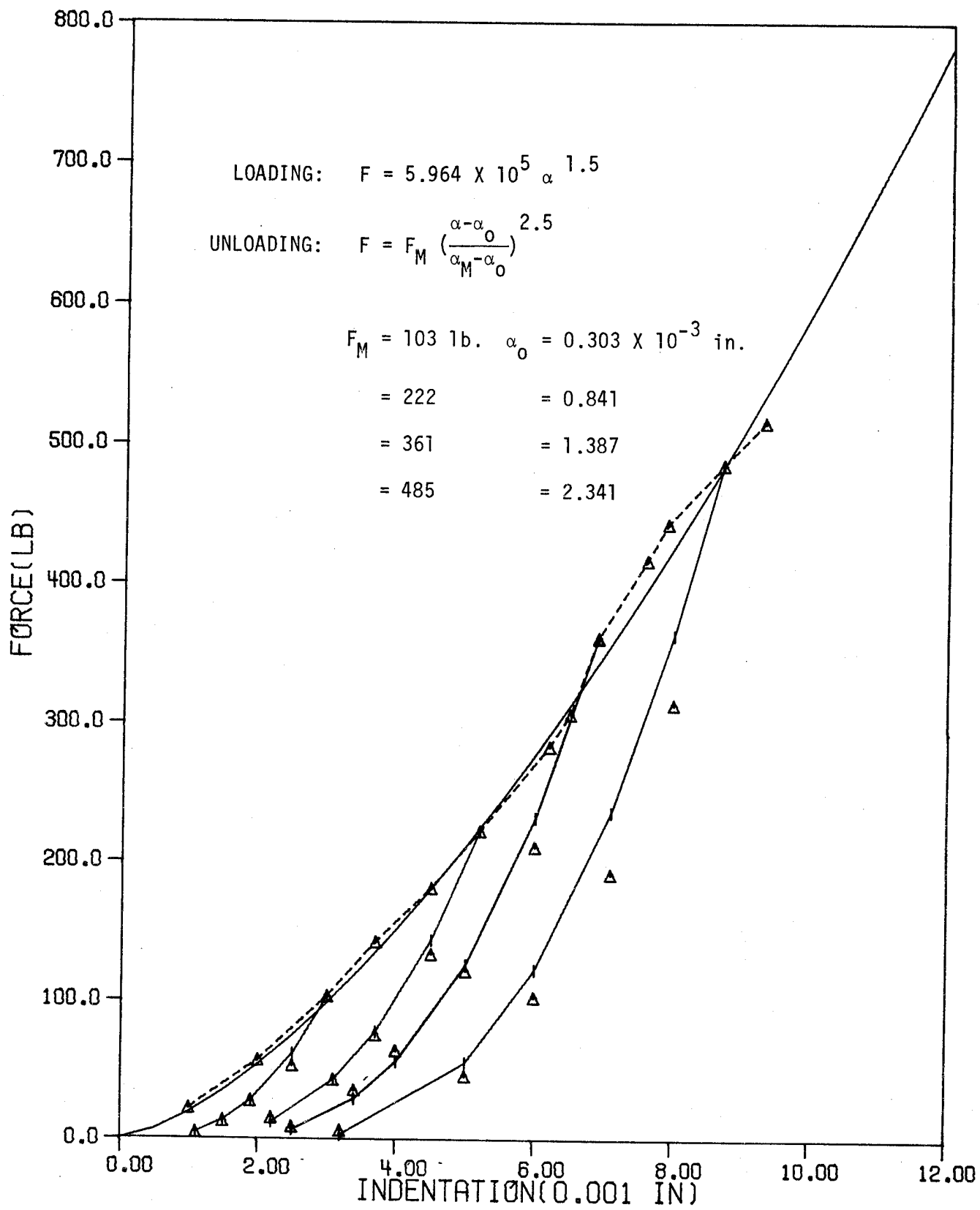


Fig. 2.14. Unloading curves for graphite/epoxy with 2-inch span.

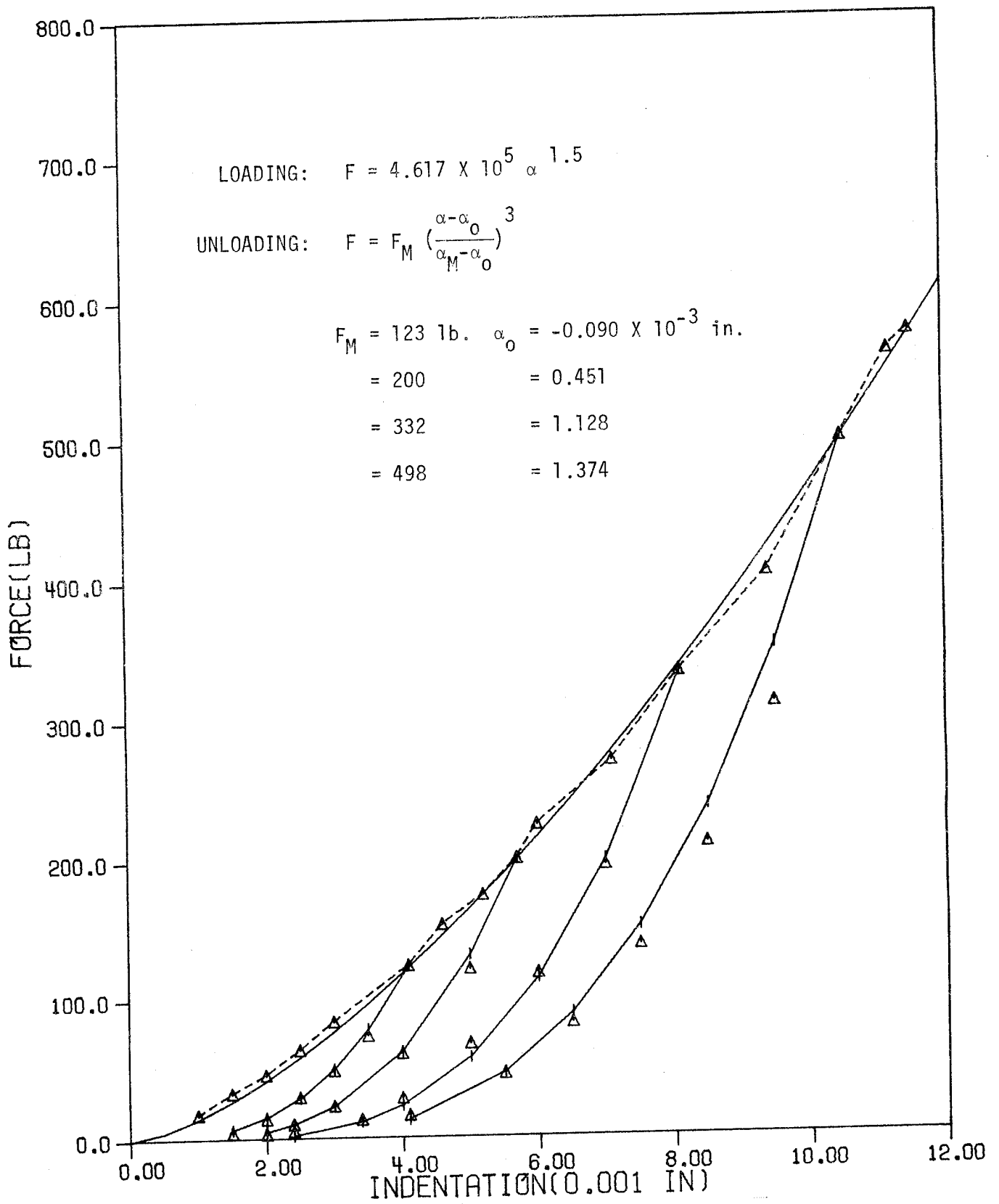


Fig. 2.15. Unloading curves for glass/epoxy with 2-inch span.

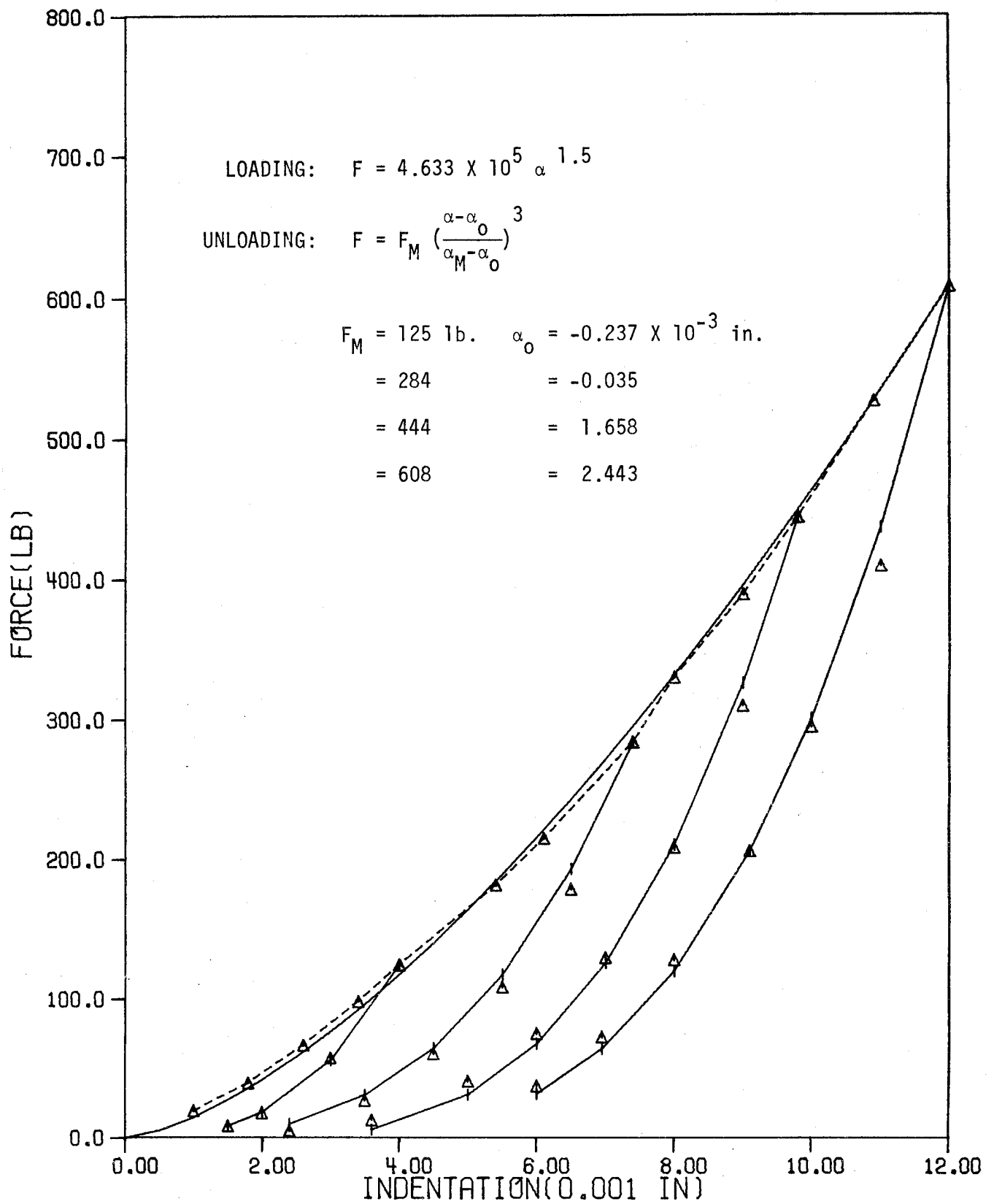


Fig. 2.16. Unloading curves for glass/epoxy with 4-inch span.

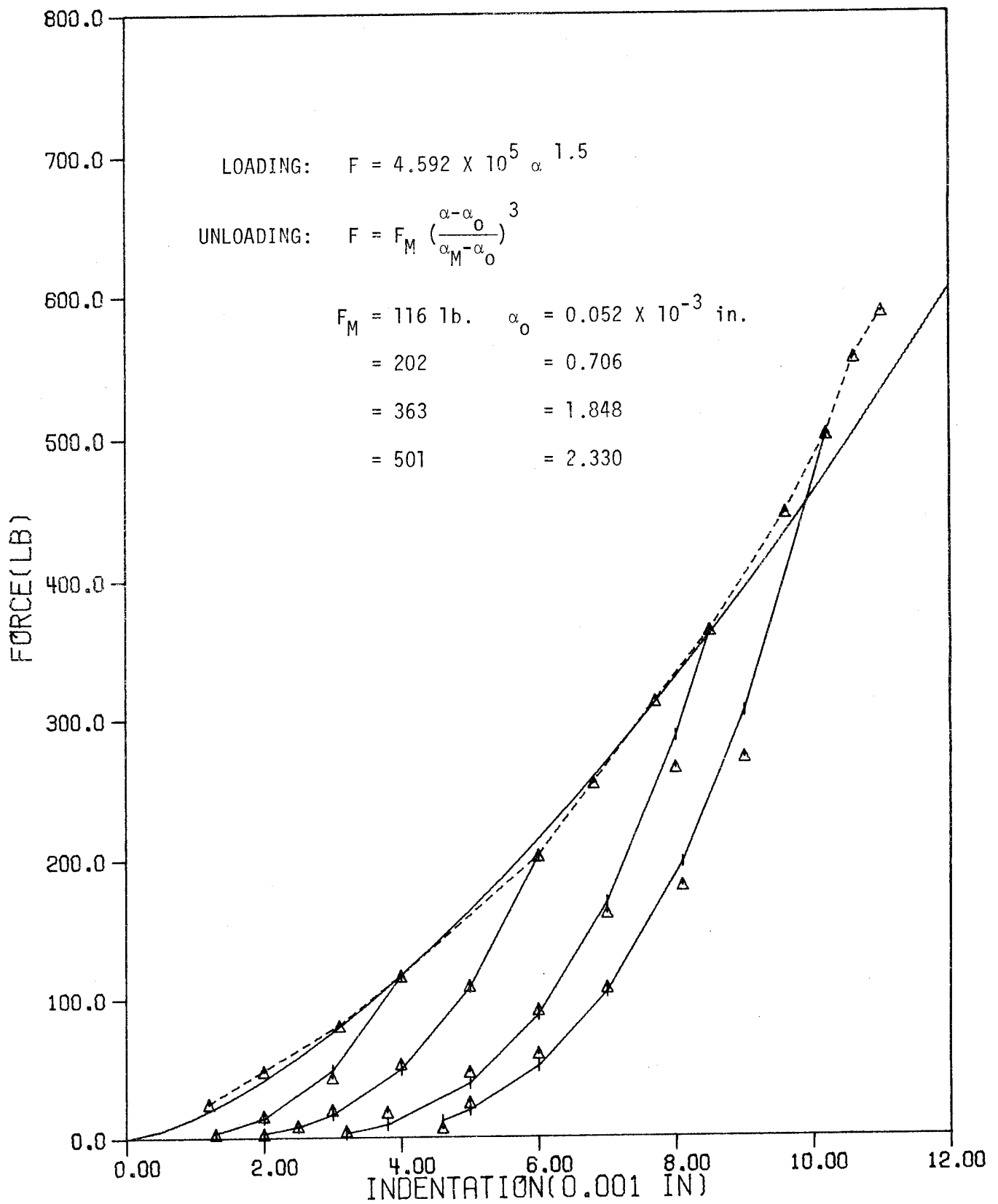


Fig. 2.17. Unloading curves for glass/epoxy with 6-inch span.

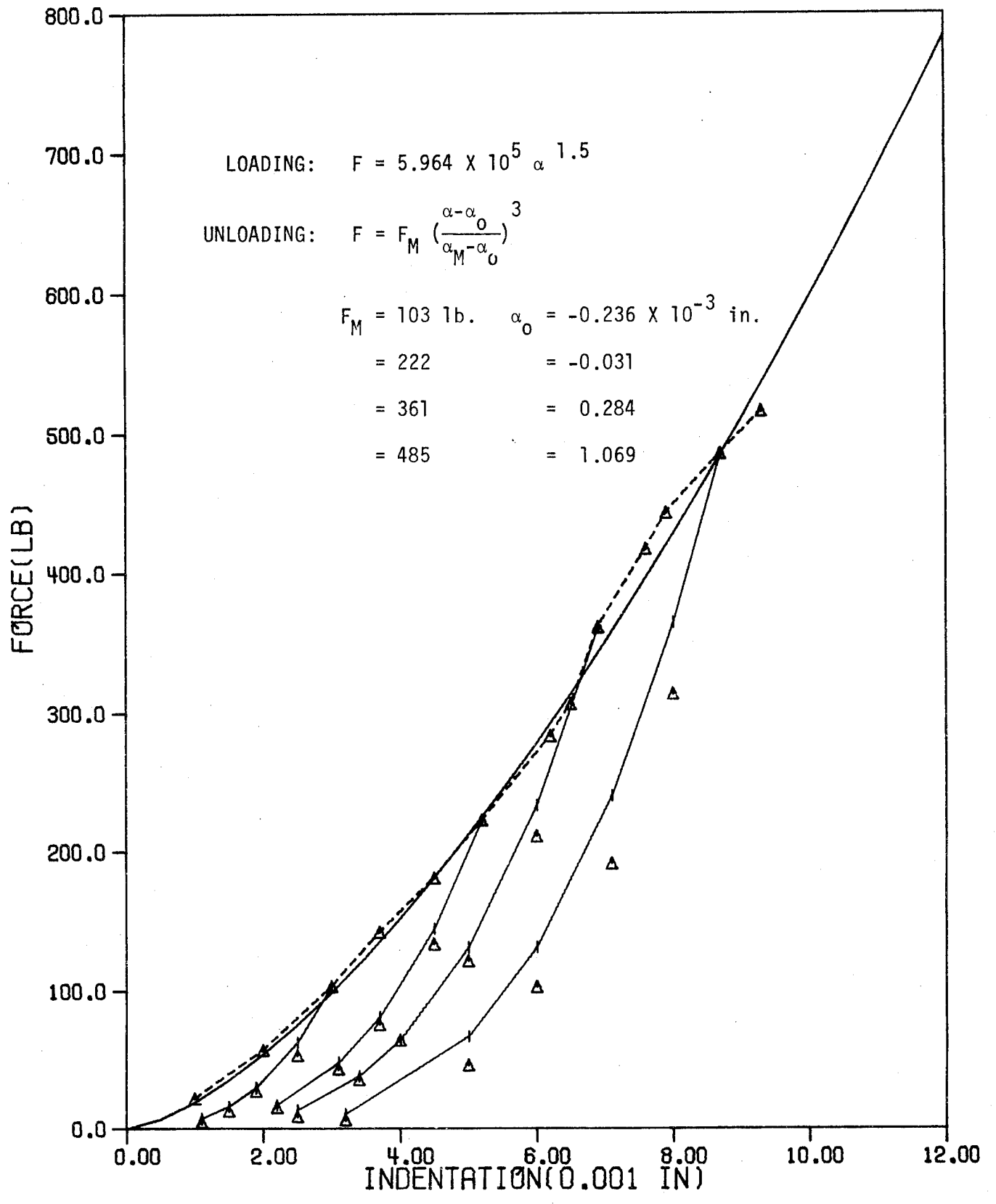


Fig. 2.18. Unloading curves for graphite/epoxy with 2-inch span.

3. IMPACT RESPONSES BY FINITE ELEMENT ANALYSIS

3.1 The Finite Element

A beam finite element with six degrees of freedom has been developed for the dynamic response of elastic isotropic beams subjected to impulsive loadings [5]. This high order beam element has been shown to be more efficient than the conventional element with four degrees of freedom. The element displacement function is taken as

$$v = a_1 + a_2x + a_3x^2 + a_4x^3 + a_5x^4 + a_6x^5 \quad (3-1)$$

where v is the transverse displacement and a_i are constant coefficients. The three degrees of freedom at each node are the transverse displacement v , the rotation θ , and the curvature κ . The coefficients a_i in Eq. (3-1) can be replaced by the six generalized nodal displacements at the two end nodes and, as a result, the displacement function can be alternatively expressed in terms of the nodal displacements.

The stiffness and mass matrices corresponding to the element displacement function has been presented elsewhere [5] and are reproduced in the following:

$$[k] = \frac{E_b I}{70L^3} \begin{bmatrix} 1200 & 600L & 30L^2 & -1200 & 600L & -30L^2 \\ & 384L^2 & 22L^3 & -600L & 216L^2 & -8L^3 \\ & & 6L^4 & -30L^2 & 8L^3 & L^4 \\ & & & 1200 & -600L & 30L^2 \\ & & & & 384L^2 & -22L^3 \\ & & & & & 6L^4 \end{bmatrix} \quad (3-2)$$

$$[m] = \frac{\rho AL}{55440} \begin{bmatrix} 21720 & 3732L & 281L^2 & 6000 & -1812L & 181L^2 \\ & 832L^2 & 69L^3 & 1812L & -532L^2 & 52L^3 \\ & & 6L^4 & 181L^2 & -52L^3 & 5L^4 \\ & & & 21720 & -3732L & 281L^2 \\ & & & & 832L^2 & -69L^3 \\ & & & & & 6L^4 \end{bmatrix} \quad (3-3)$$

where $E_b I$ is the beam bending rigidity, L is the length, ρ is the mass density, and A is the cross-sectional area. If the finite element is to be used for the analysis of laminated composite beams, then the bending rigidity $E_b I$ has to be replaced by the equivalent bending rigidity D .

3.2 Impact Response

Based upon the stiffness and mass matrices given by Eqs. (3-2) and (3-3), respectively, a computer program has been written specifically for the dynamic response of a beam subjected to transverse impact of an elastic sphere. A finite difference scheme suggested by Wilson and Clough [6] was used to integrate the time variable in the equations of motion. In [5], the classical Hertzian law of elastic contact was used to solve a few example problems and excellent results were found.

The finite element program has been modified for the analysis of impact of laminated beams. The Hertzian indentation laws, Eqs. (2-1) with Eq. (2-2) or Eq. (2-3), as well as the measured indentation formulas can be chosen for the analysis. Both elastic loading and actual loading paths can be

incorporated in the program. The computer program with a brief user's instructions is presented in Appendix A.

Figures 3.1 - 3.4 show results for some example problems of simply-supported steel beams, subjected to impact of a steel ball. The diameter of the ball is $\frac{1}{2}$ in. The classical Hertzian law of contact was used in the computation. The material constants used are given by Eq. (4-31). From these results it can be seen that the impact velocity has a great effect on the maximum contact force and contact duration. The thickness of the beam has little effect for the two beam depths studied.

As reported in Section 2, a contact of the steel ball and the glass/epoxy and graphite/epoxy composite always results in a permanent deformation. The unloading paths are substantially different from the loading path. If the actual unloading paths are used, the contact force is certainly expected to deviate from that obtained by following elastic unloadings.

Figures 3.5 and 3.6 present the results for a glass/epoxy laminated composite beam with the dimension 0.19 in. D x 1.0 in. W x 7.5 in. L. This is the composite beam used for the indentation test. The actual indentation law with $k = 4.62 \times 10^5$ and $n = 1.5$ for loading and $q = 2.5$ for unloading was used for the computation. Note that, in this case, the steel ball has a diameter of $1/4$ in. same as that of the indentor in the static indentation test. The material constants for composite are

$$E_L = 5.7 \times 10^6 \text{ psi}$$

$$E_T = 1.2 \times 10^6 \text{ psi}$$

$$G_{LT} = 0.6 \times 10^6 \text{ psi}$$

$$\nu_{LT} = 0.26$$

$$\rho = 0.002016 \text{ slug/in}^3 \quad (0.000168 \text{ lb-sec}^2/\text{in}^4)$$

From the results in these figures it can be seen that the contact force drops more rapidly after reaching its maximum value when the inelastic unloading path is followed. However, the total contact duration does not seem to be affected by the inelastic unloading.

The finite element program developed here can also be used in conjunction with the experimentally obtained contact law to compute the dynamic strain at any point on the beam. The dynamic strain can be experimentally measured by using a strain gage. By comparing the measured strain and that predicted by the finite element solution, it may be possible for us to determine the effect of a result of this comparison. The static indentation law may be modified to account for the strain rate effect. The result of the comparison will be reported in the future.

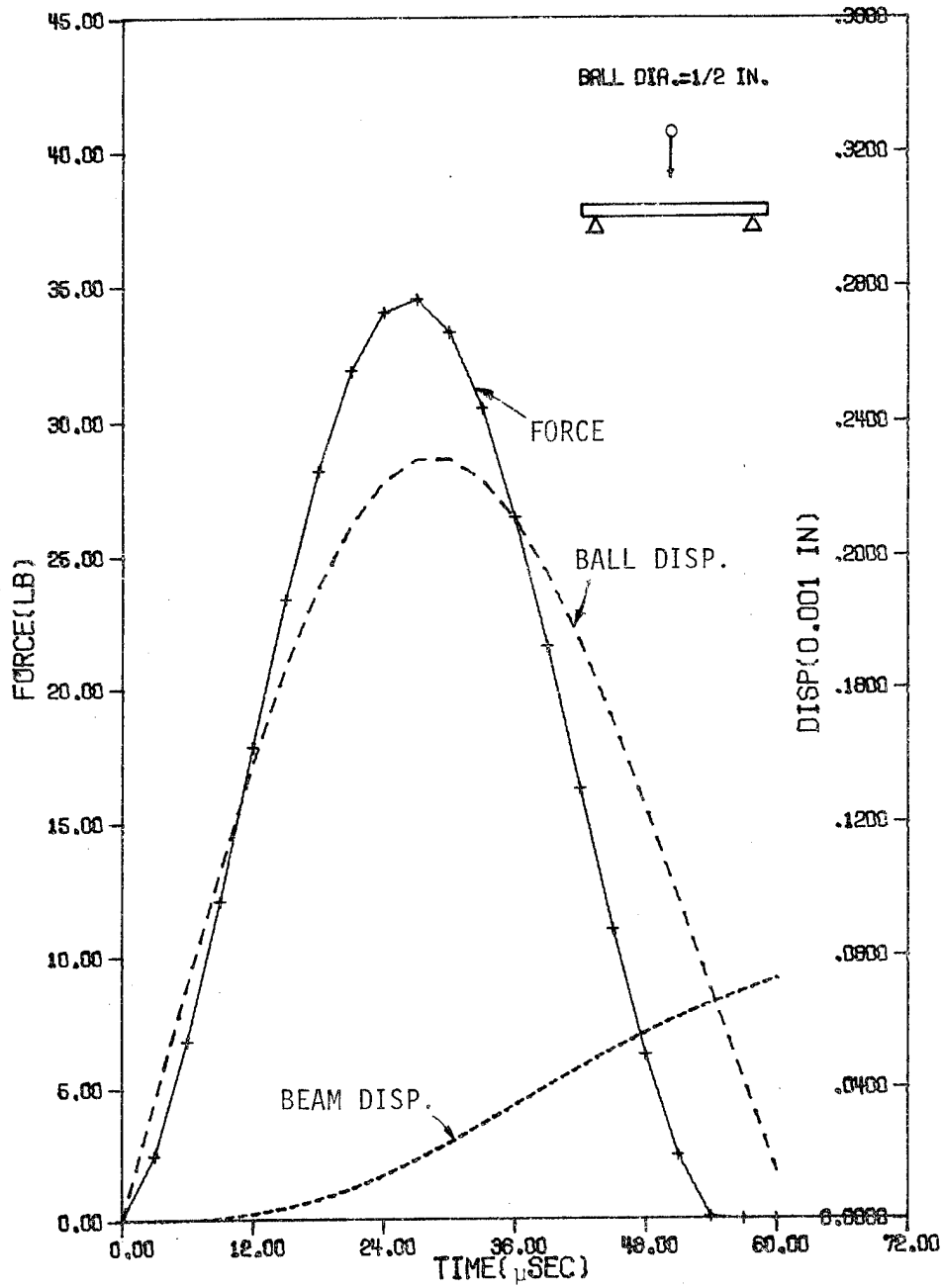


Fig. 3.1. Response of simply-supported steel beam (0.5"W X 0.5"D X 30"L) subjected to impact of a steel ball with initial velocity 12 in/sec.

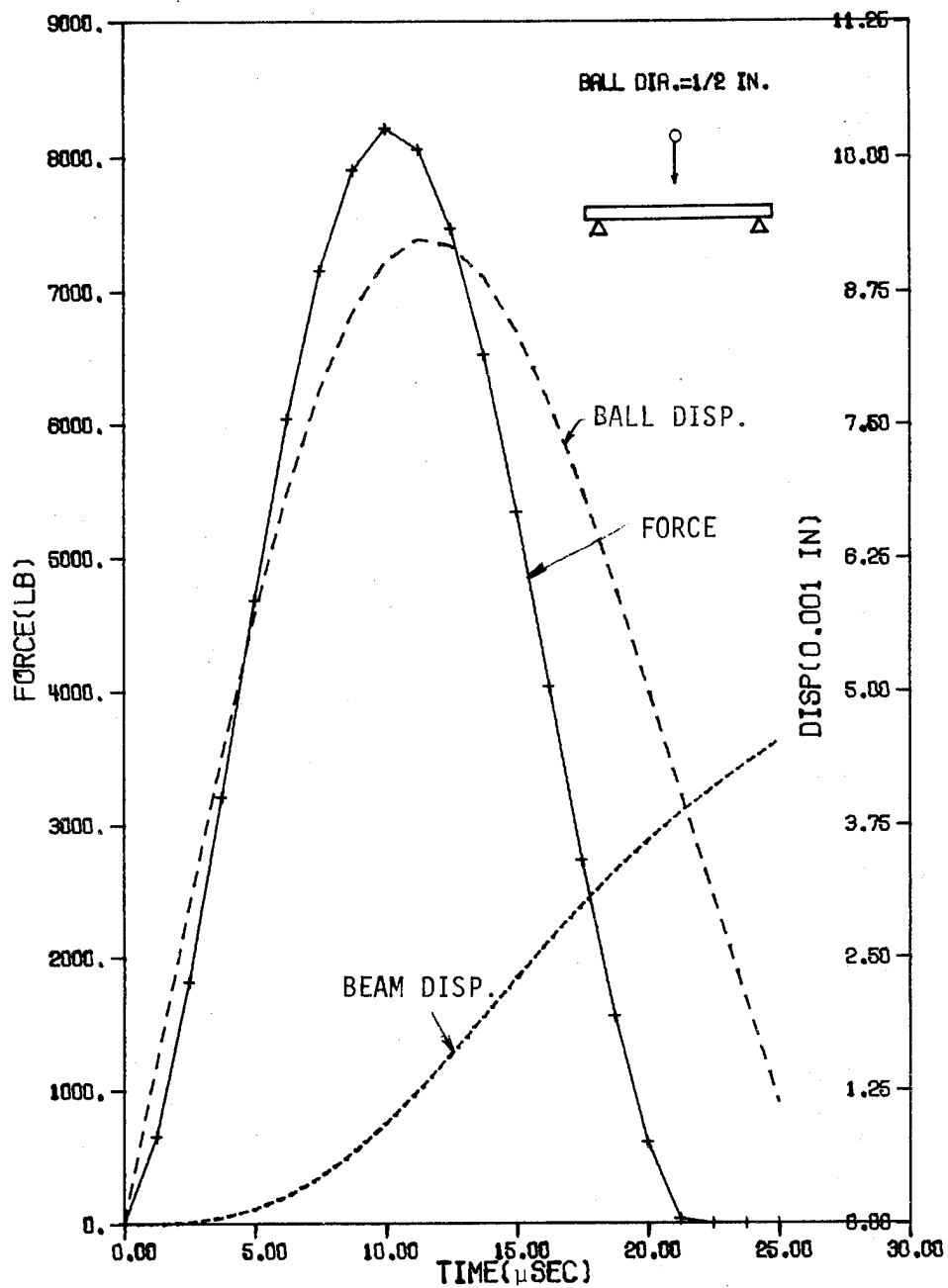


Fig. 3.2. Response of a simply-supported steel beam (0.5"W X 0.5"D X 30"L) subjected to impact of a steel ball with initial velocity 1200 in/sec.

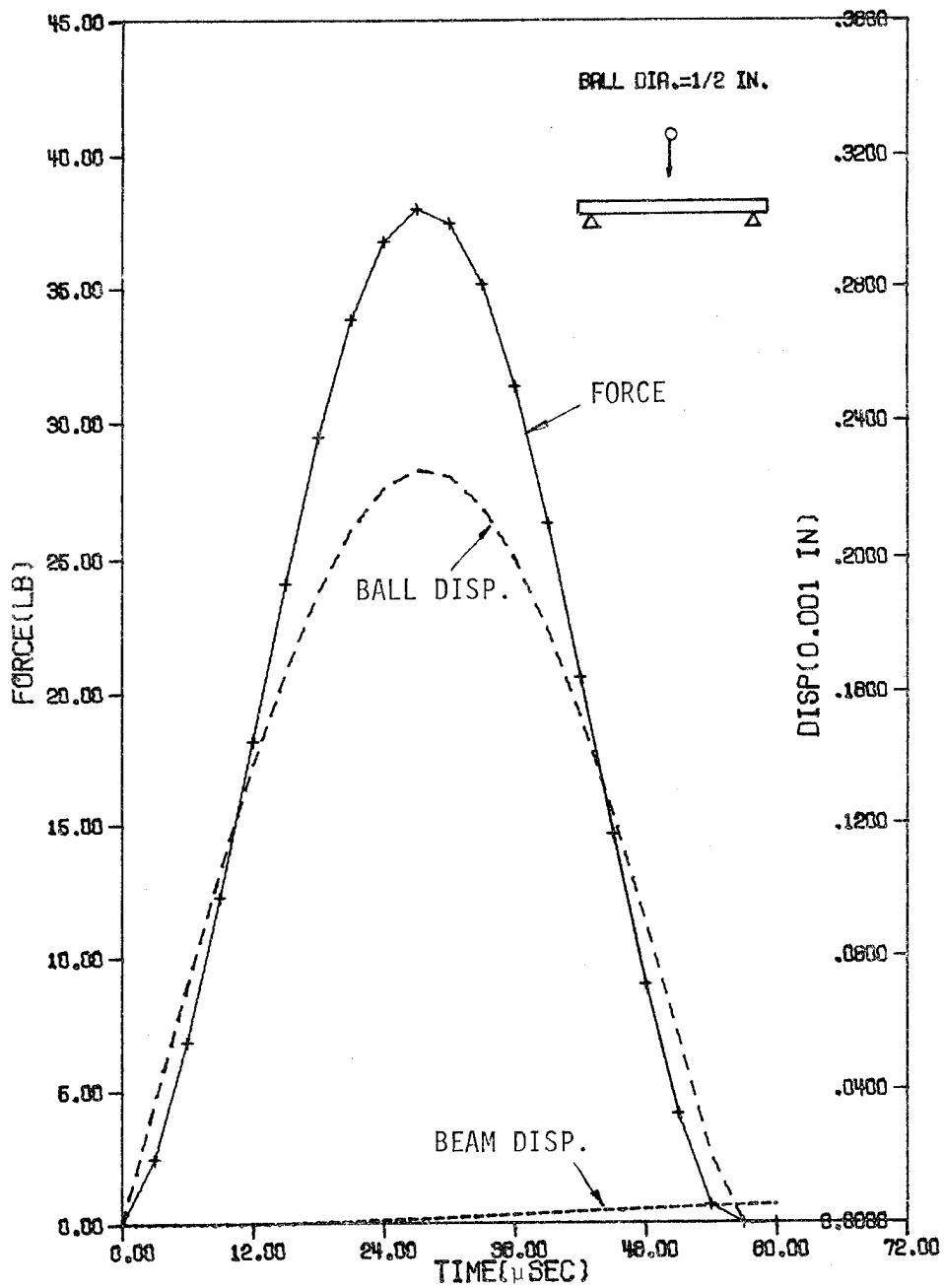


Fig. 3.3. Response of a simply-supported steel beam (0.5"W X 3.0"D X 30"L) subjected to impact of a steel ball with initial velocity 12 in/sec.

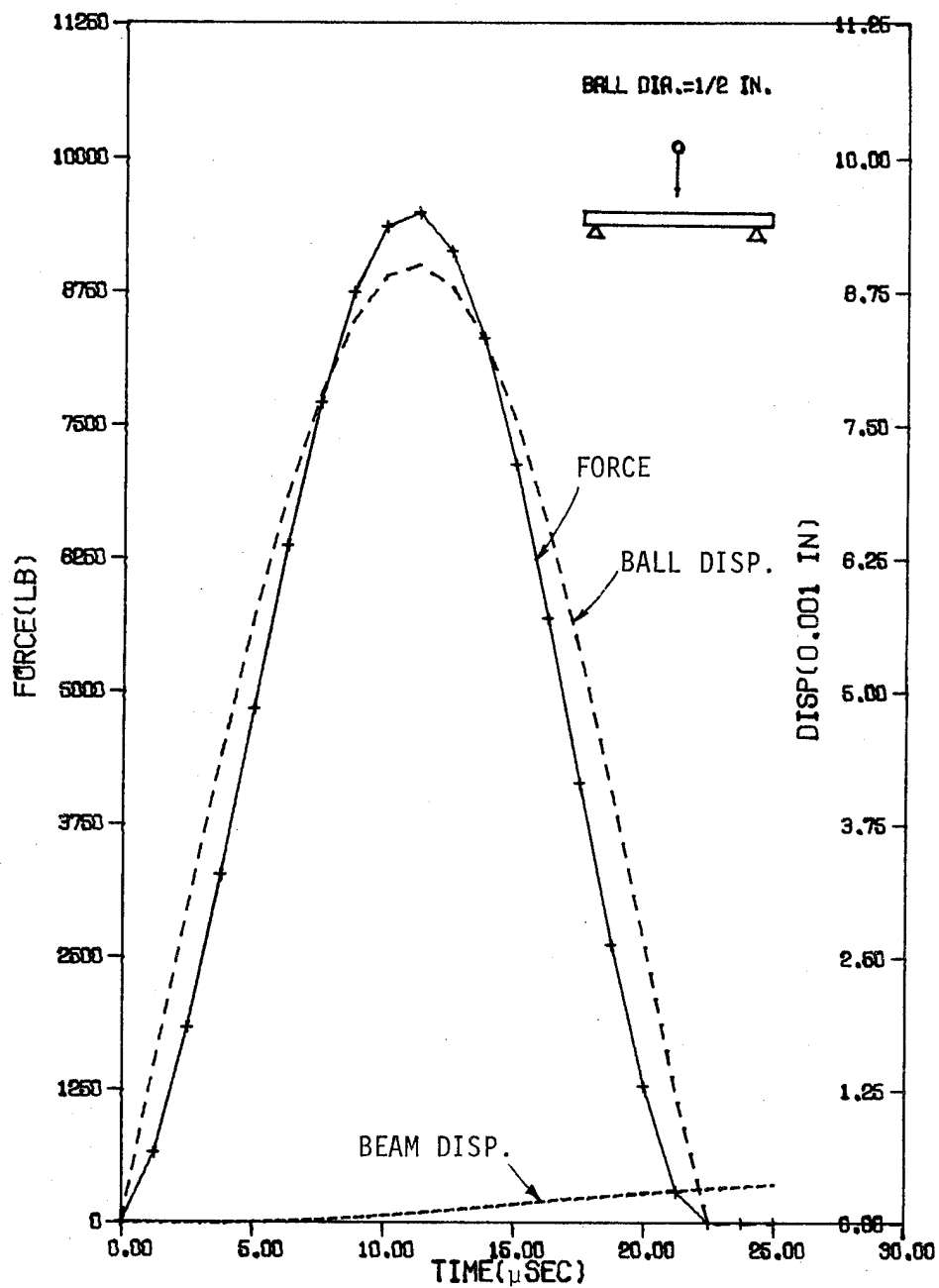


Fig. 3.4. Response of a simply-supported steel beam (0.5"W X 3"D X 30"L) subjected to impact of a steel ball with initial velocity 1200 in/sec.

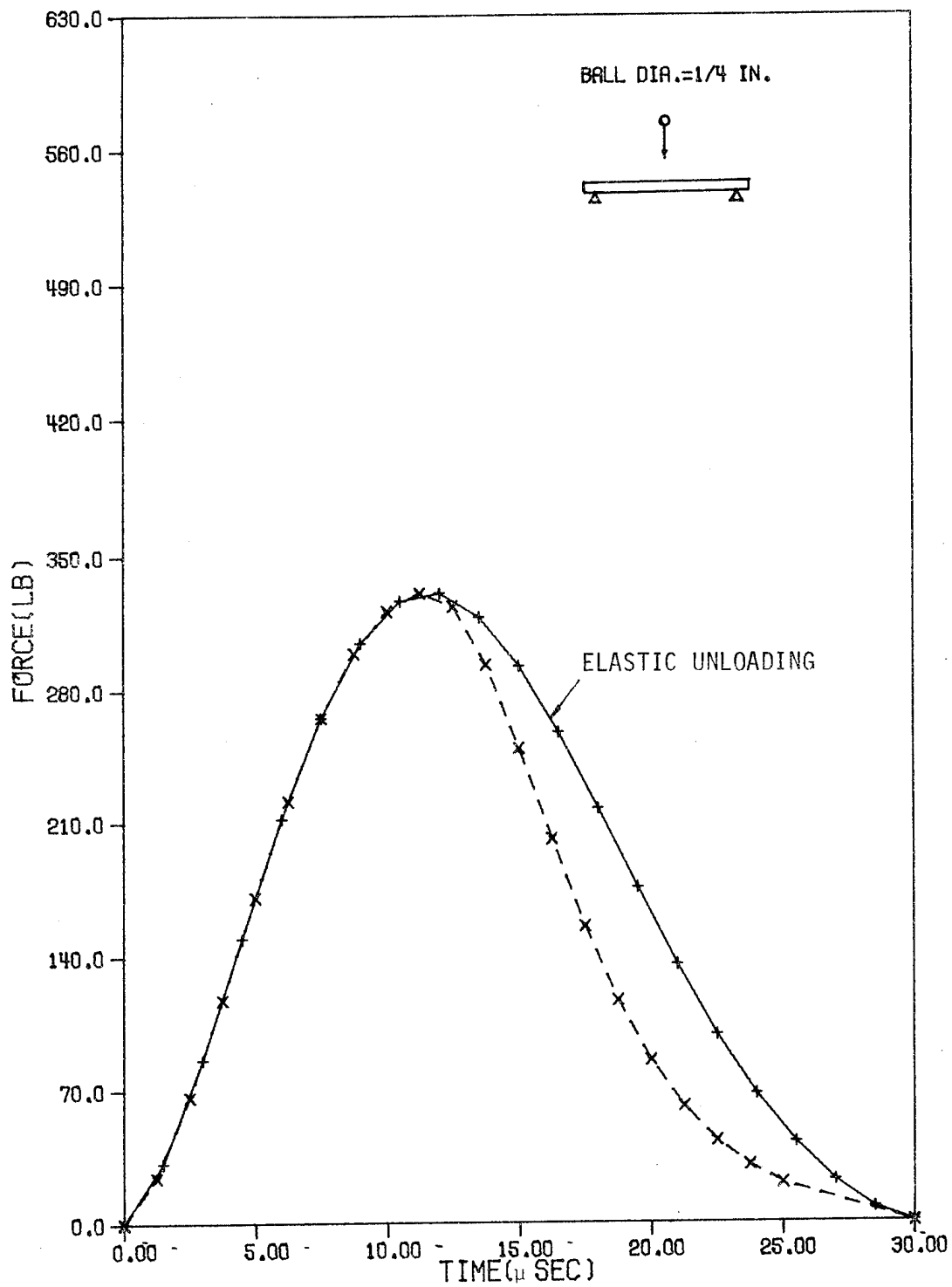


Fig. 3.5. Contact forces with elastic and inelastic unloadings in a simply-supported glass/epoxy laminated beam (1"W X 0.19"D X 7.5"L) subjected to impact of a steel ball at $v_i = 1000$ in/sec.

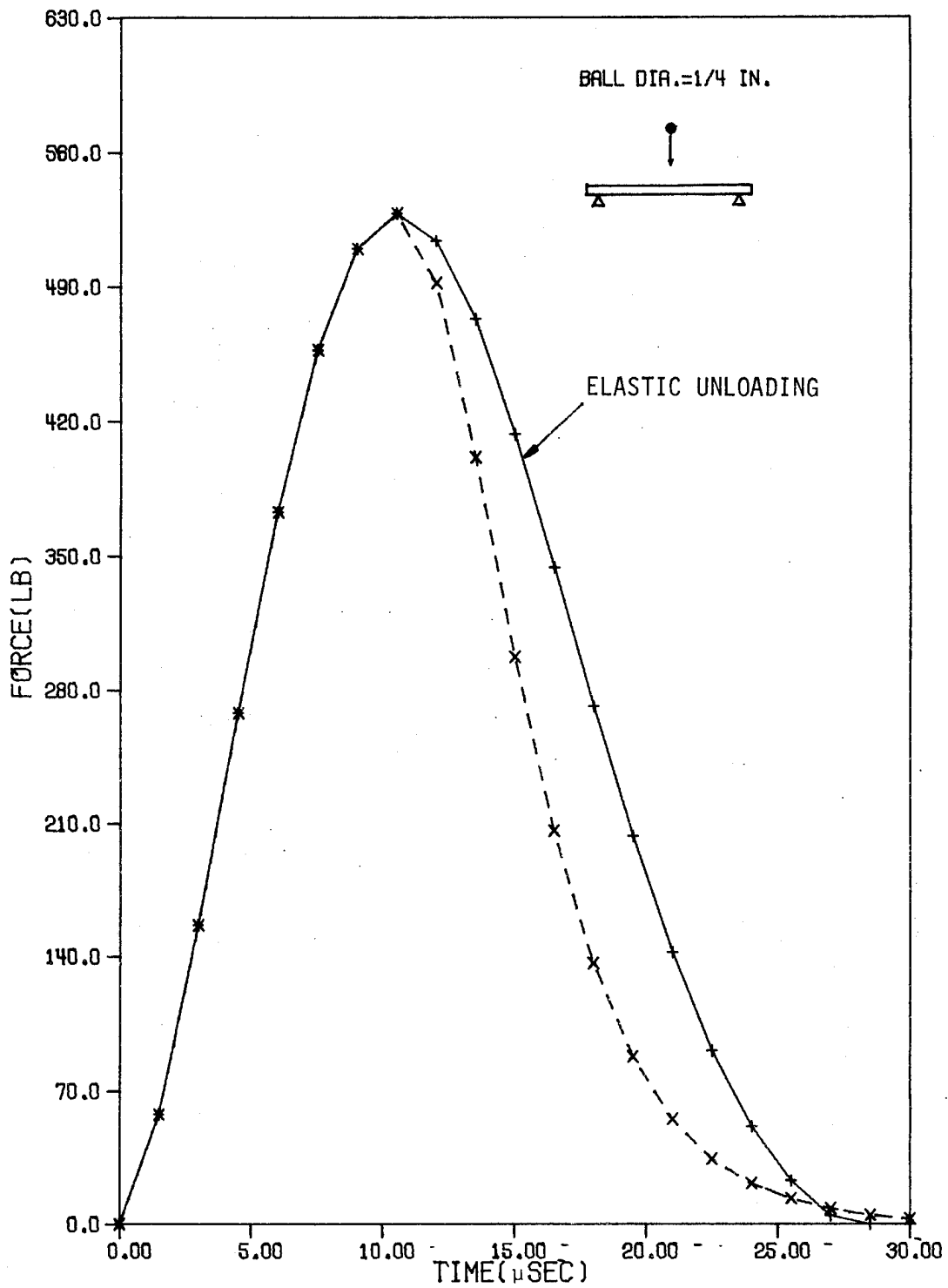


Fig. 3.6. Contact forces with elastic and inelastic unloadings in a simply-supported glass/epoxy laminated beam (1"W X 0.19"D X 7.5"L) subjected to impact of a steel ball at $v_i = 1500$ in/sec.

4. A Simple Method for Computing Contact Force and Duration in Elastic Impact

In using the finite element program described in Section 3, we have to choose a proper time increment Δt and the total length of time integration prior to the solution. A poor choice of Δt may result in poor finite difference solutions. A simple way to obtain an approximate impact duration prior to the use of the finite element program certainly will avoid futile trials. In the following, a simple method is developed for computing an approximate contact force and the contact duration.

4.1 Impact of an Elastic Sphere on a Mass with a Flat Surface

A simple analysis for a spherical projectile impacting an elastic mass with a flat surface was proposed by Timoshenko [7] as follows.

Denoting the mass and velocity of the target by m_t and v_t , respectively, and the mass and the velocity of the sphere by m_s and v_s , respectively, the rates of change of velocity during impact are

$$m_t \frac{dv_t}{dt} = F \quad (4-1)$$

$$m_s \frac{dv_s}{dt} = -F \quad (4-2)$$

where F is the contact force. The velocity of the relative approach α (the indentation) is

$$\dot{\alpha} = v_s - v_t \quad (4-3)$$

From Eqs. (4-1) to (4-3), we obtain

$$\ddot{\alpha} = -F \frac{m_t + m_s}{m_t m_s} \quad (4-4)$$

Substituting the Hertz law of contact, Eq. (2-1), in Eq. (4-4), we obtain

$$\ddot{\alpha} = -k\xi\alpha^{3/2} \quad (4-5)$$

where

$$\xi = \frac{1}{m_t} + \frac{1}{m_s} \quad (4-6)$$

Integrating Eq. (4-5), we have

$$\frac{1}{2} (\dot{\alpha}^2 - v_i^2) = -\frac{2}{5} k\xi\alpha^{5/2} \quad (4-7)$$

The maximum value of α , α_{\max} , occurs at $\dot{\alpha} = 0$. We obtain

$$\alpha_{\max} = \left(\frac{5}{4} \frac{v_i^2}{k\xi} \right)^{2/5} \quad (4-8)$$

This together with the Hertzian law yields the maximum contact force.

From Eq. (4-7), the following relation is derived:

$$dt = \frac{d\alpha}{\left(v_i^2 - \frac{4}{5} k\xi\alpha^{5/2} \right)^{1/2}} \quad (4-9)$$

By introducing

$$\eta = \left(\frac{4}{5} \frac{k\xi}{v_i^2} \right)^{2/5} \alpha = \frac{\alpha}{\alpha_{\max}} \quad (4-10)$$

Equation (4-9) can be rewritten as

$$dt = \frac{\alpha_{\max}}{v_i} \frac{d\eta}{\left(1 - \eta^{5/2} \right)^{1/2}} \quad (4-11)$$

If we assume that the maximum indentation, α_{\max} , is achieved half way through the entire contact, then the duration of impact is obtained from

integrating Eq. (4-11) as

$$T = \frac{2\alpha_{\max}}{v_i} \int_0^1 \frac{d\eta}{(1 - \eta^{5/2})^{1/2}} = 2.94 \frac{\alpha_{\max}}{v_i} \quad (4-12)$$

4.2 Equivalent Mass Model

In view of the simple formulas given by Eqs. (4-8) and (4-12), we will attempt to find an equivalent mass m_t to represent an actual beam or plate. Once this is accomplished, the maximum contact force and the contact duration can be estimated easily.

The equivalent system is developed based upon the condition that it stores the same amount of kinetic and strain energies as in the actual system. It is assumed that in both systems the strain energies in the impactors are negligible and that the kinetic energies are identical. It is also assumed that the spheres do the same amount of work on both the actual and the equivalent targets. With these assumptions, we conclude that the total kinetic energy of the equivalent mass, K_t , should be equal to the kinetic energy K plus the strain energy U of the actual elastic target, i.e.,

$$K + U = K_t \quad (4-13)$$

The kinetic energy in the equivalent target system is simply

$$K_t = \frac{1}{2} m_t v_t^2 \quad (4-14)$$

From Eq. (4-1), the velocity of the equivalent mass can be obtained by integration as

$$v_t = -\frac{1}{m_t} \int_0^t F(\tau) d\tau \quad (4-15)$$

From all the previous studies, the contact force history resembles a sine function. In view of this, we approximate the contact force as follows

$$F = F_{\max} \sin(\pi t/T) \quad (4-16)$$

Substituting Eq. (3-16) into Eq. (3-15) and integrating from $t=0$ to $t = T/2$ we obtain the velocity of the equivalent target at $t = T/2$ as

$$v_t = -\frac{1}{m_t} \frac{T}{\pi} F_{\max} \quad (4-17)$$

Substitution of Eq. (4-17) into Eq. (4-14) and then into Eq. (4-13) lead to

$$(K + U)_{t=T/2} = \frac{1}{2} \frac{1}{m_t} \left(\frac{T}{\pi}\right)^2 F_{\max}^2 \quad (4-18)$$

Since the deflection of the beam is proportional to the applied force F , both U and K contain F_{\max}^2 terms and can be factored out as

$$U = F_{\max}^2 U^*, \quad K = F_{\max}^2 K^* \quad (4-19)$$

in which U^* and K^* do not depend on F_{\max} . Equation (3-18) can now be written as

$$\frac{T^2}{2m_t\pi^2} = (U^* + K^*)_{t=T/2} \quad (4-20)$$

From Eqs. (4-6), and (4-8) and (4-12), we note that the contact duration T is a function of the equivalent mass m_t . Thus, Eq. (4-20) is basically a nonlinear equation for m_t . Numerical methods will be used to find solutions for this equation.

4.3 Simply-Supported Beam

Consider a beam of cross-sectional area A and bending rigidity D .

The equation of motion is

$$D \frac{\partial^4 w}{\partial x^4} + \rho A \frac{\partial^2 w}{\partial t^2} = q(x,t) \quad (4-21)$$

where ρ is the average mass density (over the thickness) and $q(x,t)$ is a time dependent forcing function. For a homogeneous elastic beam, we have

$$D = EI \quad (4-22)$$

For laminated composite beams, D is estimated according to Eq. (4-36).

If the force is a concentrated force $F(t)$ applied at $x=c$, then the solution for Eq. (4-21) can be expressed as [8]

$$w(x,t) = \frac{1}{\rho A} \sum_{n=1}^{\infty} \frac{w_n(x)w_n(c)}{\omega_n \int_0^L w_n^2(x)dx} \int_0^t F(\tau) \sin \omega_n(t-\tau) d\tau \quad (4-23)$$

where $w_n(x)$ is the shape function for the n th natural mode of vibration, and ω_n is the corresponding natural frequency.

For a simply-supported beam, we obtain

$$w_n(x) = \sin \frac{n\pi x}{L} \quad (4-24)$$

and

$$\omega_n^2 = \left(\frac{n\pi}{L}\right)^4 \frac{D}{\rho A} \quad (4-25)$$

If the concentrated force is given by Eq. (4-16), then the beam deflection w can be obtained from Eq. (4-23) as

$$w(x,t) = \frac{2F_{\max} L^3}{\pi^4 D} \sum_{n=1}^{\infty} w_n(c) \frac{1}{n^4} \left[\frac{4T^2}{4T^2 - T_n^2} \left(\sin \frac{\pi}{T} t - \frac{T_n}{2T} \sin \omega_n t \right) \right] w_n(x), \text{ for } t \leq T \quad (4-26)$$

In Eq. (4-26),

$$T_n = \frac{2\pi}{\omega_n} \quad (4-27)$$

is the period for the n th mode. The strain energy and the kinetic energy can be computed in a straightforward manner. We obtain at $t = T/2$

$$U^* = \frac{16L^3 T^4}{\pi^4 D} f_1 \quad (4-28)$$

$$K^* = \frac{16\rho AL^7 T^2}{\pi^6 D^2} g_1$$

where

$$f_1 = \sum_{n=1}^{\infty} \left\{ \frac{n^2}{4n^4 T^2 - T_1^2} \left[1 - \frac{T_1}{2n^2 T} \sin(n^2 \frac{\omega_1 T}{2}) \right] w_n(c) \right\}^2 \quad (4-29)$$

$$g_1 = \sum_{n=1}^{\infty} \left\{ \frac{1}{4n^4 T^2 - T_1^2} \cos(n^2 \frac{\omega_1 T}{2}) w_n(c) \right\}^2 \quad (4-30)$$

From the numerical examples, it has been observed that use of fifty terms in the series in Eqs. (4-29) and (4-30) should provide a converged

solution. In all examples presented in this section, the classical Hertzian law is used.

As a first evaluation of the equivalent mass concept, we consider a problem solved by Timoshenko [9] using a numerical procedure to solve a nonlinear integral equation. The steel beam considered has a 0.39 in. x 0.39 in. (1 cm x 1 cm) cross-section and 6.04 in. (15.35 cm) length. The beam is simply-supported at two ends and subjected to impact of a steel ball with 0.79 in. (2 cm) diameter. The material properties are

$$\begin{aligned} E &= 31 \times 10^6 \text{ psi} \\ \nu &= 0.29 \\ \rho &= 0.00894 \text{ slug/in}^3 \text{ (0.000745 lb-sec}^2\text{/in}^4\text{)} \end{aligned} \tag{4-31}$$

It should be pointed out that in the numerical computation, the value for the mass density as given by Eq. (4-31) should be divided by a factor of 12 if the length is given in inches.

Figure 4.1 shows the contact force histories according to Timoshenko's solution and the equivalent mass model. Excellent agreement is noted.

Figures 4.2 and 4.3 show the contact forces of a simply-supported steel beam subjected to impact of a steel ball of 1/2 in. diameter with different velocities. The beam has a 1/2 in. x 1/2 in. cross-section and is 30 in. long. Both the equivalent mass model results and the finite element results are found to have a very close agreement.

The results for a thicker steel beam (1/2 in. W x 3 in. D x 30 in. L) with simple supports are presented in Figs. 4.4 and 4.5 for $v_i = 12$ in./sec. and 1200 in./sec., respectively. Again, the equivalent mass model works quite well in predicting the magnitude and duration of the contact force.

Figure 4.6, shows the results for a simple-supported thin steel beam (0.5 in. W x 0.08 in. D x 15 in. L) subjected to the impact of a steel ball of 0.5 in. diameter with $v_i = 100$ in./sec. The equivalent mass model is able to predict the maximum contact force but not the contact duration due to the long tail portion.

Figure 4.7 shows the contact force history for a composite beam of the same dimension and impact condition as the previous problem. The laminated beam consists of 16 piles of graphite/epoxy composite. The ply-thickness is 0.005 in. and the lay-up is $(0/90/0/90)_{2S}$. The material constants are

$$\begin{aligned} E_L &= 30 \times 10^6 \text{ psi}, E_T = 0.75 \times 10^6 \text{ psi} \\ G_{LT} &= 0.4 \times 10^6 \text{ psi}, \nu_{LT} = 0.25, \\ \rho &= 0.00178 \text{ slug/in}^3 \quad (0.000148 \text{ lb-sec}^2/\text{in}^4) \end{aligned} \quad (4-32)$$

The modified Hertzian law of contact given by Eq. (2-3) was used for the solution. Again, from Fig. 4.7 we find that the equivalent mass model is excellent in predicting the maximum contact force but poor in estimating the total contact time. From the numerical examples carried out, it seems that the equivalent mass model can not yield accurate contact time if the target is too thin.

4.4 Simply-Supported Rectangular Plate

The plate theory developed by Whitney and Pagano [10] for laminated composites is used for the analysis. This plate theory takes the transverse shear deformation into account and has been shown by Sun and Lai [11] to be adequate for wave propagation. For simplicity, only cross-ply laminated plates are considered, for which the equations of motion are given by

$$D_{11}\psi_{x,xx} + D_{66}\psi_{x,yy} + (D_{12} + D_{66})\psi_{y,xy} - \kappa A_{55}\psi_x - \kappa A_{55}w_{,x} = \rho I\ddot{\psi}_x \quad (4-33)$$

$$(D_{12} + D_{66})\psi_{x,xy} + D_{66}\psi_{y,xx} + D_{22}\psi_{y,yy} - \kappa A_{44}\psi_y - \kappa A_{44}w_{,y} = \rho I\ddot{\psi}_y \quad (4-34)$$

$$\kappa A_{55}\psi_{x,x} + \kappa A_{55}w_{,xx} + \kappa A_{44}\psi_{y,y} + \kappa A_{44}w_{,yy} + q = \rho h\ddot{w} \quad (4-35)$$

where a comma indicates partial differentiation, q is the lateral load, w is the transverse displacement, ψ_x and ψ_y are the rotations of the plane sections, $\kappa(=\pi^2/12)$ is a shear correction factor, ρ is the average mass density (over the thickness), h is the plate thickness, I is the rotary inertia, and

$$(A_{ij}, D_{ij}) = \int_{-h/2}^{h/2} \bar{Q}_{ij}(1, z^2) dz \quad (4-36)$$

In Eq. (4-36), \bar{Q}_{ij} are the reduced stiffnesses for the composite material.

For an isotropic elastic plate, the following relations exist:

$$D_{11} = D_{22} = \frac{E h^3}{12(1-\nu^2)}$$

$$D_{12} = \nu D_{11}$$

$$D_{66} = \frac{1-\nu}{2} D_{11}$$

$$A_{11} = A_{22} = \frac{Eh}{1-\nu^2} \quad (4-37)$$

$$A_{12} = \nu A_{11}$$

$$A_{44} = A_{55} = \frac{Eh}{2(1+\nu)}$$

The equations of motion given by Eqs. (4-33) to (4-35) reduce to those for the Mindlin's plate theory [12].

If we separate the total displacement into the bending part, w_b , and that due to the transverse shear deformation, w_s , then we have

$$\begin{aligned}\psi_x &= -w_{b,x} \\ \psi_y &= -w_{b,y} \\ w &= w_b + w_s\end{aligned}\tag{4-38}$$

In terms of w_b and w_s , the equation of motion can be written as

$$D_{11} w_{b,xxx} + (D_{12} + 2D_{66}) w_{b,xyy} + \kappa A_{55} w_{s,x} = \rho I \ddot{w}_{b,x}\tag{4-39}$$

$$(D_{12} + 2D_{66}) w_{b,xyy} + D_{22} w_{b,yyy} + \kappa A_{44} w_{s,y} = \rho I \ddot{w}_{b,y}\tag{4-40}$$

$$\kappa A_{55} w_{s,xx} + \kappa A_{44} w_{s,yy} + q = \rho h (\ddot{w}_b + \ddot{w}_s)\tag{4-41}$$

Combining equations (4-39) with (4-40), we have

$$\begin{aligned}D_{11} w_{b,xxxx} + 2(D_{12} + D_{66}) w_{b,xyyy} + D_{22} w_{b,yyyy} + \kappa A_{55} w_{s,xx} \\ + \kappa A_{44} w_{s,yy} = \rho I (\ddot{w}_{b,xx} + \ddot{w}_{b,yy})\end{aligned}\tag{4-42}$$

Equations (4-41) and (4-42) can also be expressed in the form

$$\begin{aligned}L_1 w_b + L_2 w_s &= \rho I \frac{\partial^2}{\partial t^2} \nabla^2 w_b \\ L_2 w_s + q &= \rho h \frac{\partial^2}{\partial t^2} (w_b + w_s)\end{aligned}\tag{4-43}$$

where

$$L_1 = D_{11} \frac{\partial^4}{\partial x^4} + 2(D_{12} + 2D_{66}) \frac{\partial^4}{\partial x^2 \partial y^2} + D_{22} \frac{\partial^4}{\partial y^4}$$

$$L_2 = \kappa A_{55} \frac{\partial^2}{\partial x^2} + \kappa A_{44} \frac{\partial^2}{\partial y^2}$$

$$\nabla^2 = \frac{\partial^2}{\partial x^2} + \frac{\partial^2}{\partial y^2}$$

Applying Laplace transform to equations (4-43) yields

$$L_1 \bar{w}_b + L_2 \bar{w}_s = \rho I s^2 \nabla^2 \bar{w}_b \quad (4-44)$$

$$L_2 \bar{w}_s + \bar{q} = \rho h s^2 (\bar{w}_b + \bar{w}_s)$$

where \bar{w}_b and \bar{w}_s are the transformed functions of w_b and w_s , respectively, and s is the Laplace transform parameter. Since the rotatory inertia is small, it is neglected in this study.

Solving Eqs. (4-44), we obtain

$$\left[(L_2 - L_1) \rho h s^2 + L_1 L_2 \right] \bar{w} = (-L_1 + L_2) \bar{q} \quad (4-45)$$

We expand the displacement w and the load q in terms of the shape functions $w_{mn}(x,y)$ of the natural modes of the plate as

$$w = \sum_m \sum_n B_{mn}(t) w_{mn}(x,y) \quad (4-46)$$

$$q = \sum_m \sum_n q_{mn}(t) w_{mn}(x,y)$$

For a simply-supported rectangular plate, the shape function for the (m,n) mode is given by

$$w_{mn}(x,y) = \sin \frac{m\pi x}{a} \sin \frac{n\pi y}{b} \quad (4-47)$$

where a and b are the lateral dimensions of the plate.

Applying Laplace transform to Eq. (4-46) we obtain

$$\bar{w} = \sum_m \sum_n \bar{B}_{mn}(s) w_{mn}(x,y) \quad (4-48)$$

$$\bar{q} = \sum_m \sum_n \bar{q}_{mn}(s) w_{mn}(x,y)$$

Substitution of Eqs. (4-48) and (4-47) into Eq. (4-45) leads to

$$\bar{B}_{mn}(s) = \frac{1}{\rho h} \frac{1}{s^2 + \omega_{mn}^2} \bar{q}_{mn}(s) \quad (4-49)$$

where

$$\omega_{mn}^2 = \frac{1}{h} \frac{C_{mn} E_{mn}}{C_{mn} + E_{mn}}$$

$$C_{mn} = D_{11} \left(\frac{m\pi}{a}\right)^4 + 2(D_{12} + 2D_{66}) \left(\frac{m\pi}{a}\right)^2 \left(\frac{n\pi}{b}\right)^2 + D_{22} \left(\frac{n\pi}{b}\right)^4$$

$$E_{mn} = \kappa A_{55} \left(\frac{m\pi}{a}\right)^2 + \kappa A_{44} \left(\frac{n\pi}{b}\right)^2 \quad (4-50)$$

The quantity ω_{mn} is the angular natural frequency for the (m,n) mode. If the transverse shear deformation is neglected (i.e. the classical plate theory), then

$$\omega_{mn}^2 = \frac{C_{mn}}{\rho h} \quad (4-51)$$

The solution for w can be obtained by applying inverse transform.

We obtain

$$w = \frac{1}{\rho h} \sum_m \sum_n \sin \frac{m\pi x}{a} \sin \frac{n\pi y}{b} \int_0^t q_{mn}(\tau) \frac{\sin \omega_{mn}(t-\tau)}{\omega_{mn}} d\tau \quad (4-52)$$

where

$$q_{mn}(t) = \frac{4}{ab} \int_0^a \int_0^b q(x,y,t) \sin \frac{m\pi x}{a} \sin \frac{n\pi y}{b} dx dy \quad (4-53)$$

Consider a contact force given as a sine function, see Eq. (4-16), which is applied at the point (x_1, y_1) . Then

$$\begin{aligned} q_{mn}(t) &= \frac{4}{ab} \int_0^a \int_0^b q(x,y,t) \sin \frac{m\pi x}{a} \sin \frac{n\pi y}{b} dx dy \\ &= \frac{4}{ab} F_{\max} \sin\left(\frac{\pi t}{T}\right) \sin \frac{m\pi x_1}{a} \sin \frac{n\pi y_1}{b} \text{ for } t \leq T \end{aligned} \quad (4-54)$$

Substitution of Eq. (4-54) into Eq. (4-52) yields

$$\begin{aligned} w(x,y,t) &= \frac{4F_{\max}}{\rho h ab} \sum_m \sum_n \left[\left(\sin \frac{m\pi x_1}{a} \sin \frac{n\pi y_1}{b} \right) \left(\sin \frac{m\pi x}{a} \sin \frac{n\pi y}{b} \right) \right. \\ &\quad \left. \frac{1}{\omega_{mn}^2} \frac{1}{1 - \left(\frac{\pi}{\omega_{mn} T}\right)^2} \left(\sin \frac{\pi}{T} t - \frac{\pi}{T \omega_{mn}} \sin \omega_{mn} t \right) \right] \end{aligned} \quad (4-55)$$

for $0 \leq t \leq T$. For $x_1 = a/2$, $y_1 = b/2$, Eq. (4-55) becomes

$$w(x,y,t) = \frac{4F_{\max}}{\rho h a b} \sum_{m=1}^{\infty} \sum_{n=1}^{\infty} \left[\left(\sin \frac{m\pi x}{a} \sin \frac{n\pi y}{b} \right) \frac{1}{\omega_{mn}^2} \right. \\ \left. \frac{1}{1 - \left(\frac{\pi}{\omega_{mn} T} \right)^2} \left(\sin \frac{\pi}{T} t - \frac{\pi}{T \omega_{mn}} \sin \omega_{mn} t \right) \right] \sin \frac{m\pi}{2} \sin \frac{n\pi}{2} \quad (4-56)$$

comparing Eq. (4-46) with (4-56) we find

$$B_{mn}(t) = \frac{4F_{\max}}{\rho h a b} \frac{1}{\omega_{mn}^2} \frac{1}{1 - \left(\frac{\pi}{\omega_{mn} T} \right)^2} x \sin \frac{m\pi}{2} \sin \frac{n\pi}{2} x \left(\sin \frac{\pi}{T} t - \frac{\pi}{T \omega_{mn}} \sin \omega_{mn} t \right) \quad (4-57)$$

The kinetic energy in the plate at any time $t \leq T$ is given by

$$K(t) = \frac{\rho h}{2} \int_0^a \int_0^b \left(\frac{\partial w}{\partial t} \right)^2 dx dy \quad (4-58)$$

Substituting Eq. (4-57) into Eq. (4-46) and then into Eq. (4-58) we obtain

$$K(t) = \frac{\rho h a b}{8} \sum_m \sum_n \dot{B}_{mn}^2(t) \quad (4-59)$$

By introducing the stiffness, K_{mn} , of the plate system for the (m, n) mode, the total strain energy can be formally written as

$$U(t) = \frac{1}{2} \sum_m \sum_n K_{mn} B_{mn}^2(t) \quad (4-60)$$

Upon substitution of Eqs. (4-59) and (4-60) into the Lagrangian equation of motion we obtain

$$\frac{1}{4} \rho h a b \ddot{B}_{mn}(t) + K_{mn} B_{mn}(t) = Q_{mn} \quad (4-61)$$

where Q_{mn} is the generalized force. From Eq. (4-61) we obtain the natural frequency ω_{mn} for the (m,n) mode as

$$\omega_{mn}^2 = \frac{4}{\rho h a b} K_{mn} \quad (4-62)$$

from which

$$K_{mn} = \frac{\rho h a b}{4} \omega_{mn}^2 \quad (4-63)$$

Substituting Eqs. (4-63) and (4-57) into Eq. (4-60) we obtain

$$U(t) = \frac{2F_{\max}^2}{\rho h a b} \sum_m \sum_n \left[\frac{1}{\omega_{mn}} \frac{1}{1 - \left(\frac{\pi}{\omega_{mn} T}\right)^2} x \sin \frac{m\pi}{2} \sin \frac{n\pi}{2} x \right. \\ \left. x \left(\sin \frac{\pi}{T} t - \frac{\pi}{T \omega_{mn}} \sin \omega_{mn} t \right) \right]^2 \quad (4-64)$$

With Eqs. (4-60) and (4-64), the quantities U^* and K^* in the equivalent mass mode can be obtained. We have

$$U^* (T/2) = \frac{2}{\rho h a b} f_3 \quad (4-65)$$

$$K^* (T/2) = \frac{2\pi^2}{\rho h a b T^2} g_3 \quad (4-66)$$

where

$$f_3 = \sum_m \sum_n \left[\frac{1}{\omega_{mn}} \frac{1}{1 - \left(\frac{\pi}{\omega_{mn} T}\right)^2} \left(1 - \frac{\pi}{T \omega_{mn}} \sin \frac{\omega_{mn} T}{2}\right) \sin \frac{m\pi}{2} \sin \frac{n\pi}{2} \right]^2 \quad (4-67)$$

$$g_3 = \sum_m \sum_n \left[\frac{1}{\omega_{mn}^2} \frac{1}{1 - \left(\frac{\pi}{\omega_{mn} T}\right)^2} \cos \left(\frac{\omega_{mn} T}{2}\right) \sin \frac{m\pi}{2} \sin \frac{n\pi}{2} \right]^2 \quad (4-68)$$

Karas [13] considered the impact of a steel ball of 2 cm in diameter on a simply-supported square steel plate with $a=b=20$ cm and $h = 0.8$ cm by using the classical plate theory. The impact velocity of the ball was 100 cm/sec. The contact force histories obtained by Karas and by using the equivalent mass model are shown in Fig. 4.8. It is seen that the equivalent mass model yields a good estimate of the maximum contact force and contact duration.

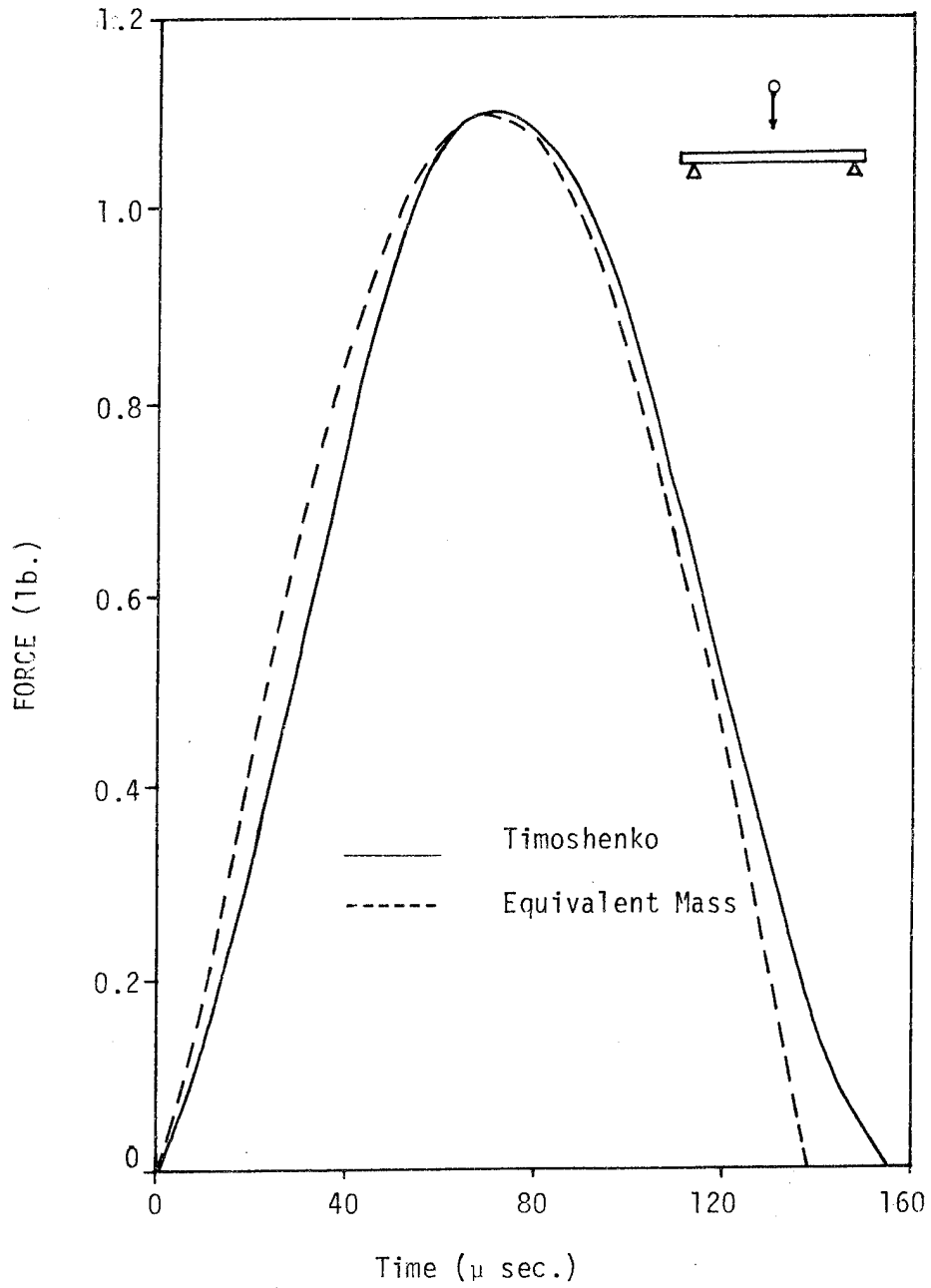


Fig. 4.1 Contact force history for the Timoshenko problem.

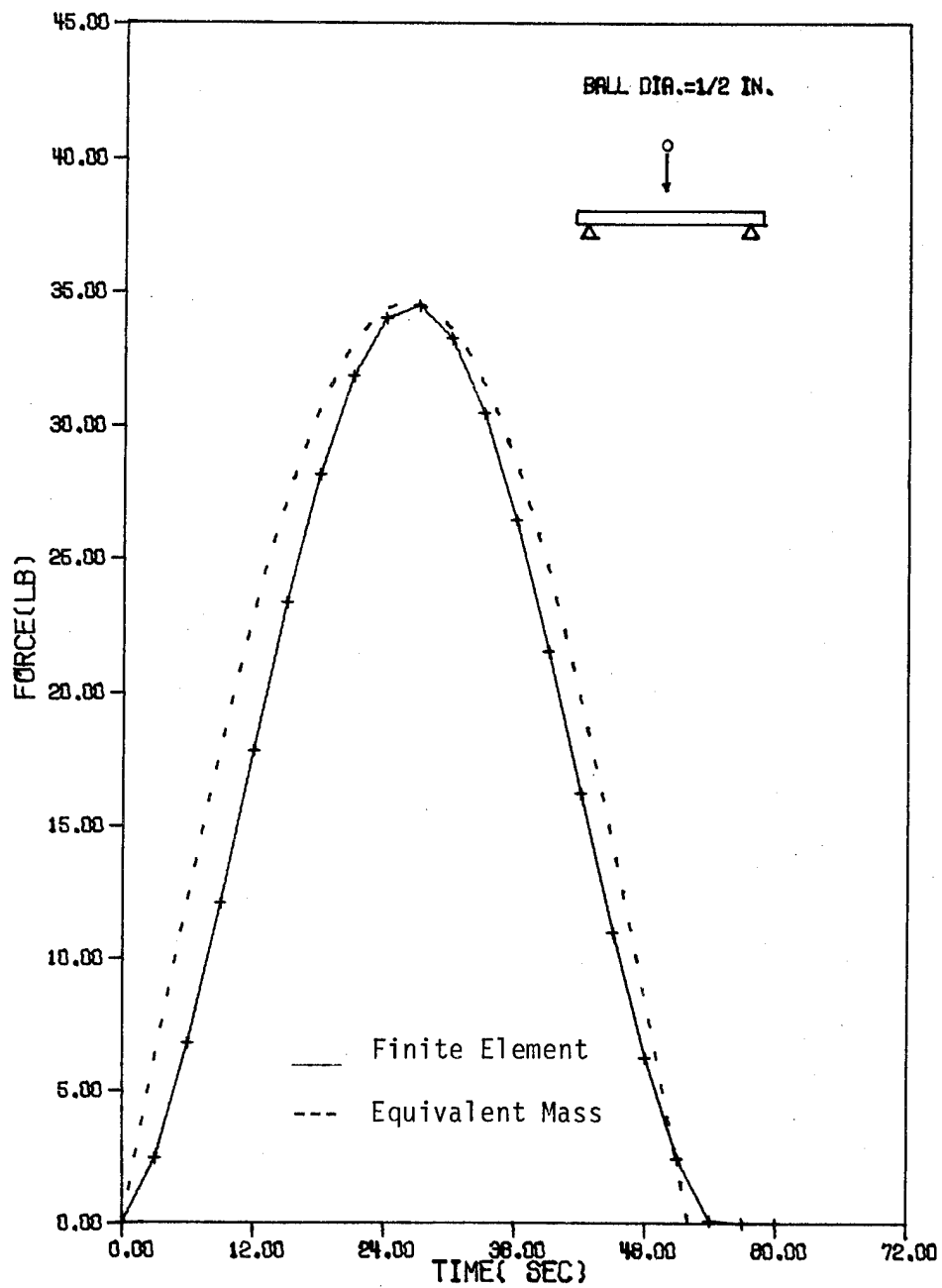


Fig. 4.2. Simply-supported steel beam (0.5"W x 0.5"D x 30"L) subjected to impact of a steel ball at 12 in/sec.

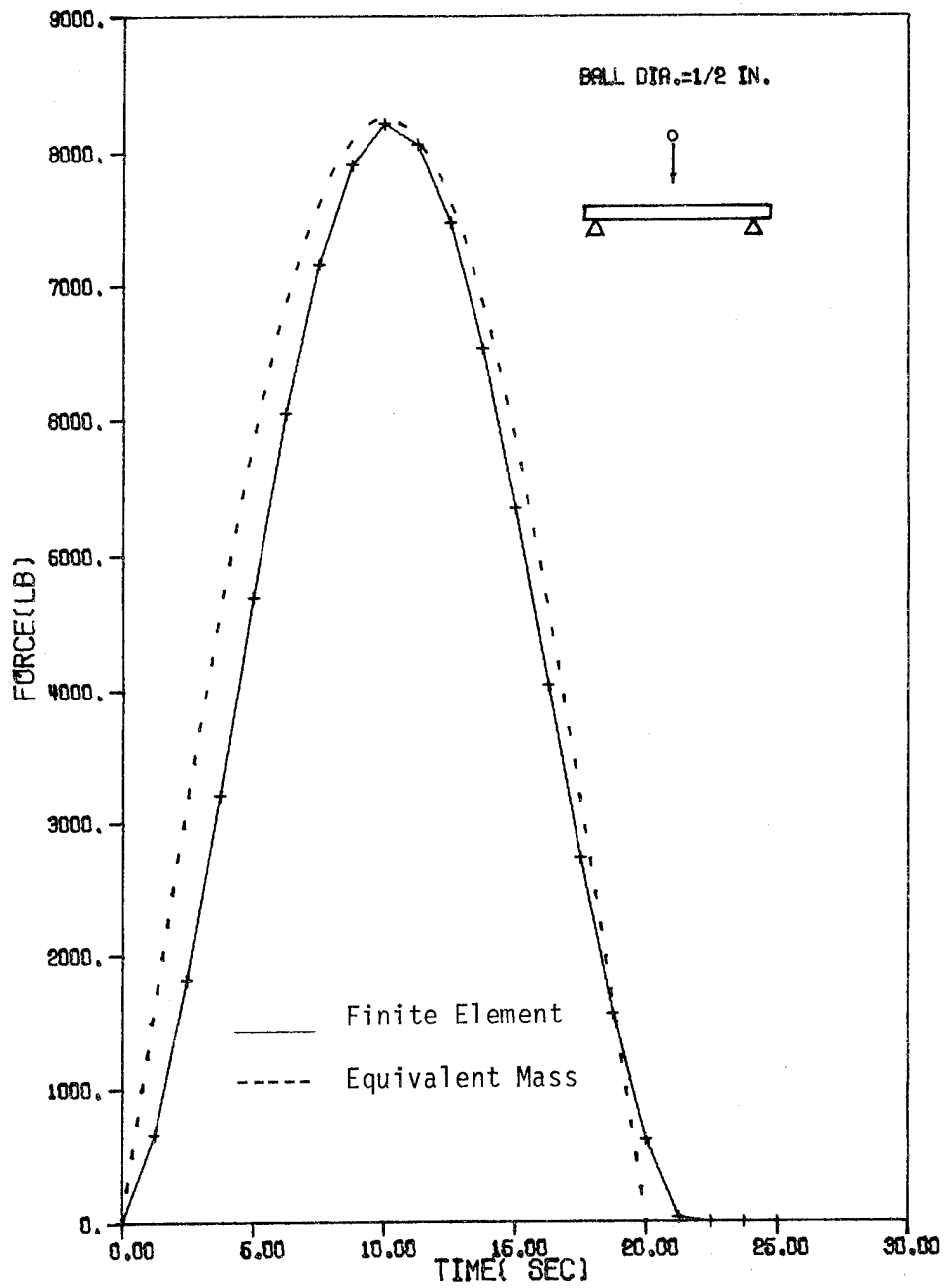


Fig. 4.3 Simply-supported steel beam (0.5"W x 0.5"D x 30"L) subjected to impact of a steel ball at 1200 in/sec.

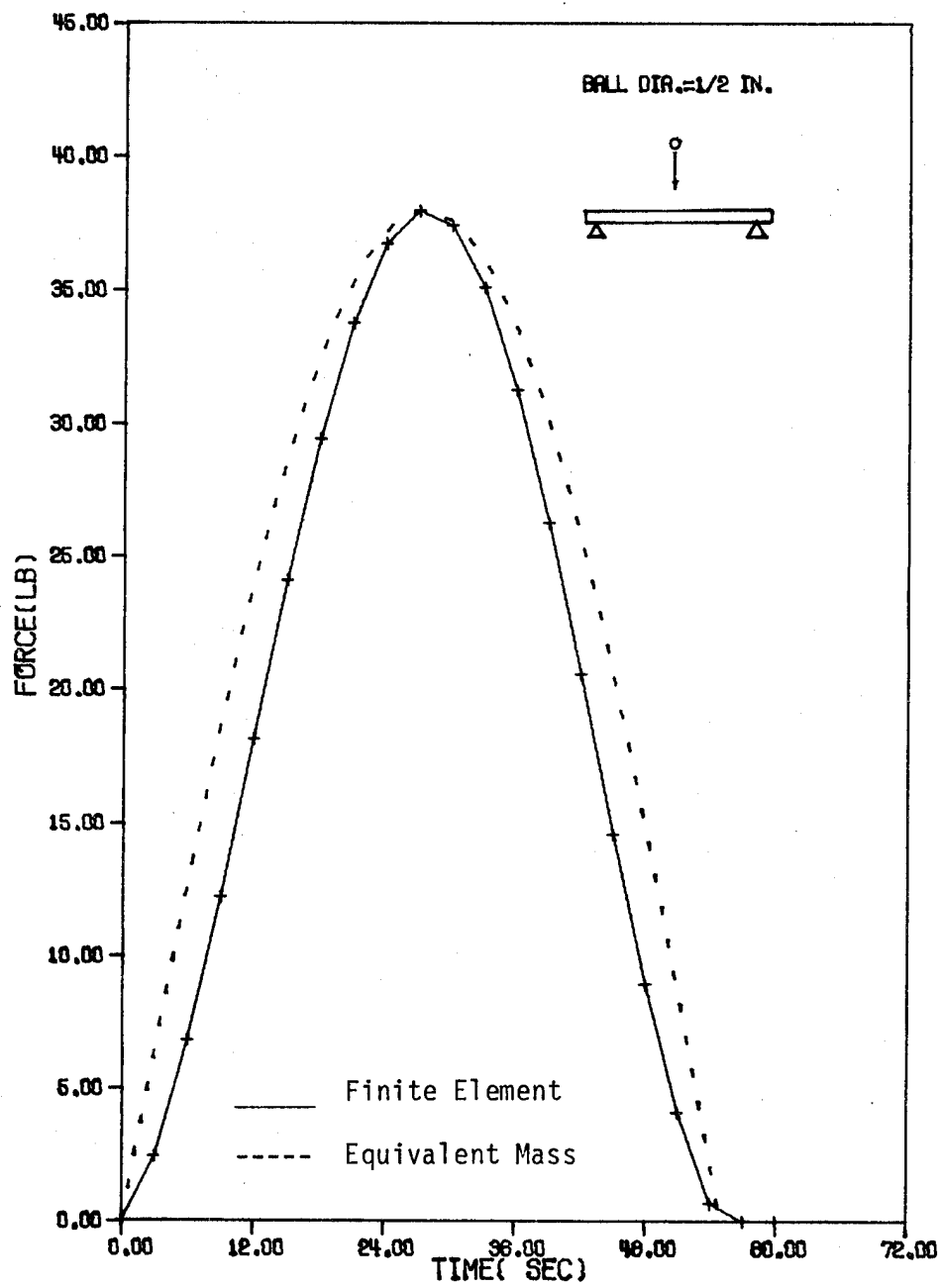


Fig. 4.4 Simply-supported steel beam (0.5"W x 3"D x 30"L) subjected to impact of a steel ball at 12 in/sec.

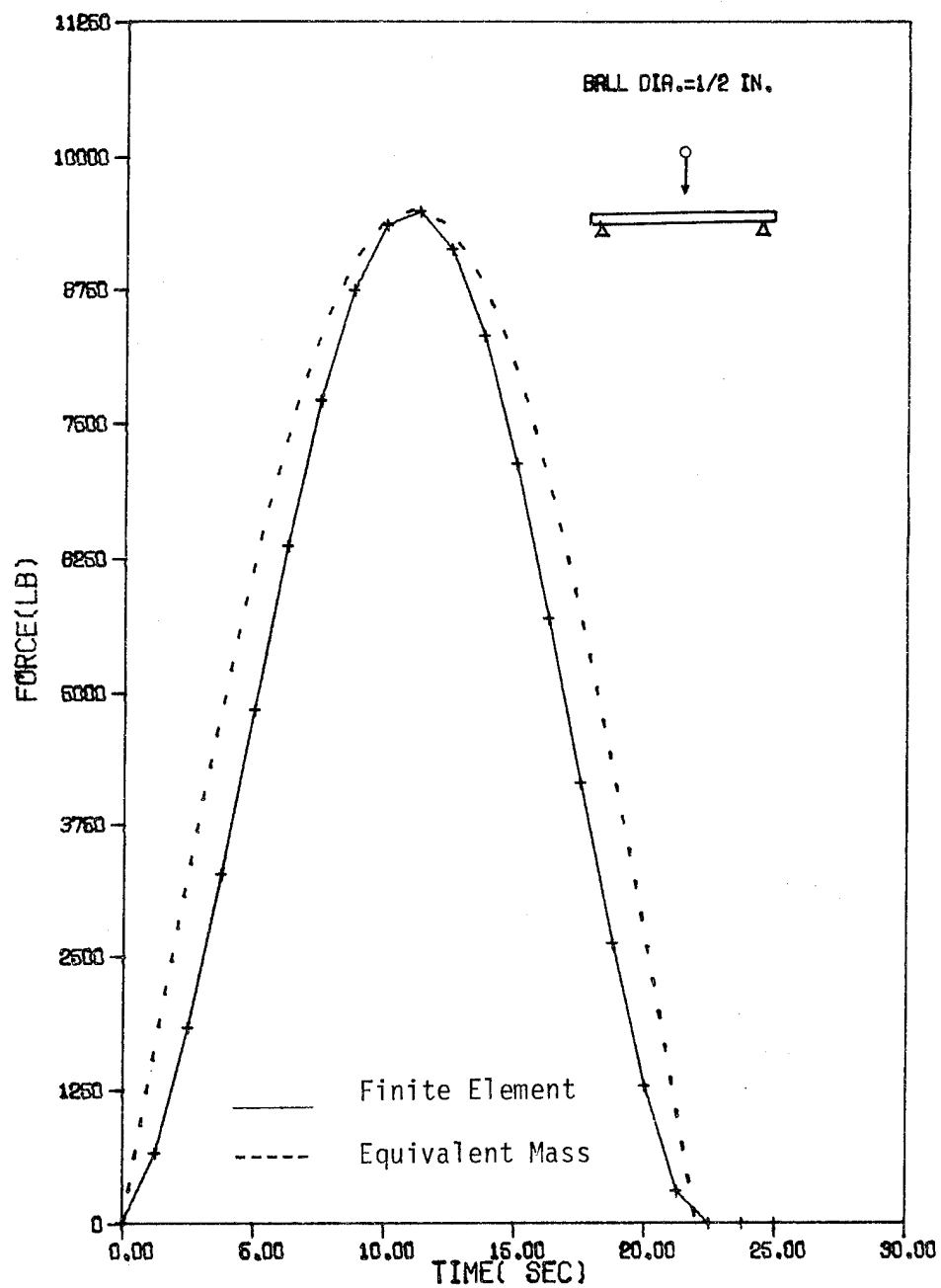


Fig. 4.5 Simply-supported steel beam (0.5"W x 3"D x 30"L) subjected to impact of a steel ball at 1200 in/sec.

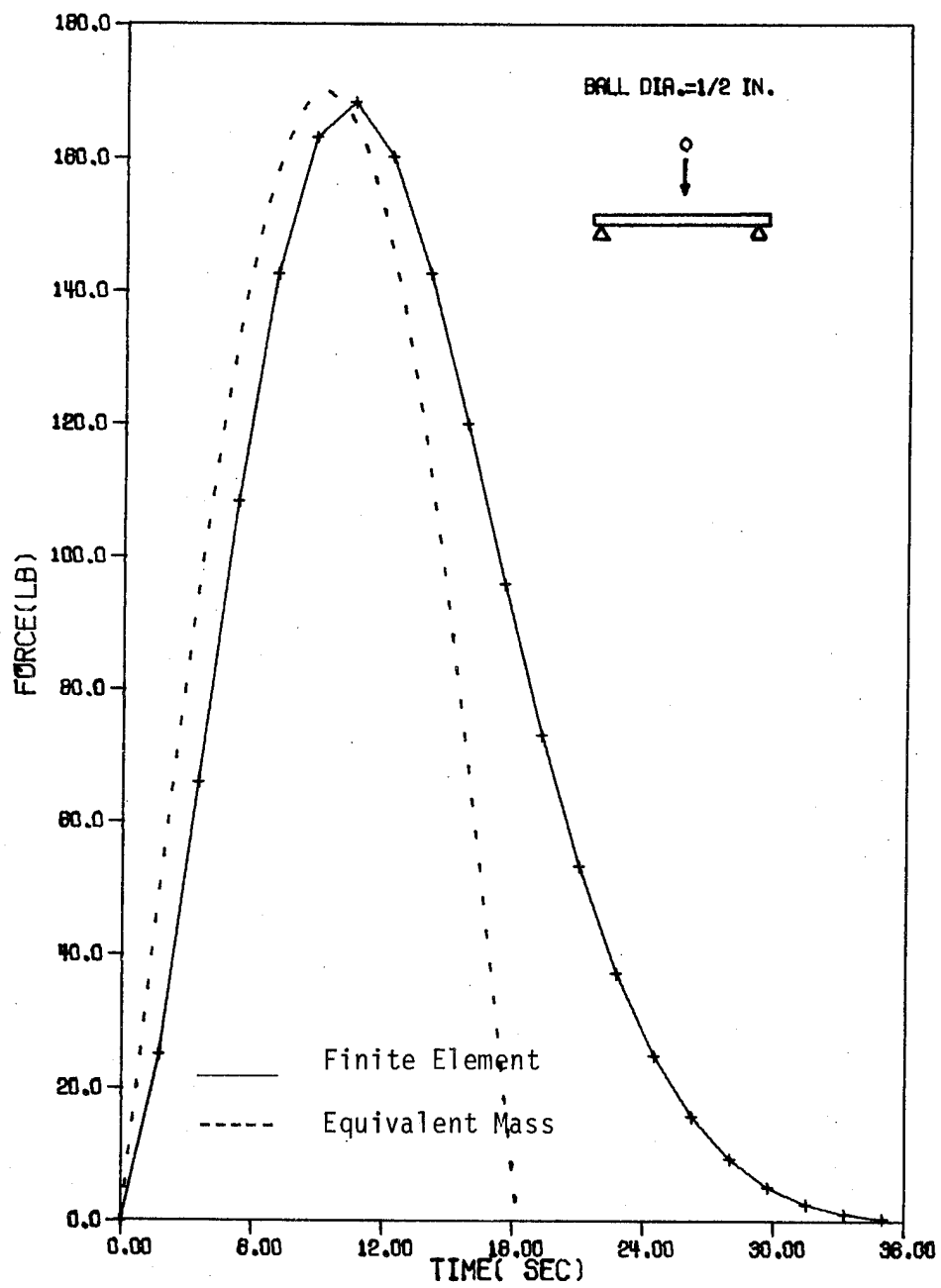


Fig. 4.6 Simply-supported steel beam (0.5"W x 0.08"D x 15"L) subjected to impact of a steel ball at 100 in/sec.

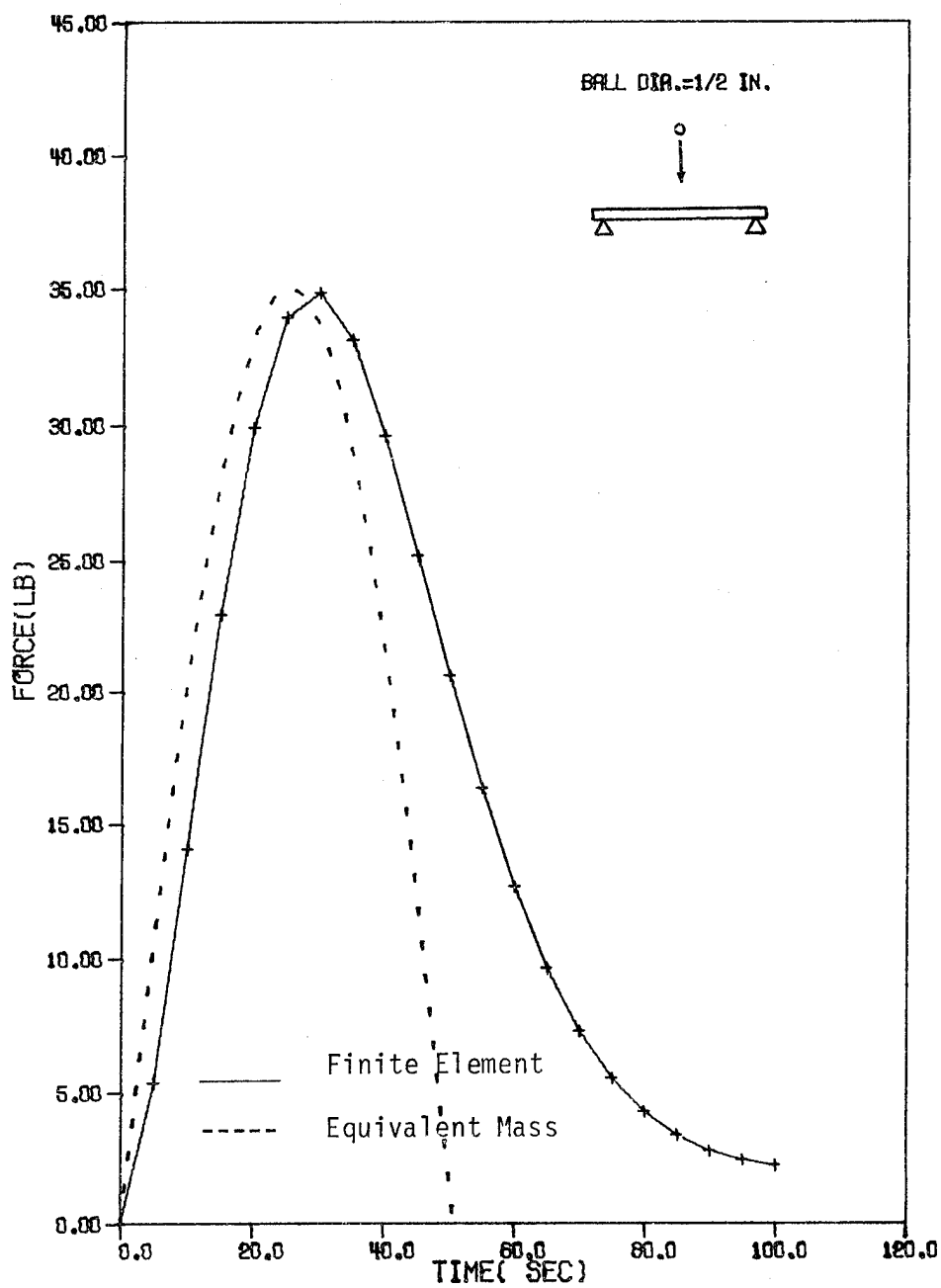


Fig. 4.7 Simply-supported graphite/epoxy beam (0.5"W x 0.08"D x 15"L) subjected to impact of a steel ball at 100 in/sec.

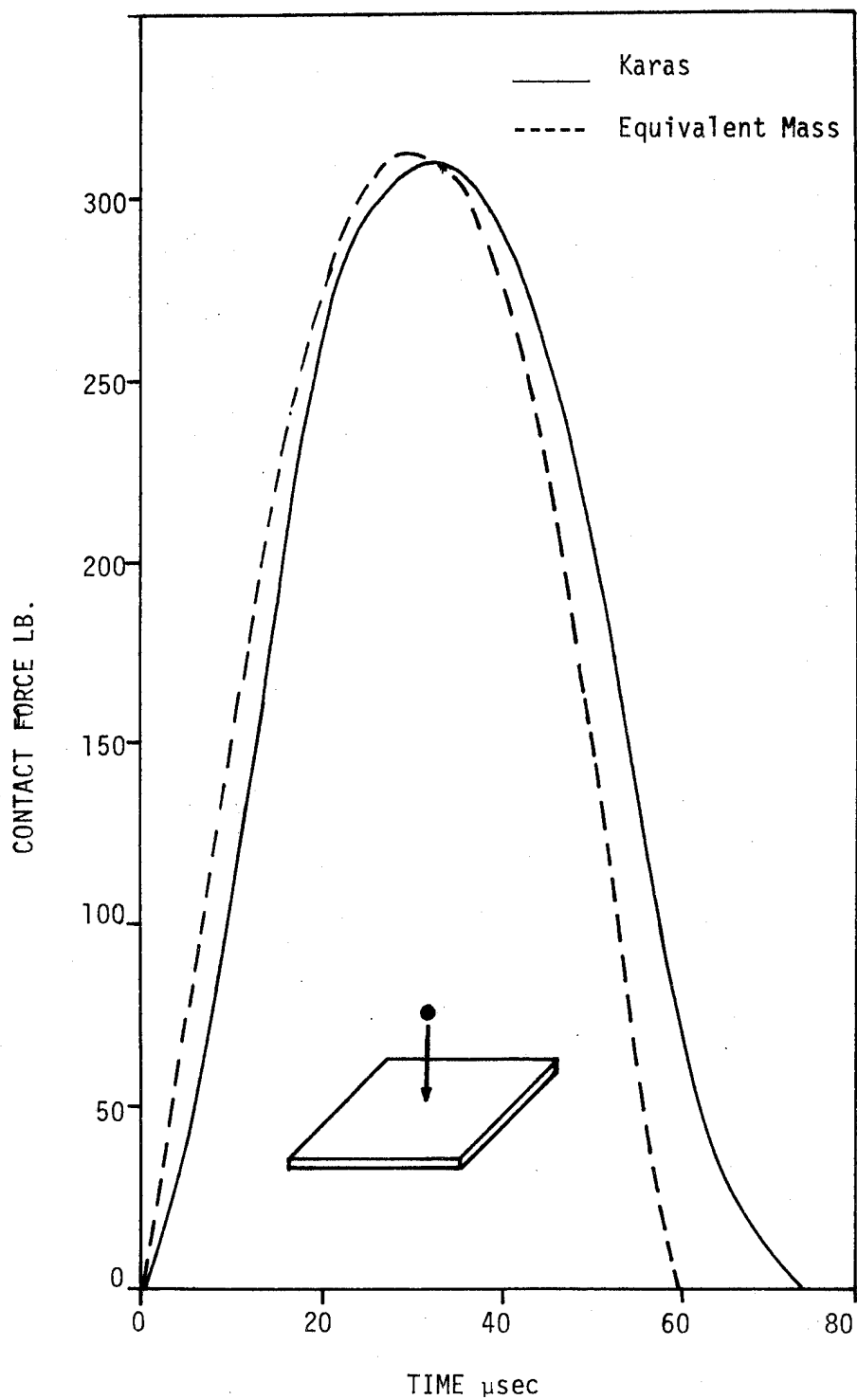


Fig. 4.8 Contact force history for a simply-supported steel plate (20 cm x 20 cm x 0.8 cm) subjected to impact of a steel ball (2 cm diameter) at 100 cm/sec.

5. Conclusions

Static indentation tests have been performed to determine the law of contact between a steel ball and two laminated composites, namely, glass/epoxy and graphite/epoxy. It has been found that the loading path followed very well the power law

$$F = k \alpha^{1.5}$$

where F is the contact force, k is a coefficient, and α is the indentation depth. Tests were conducted with beams clamped at two ends with various spans. The results indicated that the indentation law does not seem to depend on the span between the clamps. The experimental results have also revealed that both composites tested possessed a pronounced inelastic behavior even at very low contact force levels. The unloading paths from various loading points have been obtained experimentally and fitted into a power law for the computational purpose.

An efficient high order beam finite element has been employed together with the classical Hertzian contact law or the measured contact law for analyzing the impact response. The finite element program is capable of computing the contact force, contact duration, and all the dynamic responses in the laminated composite. A simple method for estimating the contact force and duration has been developed and shown to be quite accurate except for very thin beams.

6. References

- [1] Hertz, H., "Über die Berührung fester elastischer Körper", Journal Reine Angle Math (Crelle), Vol. 92, 1881, p. 155.
- [2] Willis, J.R., "Hertzian Contact of Anisotropic Bodies," Journal of Mechanics and Physics of Solids, Vol. 14, 1966, p. 163.
- [3] Sun, C.T., "An Analytical Method for Evaluation of Impact Damage Energy of Laminated Composites," ASTM STP617, 1977, p. 427.
- [4] Barnhart, K.E., and Goldsmith, W., "Stresses in Beams during Transverse Impact," J. Appl. Mech., Vol. 24, 1957, p. 440.
- [5] Sun, C.T., and Huang, S.N., "Transverse Impact Problems by Higher Order Beam Finite Element," Journal of Computers and Structures, Vol. 5, pp. 297-303, 1975.
- [6] Wilson, E.L. and Clough, R.W., "Dynamic Response by Step by Step Matrix Analysis," Symposium on Use of Computers in Civil Engineering, October 1962.
- [7] Timoshenko, S.P., Theory of Elasticity, McGraw-Hill, New York, 1934.
- [8] Goldsmith, W., Impact, Edward Arnold, London, 1960, p. 58.
- [9] Timoshenko, S. "Zür Frage nach der wirkung eines Stosse auf einer Balken," Zaitschrift für Mathematik und Physik, Vol. 62, 1913, pp. 198-209.
- [10] Whitney, J.M., and Pagano, N.J., "Shear Deformation in Heterogeneous Anisotropic Plates," J. Applied Mechanics, Vol. 37, 1970, pp. (031-1036).
- [11] Sun, C.T., and Lai, R.Y.S., "Exact and Approximate Analysis of Transient Wave Propagation in an Anistropic Plate," AIAA Journal, Vol. 12, 1974, pp. 1415-1417.
- [12] Mindlin, R.D., "Influence of Rotary Inertia and Shear on Flexural Vibrations of Isotropic, Elastic Plates," J. Applied Mechanics, Vol. 18, 1951, pp. 31-38.
- [13] Karas, K., "Platten Unter Seitlichem Stoss," Ingenieur-Archiv, Vol. 10, 1939, pp. 237-250.

APPENDIX A

A COMPUTER PROGRAM FOR FINITE ELEMENT ANALYSIS OF THE TRANSVERSE IMPACT
OF A BEAM

The following is a description of the input data required to analyze the transverse impact of a beam. The description is by card sections, and where applicable, the number of cards precedes the name. The arrangement of the cards is shown in Fig. A-1.

1. Heading Card(s) (I2, 10A7)

One card is required for each problem.

Cols. 1-2 Problem number (NPROB)

3-72 Arbitrary problem identification (TITLE)

2. 1-Control Card (9I5)

Cols. 1-5 Number of nodal points (NP)

6-10 Number of elements (NE)

11-15 Number of restrained boundary nodes (NB)

16-20 Number of output printing cycles (NTM)

21-25 Number of material types (NMAT)

For isotropic materials, this number is limited to 24 plus one for the sphere. However, for a laminated composite, this number can only be two.

26-30 Output printing frequency in $\frac{1}{10}$ μ sec (NDIN)

31-35 Beam material type (MATP)

0 - if beam is isotropic

1 - if beam is a laminated composite

36-50 Number of nodal data cards (NDC)

Explained later.

41-45 Control for print of input data (11)

0 - Input printed at beginning of first problem only.

1 - Input printed for each new problem.

Input for the printing scheme outlines the cycle and frequency at which the output is printed. The integer, NTM, indicates how many times output is printed after the sphere makes contact and the integer, NDIN, indicates how much time elapses between printing of the output. In addition, NDIM is measured in tenths of a microsecond. As an example, if one wishes to print output every 5 μ sec for 10 cycles, then NDIN equals 50 (in $\frac{1}{10}$ μ sec) and NTM=10. Observe that (NDON x NTRM)/10 yields the time at which computations stop, in this case its 50 μ sec.

3. 1 - Dimension Card (3F10.0)

Cols. 1-10 Beam thickness (TB)

11-20 Beam width (WB)

21-30 Sphere radius (R)

4. 1 - Nodal Impact Card (I5,2F10.0)

Cols. 1-5 Impacted node (NQ)

6-15 Impact velocity (Q2)

16-25 Time increment (DT)

5. Element Type Material Properties Card (s) (I5,5F10.0)

1 card per material

Cols. 1-5 Material number (IMAT)

6-15 Longitudinal Young's modulus (ORT(N,1))

16-25 Transverse Young's modulus (ORT(N,2))

26-35 Shear modulus (ORT(N,3))

36-45 Poisson's ratio (ORT(N,4))

46-55 Mass density, ρ (ORT(N,5))

The last material card must contain the material properties of the impacting sphere. If the sphere and the beam possess identical material properties, then only one material card (NMAT = 1) is necessary.

6. 1 - Indentation Law Card (E10.3,2F10.0)

Cols. 1-10 Loading coefficient k (STF)

11-20 Permanent deformation α_0 (DISPEM)

21-30 Unloading power q (QP)

If the Hertzian law is used for loading, set STF = 0.0. If elastic unloading is followed, then set DISPEM = 0.0 and the input for QP will be ignored.

7. Nodal Data Card(s) (2I5, 2F10.0, I5)

1 card is required for each set of identical elements.

Cols. 1-5 Beginning node in the set (ND1)

6-10 Final node in the set (ND2)

11-20 x-position of beginning node (X1)

21-30 x-position of final node (X2)

31-35 Element material type of set (IMT)

This input provides information for the automatic element generator in the program. Given the above information for each set of identical elements, the program computes the x-position of each node and assigns each element a material type and the Ith and Jth nodes. The number of these cards is equal to NDC, which is input on the control card.

NOTE: Node 1 must begin at position $x = 0$.

8. Boundary Conditions Card(s) (2I5)

1 card per restrained node

Cols. 1-5 Restrained node (NBC)

6-10 Boundary condition code (NFIIX)

The boundary condition code is an integer containing three digits.

Each digit in the code is either 1-restrained or 0-free. The ones digit controls the curvature, the tens digit controls the slope, and the hundreds digit controls the displacement. As an example, if one node was clamped, then the displacement and slope are zero and the curvature is nonzero, or

$$v = 0 \quad \theta = 0 \quad \kappa \neq 0 \quad \text{therefore} \quad \text{Code 110}$$

NOTE: Boundary conditions may be specified at any node with any code.

8. Number of layers in laminate (15) (MLAYER)

9. Laminate data (15, F5.0, F10.0)

1 card per layer.

Cols. 1-5 Layer number (L)

6-10 Fiber orientation (TH)

11-20 Layer thickness (TK)

If a laminated composite beam is to be examined under impact, two major alterations in the program must be made. This program provides for both, with the proper indication on the control card (MATP = 1). From the laminate data given, an equivalent bending rigidity is computed, or $D_{11} = EI$. In addition, the contact coefficient in the Hertzian Contact Law is also computed differently for composite beams.

NOTE: If an isotropic beam is used, skip Cards 8 and 9.

10. Termination Card

EXAMPLE 1

Consider the impact of a steel sphere on a steel cantilever beam. The dimensions of the beam are 0.5" W x 0.08" D x 15" L and the sphere has a diameter of 0.5" in. The initial velocity of the sphere is 100 in/sec., with the point of impact located at the mid-point. Numerical solutions are to be obtained up to 100 μ sec by using 30 finite elements.

The material constants used in this computation are

$$E = 30 \times 10^6 \text{ psi}, \nu = 0.25 \text{ and } \rho = 0.00880 \text{ slug/in}^3 (0.000733 \text{ lb} \cdot \text{sec}^2/\text{in}^4).$$

Note that the value of ρ in slug should be divided by 12 if length is measured in inches.

The sample inputs and outputs for Example 1 and Example 2 are listed following Fig. A-1. The results for the contact force, the displacement of the sphere and the deflection of the beam at the impact point are shown in Fig. A-2. The displacement profiles of the beam at the impact point are shown in Fig. A-2. The displacement profiles of the beam at various times are presented in Fig. A-3.

EXAMPLE 2

This example is identical to the previous example except that the beam is now a laminated composite which consists of 16 layers of graphite/epoxy composite. The ply-thickness is 0.005" and the lay-up is $(0/90/0/90)_{2s}$. The material constants are

$$E_{11} = 30 \times 10^6 \text{ psi} \quad E_{22} = 0.75 \times 10^6 \text{ psi} \quad G_{12} = 0.4 \times 10^6 \text{ psi}$$

$$\nu_{12} = 0.25 \quad , \quad \rho = 0.00178 \text{ slug/in}^3 (0.000148 \text{ lb} \cdot \text{sec}^2/\text{in}^4)$$

The corresponding results are shown in Figs. A-4 and A-5.

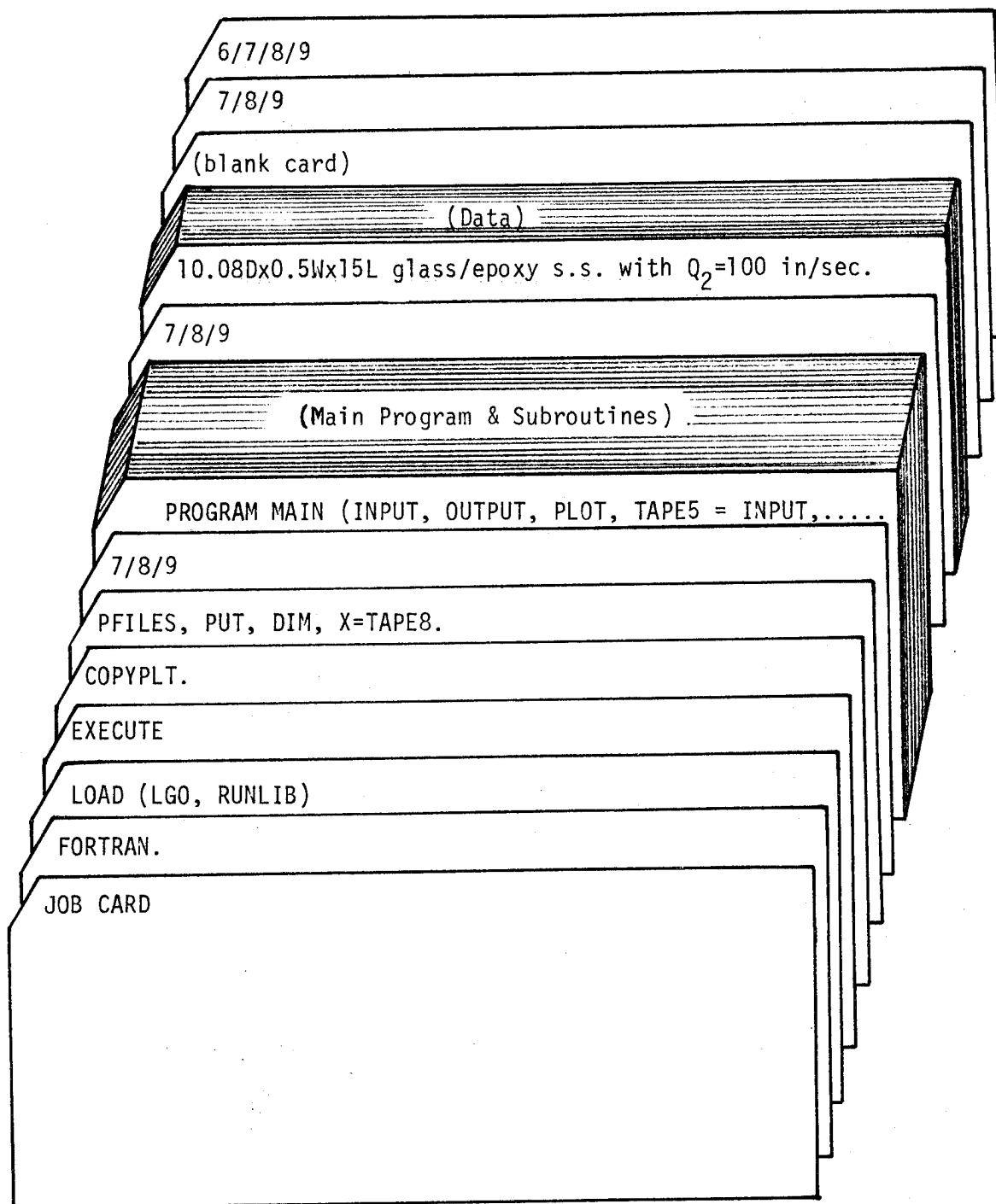


Fig. A-1 Deck set-up

Sample Output for Example 1

1 0.08DX0.5WX15L ISO. CANTILEVER WITH Q2=100 IN/SEC.

NODAL POINTS 31
 ELEMENTS 30
 BOUNDARY CONDITIONS 1
 OUTPUT LIMIT 1000
 DEGREES OF FREEDOM 3
 MATERIALS 1

BEAM THICKNESS .080
 BEAM WIDTH .500
 SPHERE DENSITY .000733
 SPHERE RADIUS .250

IMPACT NODE 16
 IMPACT VELOCITY 100.0
 INTEGRATION TIME INCREMENT(X E-06 SEC) 3.500E-08

MATERIAL PROPERTIES					
MAT. NO.	E1	E2	G12	U12	RHO
1	30000000.0	30000000.0	11500000.0	.300	.000733

PERMANENT DEFORMATION(IN) *.000000

NODAL POINTS		
	X	Y
1	0.000	0.000
2	.500	0.000
3	1.000	0.000
4	1.500	0.000
5	2.000	0.000
6	2.500	0.000
7	3.000	0.000
8	3.500	0.000
9	4.000	0.000
10	4.500	0.000
11	5.000	0.000
12	5.500	0.000
13	6.000	0.000
14	6.500	0.000
15	7.000	0.000
16	7.500	0.000
17	8.000	0.000
18	8.500	0.000
19	9.000	0.000
20	9.500	0.000
21	10.000	0.000
22	10.500	0.000
23	11.000	0.000
24	11.500	0.000
25	12.000	0.000
26	12.500	0.000
27	13.000	0.000
28	13.500	0.000
29	14.000	0.000
30	14.500	0.000
31	15.000	0.000

ELEMENTS	I	J	K		MAT
1	1	2	0	0	1
2	2	3	0	0	1
3	3	4	0	0	1
4	4	5	0	0	1
5	5	6	0	0	1
6	6	7	0	0	1
7	7	8	0	0	1
8	8	9	0	0	1
9	9	10	0	0	1
10	10	11	0	0	1
11	11	12	0	0	1
12	12	13	0	0	1
13	13	14	0	0	1
14	14	15	0	0	1
15	15	16	0	0	1
16	16	17	0	0	1
17	17	18	0	0	1
18	18	19	0	0	1
19	19	20	0	0	1
20	20	21	0	0	1
21	21	22	0	0	1
22	22	23	0	0	1
23	23	24	0	0	1
24	24	25	0	0	1
25	25	26	0	0	1
26	26	27	0	0	1
27	27	28	0	0	1
28	28	29	0	0	1
29	29	30	0	0	1
30	30	31	0	0	1

BOUNDARY CONDITIONS
31 110

PRINTING SCHEME

1. REPORT OUTPUT EVERY 5.00 MSEC
2. TERMINATE OUTPUT AT 100.00 MSEC

TYPICAL STIFNESS MATRIX OF AN ELEMENT

8.777E+04	2.194E+04	5.486E+02	-8.777E+04	2.194E+04	-5.486E+02
2.194E+04	7.022E+03	2.011E+02	-2.194E+04	3.950E+03	-7.314E+01
5.486E+02	2.011E+02	2.743E+01	-5.486E+02	7.314E+01	4.571E+00
-8.777E+04	-2.194E+04	-5.486E+02	8.777E+04	-2.194E+04	5.486E+02
2.194E+04	3.950E+03	7.314E+01	-2.194E+04	7.022E+03	-2.011E+02
-5.486E+02	-7.314E+01	4.571E+00	5.486E+02	-2.011E+02	2.743E+01

TYPICAL MASS MATRIX OF AN ELEMENT

5.743E-06	4.934E-07	1.858E-08	1.587E-06	-2.396E-07	1.197E-08
4.934E-07	5.500E-08	2.281E-09	2.396E-07	-3.517E-08	1.719E-09
1.858E-08	2.281E-09	9.916E-11	1.197E-08	-1.719E-09	8.263E-11
1.587E-06	2.396E-07	1.197E-08	5.743E-06	-4.934E-07	1.858E-08
-2.396E-07	-3.517E-08	-1.719E-09	-4.934E-07	5.500E-08	-2.281E-09
1.197E-08	1.719E-09	8.263E-11	1.858E-08	-2.281E-09	9.916E-11

0.08DX0.5HX15L ISO. CANTILEVER WITH Q2=100 IN/SEC.

TIME ELAPSED(MSEC)	10.500
FORCE(LB)	1.684E+02
MASS DISPLACEMENT(IN)	9.747E-04
MASS VELOCITY(IN/SEC)	7.849E+01
MASS ACCEL. (IN/SEC2)	-3.509E+06
INDENTATION(IN)	6.197E-04

NODE	DISP	STRAIN-XX	STRAIN-YY	STRESS-XX
1	1.670E-11	-9.892E-11	2.968E-11	-2.968E-03
2	-2.051E-11	5.506E-10	-1.652E-10	1.652E-02
3	3.951E-11	-9.258E-10	2.777E-10	-2.777E-02
4	-3.684E-11	3.027E-10	-9.081E-11	9.081E-03
5	-1.222E-10	5.425E-09	-1.628E-09	1.628E-01
6	8.400E-10	-2.698E-08	8.093E-09	-8.093E-01
7	-2.888E-09	8.059E-08	-2.418E-08	2.418E+00
8	6.521E-09	-1.550E-07	4.650E-08	-4.650E+00
9	-6.891E-09	8.597E-08	-2.579E-08	2.579E+00
10	-1.677E-08	6.471E-07	-1.941E-07	1.941E+01
11	1.002E-07	-2.525E-06	7.574E-07	-7.574E+01
12	-1.803E-07	2.561E-06	-7.683E-07	7.683E+01
13	-4.412E-07	1.034E-05	-3.101E-06	3.101E+02
14	-3.972E-07	2.215E-05	-6.645E-06	6.645E+02
15	-3.358E-05	1.188E-04	-3.565E-05	3.565E+03
16	3.578E-04	-7.110E-04	2.133E-04	-2.133E+04
17	-3.358E-05	1.188E-04	-3.565E-05	3.565E+03
18	-3.972E-07	2.215E-05	-6.645E-06	6.645E+02
19	-4.412E-07	1.034E-05	-3.101E-06	3.101E+02
20	-1.803E-07	2.561E-06	-7.683E-07	7.683E+01
21	1.002E-07	-2.525E-06	7.574E-07	-7.574E+01
22	-1.677E-08	6.471E-07	-1.941E-07	1.941E+01
23	-6.891E-09	8.597E-08	-2.579E-08	2.579E+00
24	6.521E-09	-1.550E-07	4.650E-08	-4.650E+00
25	-2.888E-09	8.059E-08	-2.418E-08	2.418E+00
26	8.400E-10	-2.698E-08	8.093E-09	-8.093E-01
27	-1.221E-10	5.424E-09	-1.627E-09	1.627E-01
28	-3.697E-11	3.067E-10	-9.201E-11	9.201E-03
29	3.985E-11	-9.352E-10	2.806E-10	-2.806E-02
30	-2.116E-11	5.698E-10	-1.709E-10	1.709E-02
31	1.306E-21	-2.755E-10	8.264E-11	-8.264E-03

0.08DX0.5WX15L ISO. CANTILEVER WITH Q2=100 IN/SEC.

TIME ELAPSED(MSEC)	35.000
FORCE(LB)	3.223E-01
MASS DISPLACEMENT(IN)	2.332E-03
MASS VELOCITY(IN/SEC)	4.839E+01
MASS ACCEL.(IN/SEC2)	-6.718E+03
INDENTATION(IN)	1.139E-05

NODE	DISP	STRAIN-XX	STRAIN-YY	STRESS-XX
1	-1.639E-08	1.939E-07	-5.817E-08	5.817E+00
2	-4.074E-08	1.315E-06	-3.944E-07	3.944E+01
3	1.731E-07	-3.163E-06	9.490E-07	-9.490E+01
4	8.057E-08	-1.543E-06	4.630E-07	-4.630E+01
5	-1.623E-07	1.457E-06	-4.371E-07	4.371E+01
6	-5.161E-07	6.356E-06	-1.907E-06	1.907E+02
7	-8.232E-07	8.349E-06	-2.505E-06	2.505E+02
8	-1.621E-06	1.321E-05	-3.964E-06	3.964E+02
9	-3.188E-06	1.493E-05	-4.478E-06	4.478E+02
10	-1.613E-07	-1.602E-05	4.806E-06	-4.806E+02
11	2.248E-05	-5.990E-05	1.797E-05	-1.797E+03
12	-4.545E-05	1.443E-04	-4.329E-05	4.329E+03
13	9.286E-05	-2.545E-04	7.636E-05	-7.636E+03
14	-3.946E-04	4.636E-04	-1.391E-04	1.391E+04
15	1.079E-03	-6.524E-05	1.957E-05	-1.957E+03
16	2.322E-03	-4.584E-04	1.375E-04	-1.375E+04
17	1.079E-03	-6.524E-05	1.957E-05	-1.957E+03
18	-3.946E-04	4.636E-04	-1.391E-04	1.391E+04
19	9.286E-05	-2.545E-04	7.636E-05	-7.636E+03
20	-4.545E-05	1.443E-04	-4.329E-05	4.329E+03
21	2.248E-05	-5.990E-05	1.797E-05	-1.797E+03
22	-1.612E-07	-1.602E-05	4.807E-06	-4.807E+02
23	-3.188E-06	1.493E-05	-4.478E-06	4.478E+02
24	-1.621E-06	1.322E-05	-3.966E-06	3.966E+02
25	-8.225E-07	8.333E-06	-2.500E-06	2.500E+02
26	-5.171E-07	6.379E-06	-1.914E-06	1.914E+02
27	-1.620E-07	1.454E-06	-4.362E-07	4.362E+01
28	8.263E-08	-1.598E-06	4.793E-07	-4.793E+01
29	1.684E-07	-3.057E-06	9.171E-07	-9.171E+01
30	-3.759E-08	1.254E-06	-3.762E-07	3.762E+01
31	-2.132E-18	5.192E-08	-1.558E-08	1.558E+00

Sample Output for Example 2

1 0.08DX0.5WX15L COMP. CANTILEVER WITH Q2=100 IN/SEC

NODAL POINTS 31
 ELEMENTS 30
 BOUNDARY CONDITIONS 1
 OUTPUT LIMIT 1000
 DEGREES OF FREEDOM 3
 MATERIALS 2

BEAM THICKNESS .080
 BEAM WIDTH .500
 SPHERE DENSITY .000733
 SPHERE RADIUS .250

IMPACT NODE 16
 IMPACT VELOCITY 100.0
 INTEGRATION TIME INCREMENT(X E-06 SEC) 1.000E-07

MATERIAL PROPERTIES					
MAT. NO.	E1	E2	G12	U12	RHO
1	30000000.0	750000.0	400000.0	.250	.000148
2	30000000.0	30000000.0	11500000.0	.300	.000733

PERMANENT DEFORMATION(IN) *.000000

ABD MATRIX

1.232E+06	1.502E+04	-5.912E-39	-2.910E-11	3.183E-12	-9.788E-55
1.502E+04	1.232E+06	-1.994E-09	3.183E-12	3.402E-10	-4.653E-25
-5.912E-39	-1.994E-09	3.200E+04	-9.788E-55	-4.653E-25	4.547E-12
-2.910E-11	3.183E-12	-9.788E-55	7.742E+02	8.013E+00	-2.562E-42
3.183E-12	3.402E-10	-4.653E-25	8.013E+00	5.398E+02	-8.639E-13
-9.788E-55	-4.653E-25	4.547E-12	-2.562E-42	-8.639E-13	1.707E+01

NODAL POINTS

	X	Y
1	0.000	0.000
2	.500	0.000
3	1.000	0.000
4	1.500	0.000
5	2.000	0.000
6	2.500	0.000
7	3.000	0.000
8	3.500	0.000
9	4.000	0.000
10	4.500	0.000
11	5.000	0.000
12	5.500	0.000
13	6.000	0.000
14	6.500	0.000
15	7.000	0.000
16	7.500	0.000
17	8.000	0.000
18	8.500	0.000
19	9.000	0.000
20	9.500	0.000
21	10.000	0.000
22	10.500	0.000
23	11.000	0.000
24	11.500	0.000
25	12.000	0.000
26	12.500	0.000
27	13.000	0.000
28	13.500	0.000
29	14.000	0.000
30	14.500	0.000
31	15.000	0.000

ELEMENTS	I	J	K	MAT	
1	1	2	0	0	1
2	2	3	0	0	1
3	3	4	0	0	1
4	4	5	0	0	1
5	5	6	0	0	1
6	6	7	0	0	1
7	7	8	0	0	1
8	8	9	0	0	1
9	9	10	0	0	1
10	10	11	0	0	1
11	11	12	0	0	1
12	12	13	0	0	1
13	13	14	0	0	1
14	14	15	0	0	1
15	15	16	0	0	1
16	16	17	0	0	1
17	17	18	0	0	1
18	18	19	0	0	1
19	19	20	0	0	1
20	20	21	0	0	1
21	21	22	0	0	1
22	22	23	0	0	1
23	23	24	0	0	1
24	24	25	0	0	1
25	25	26	0	0	1
26	26	27	0	0	1
27	27	28	0	0	1
28	28	29	0	0	1
29	29	30	0	0	1
30	30	31	0	0	1

BOUNDARY CONDITIONS

31 110

PRINTING SCHEME

1. REPORT OUTPUT EVERY 5.00 MSEC
2. TERMINATE OUTPUT AT 100.00 MSEC

TYPICAL STIFFNESS MATRIX OF AN ELEMENT

1.062E+05	2.654E+04	6.636E+02	-1.062E+05	2.654E+04	-6.636E+02
2.654E+04	8.494E+03	2.433E+02	-2.654E+04	4.778E+03	-8.848E+01
6.636E+02	2.433E+02	3.318E+01	-6.636E+02	8.848E+01	5.530E+00
-1.062E+05	-2.654E+04	-6.636E+02	1.062E+05	-2.654E+04	6.636E+02
2.654E+04	4.778E+03	8.848E+01	-2.654E+04	8.494E+03	-2.433E+02
-6.636E+02	-8.848E+01	5.530E+00	6.636E+02	-2.433E+02	3.318E+01

TYPICAL MASS MATRIX OF AN ELEMENT

1.160E-06	9.963E-08	3.751E-09	3.203E-07	-4.837E-08	2.416E-09
9.963E-08	1.111E-08	4.605E-10	4.837E-08	-7.101E-09	3.470E-10
3.751E-09	4.605E-10	2.002E-11	2.416E-09	-3.470E-10	1.668E-11
3.203E-07	4.837E-08	2.416E-09	1.160E-06	-9.963E-08	3.751E-09
-4.837E-08	-7.101E-09	-3.470E-10	-9.963E-08	1.111E-08	-4.605E-10
2.416E-09	3.470E-10	1.668E-11	3.751E-09	-4.605E-10	2.002E-11

0.08DX0.5WX15L COMP. CANTILEVER WITH Q2=100 IN/SEC

TIME ELAPSED(MSEC)	20.000
FORCE(LB)	2.989E+01
MASS DISPLACEMENT(IN)	1.963E-03
MASS VELOCITY(IN/SEC)	9.407E+01
MASS ACCEL.(IN/SEC2)	-6.230E+05
INDENTATION(IN)	1.557E-03

NODE	DISP	STRAIN-XX	STRAIN-YY	STRESS-XX
1	4.354E-09	-1.203E-08	3.008E-09	-3.610E-01
2	1.211E-09	-1.140E-08	2.850E-09	-3.420E-01
3	1.594E-09	-1.941E-08	4.853E-09	-5.824E-01
4	4.063E-09	-5.353E-08	1.338E-08	-1.606E+00
5	1.002E-08	-1.048E-07	2.619E-08	-3.143E+00
6	2.165E-08	-1.112E-07	2.780E-08	-3.336E+00
7	2.325E-08	-4.028E-08	1.007E-08	-1.209E+00
8	-7.712E-08	3.099E-07	-7.748E-08	9.297E+00
9	-2.602E-08	-1.633E-07	4.081E-08	-4.898E+00
10	3.666E-07	-2.982E-07	7.454E-08	-8.945E+00
11	-1.191E-06	8.802E-07	-2.201E-07	2.641E+01
12	2.941E-06	-8.390E-08	2.098E-08	-2.517E+00
13	-1.862E-06	-9.902E-06	2.476E-06	-2.971E+02
14	-3.526E-05	3.434E-05	-8.586E-06	1.030E+03
15	1.289E-04	3.957E-05	-9.892E-06	1.187E+03
16	4.115E-04	-1.934E-04	4.835E-05	-5.802E+03
17	1.289E-04	3.957E-05	-9.892E-06	1.187E+03
18	-3.526E-05	3.434E-05	-8.586E-06	1.030E+03
19	-1.862E-06	-9.902E-06	2.476E-06	-2.971E+02
20	2.941E-06	-8.370E-08	2.092E-08	-2.511E+00
21	-1.191E-06	8.798E-07	-2.199E-07	2.639E+01
22	3.666E-07	-2.978E-07	7.446E-08	-8.935E+00
23	-2.603E-08	-1.629E-07	4.073E-08	-4.888E+00
24	-7.707E-08	3.088E-07	-7.721E-08	9.265E+00
25	2.321E-08	-3.940E-08	9.850E-09	-1.182E+00
26	2.164E-08	-1.112E-07	2.779E-08	-3.335E+00
27	1.003E-08	-1.050E-07	2.624E-08	-3.149E+00
28	4.071E-09	-5.328E-08	1.332E-08	-1.599E+00
29	1.696E-09	-2.162E-08	5.406E-09	-6.487E-01
30	1.136E-09	-9.681E-09	2.420E-09	-2.904E-01
31	2.507E-18	-3.823E-08	9.556E-09	-1.147E+00

0.08DX0.5WX15L COMP. CANTILEVER WITH Q2=100 IN/SEC :

TIME ELAPSED(MSEC)	90.000
FORCE(LB)	2.785E+00
MASS DISPLACEMENT(IN)	7.288E-03
MASS VELOCITY(IN/SEC)	6.770E+01
MASS ACCEL.(IN/SEC ²)	-5.805E+04
INDENTATION(IN)	3.264E-04

NODE	DISP	STRAIN-XX	STRAIN-YY	STRESS-XX
1	3.708E-05	-2.198E-08	5.496E-09	-6.595E-01
2	-3.087E-05	2.453E-05	-6.132E-06	7.358E+02
3	2.007E-05	-1.937E-06	4.844E-07	-5.812E+01
4	5.413E-05	-3.431E-05	8.577E-06	-1.029E+03
5	-7.656E-05	1.602E-05	-4.004E-06	4.805E+02
6	-1.137E-04	5.467E-05	-1.367E-05	1.640E+03
7	1.365E-04	-3.582E-06	8.954E-07	-1.074E+02
8	3.434E-04	-9.696E-05	2.424E-05	-2.909E+03
9	5.487E-06	-7.986E-05	1.996E-05	-2.396E+03
10	-7.572E-04	6.927E-05	-1.732E-05	2.078E+03
11	-1.100E-03	1.993E-04	-4.982E-05	5.978E+03
12	-2.664E-04	1.998E-04	-4.995E-05	5.994E+03
13	1.748E-03	7.519E-05	-1.880E-05	2.256E+03
14	4.217E-03	-8.072E-05	2.018E-05	-2.422E+03
15	6.202E-03	-1.999E-04	4.998E-05	-5.998E+03
16	6.969E-03	-2.614E-04	6.536E-05	-7.843E+03
17	6.202E-03	-1.999E-04	4.998E-05	-5.998E+03
18	4.217E-03	-8.072E-05	2.018E-05	-2.422E+03
19	1.748E-03	7.519E-05	-1.880E-05	2.256E+03
20	-2.664E-04	1.998E-04	-4.995E-05	5.994E+03
21	-1.100E-03	1.993E-04	-4.982E-05	5.978E+03
22	-7.572E-04	6.927E-05	-1.732E-05	2.078E+03
23	5.487E-06	-7.986E-05	1.997E-05	-2.396E+03
24	3.434E-04	-9.696E-05	2.424E-05	-2.909E+03
25	1.365E-04	-3.579E-06	8.949E-07	-1.074E+02
26	-1.137E-04	5.467E-05	-1.367E-05	1.640E+03
27	-7.654E-05	1.603E-05	-4.007E-06	4.808E+02
28	5.425E-05	-3.428E-05	8.571E-06	-1.029E+03
29	2.033E-05	-2.156E-06	5.389E-07	-6.467E+01
30	-3.311E-05	2.110E-05	-5.275E-06	6.330E+02
31	-3.552E-15	-3.097E-05	7.743E-06	-9.291E+02

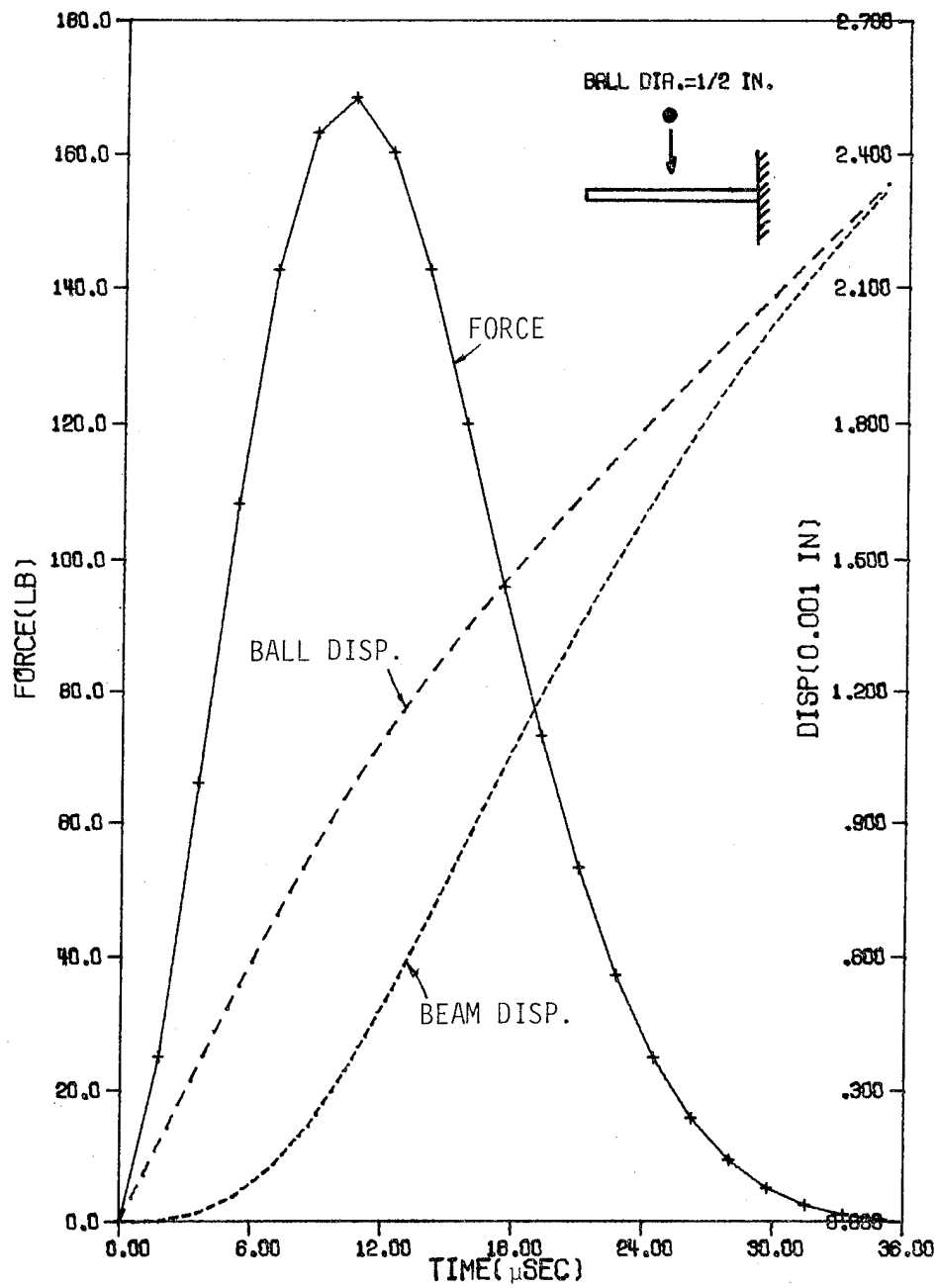


Fig. A-2 Response of a cantilever steel beam (0.5"W x 0.08"D x 15"L) subjected to impact of a steel ball at 100 in./sec.

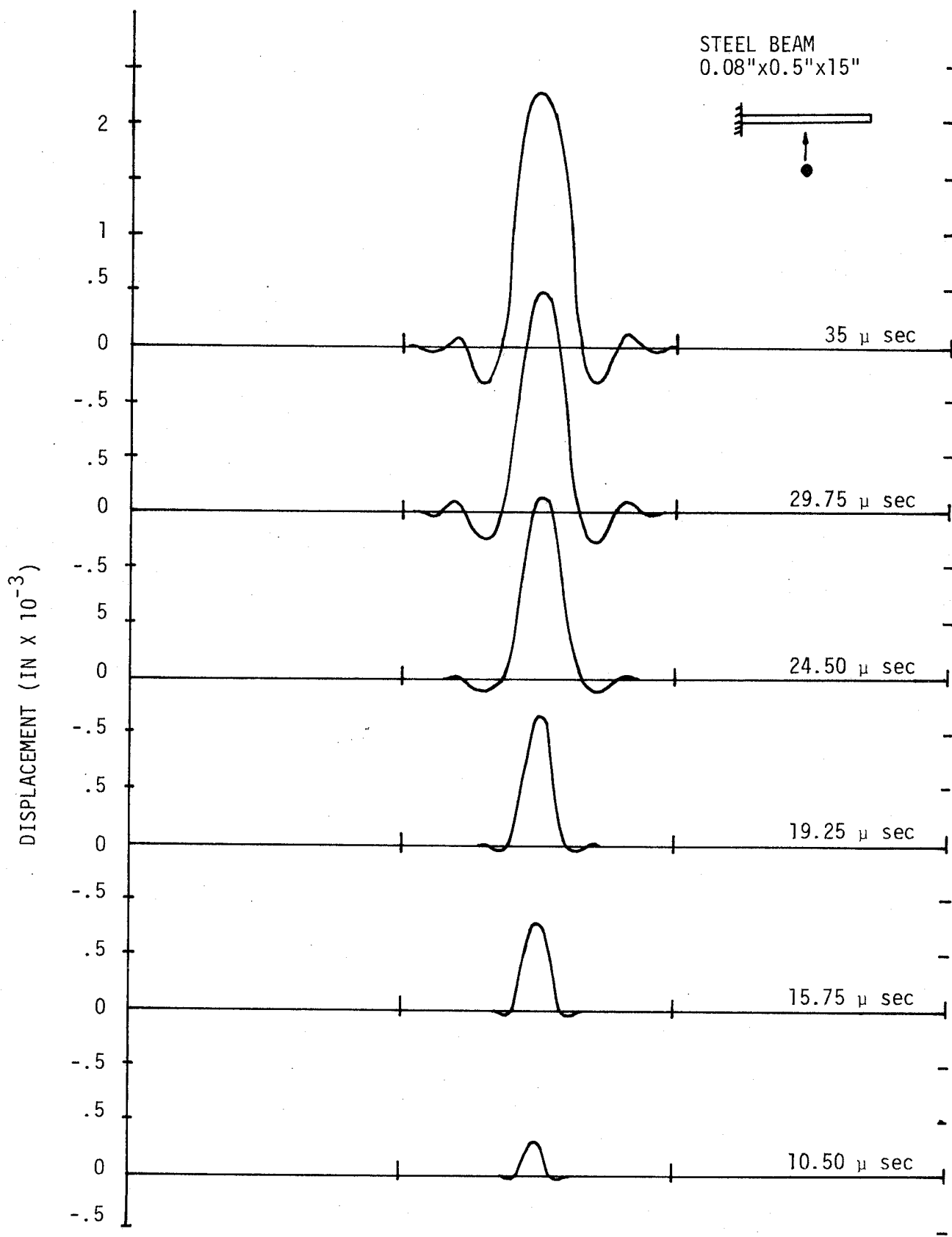


Fig. A-3 Displacement profiles at various times after impact of the steel beam.

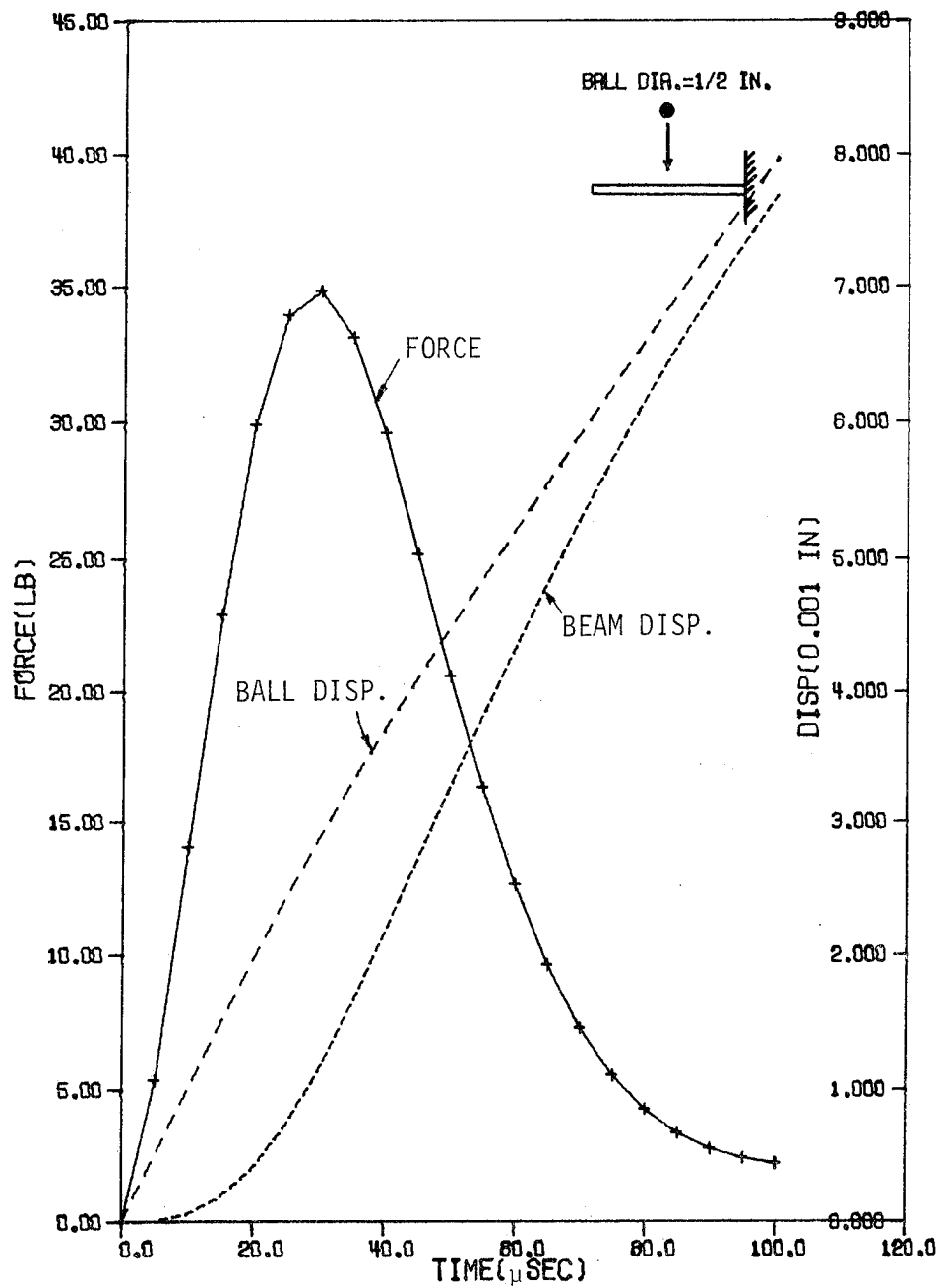


Fig. A-4 Response of a cantilever graphite/epoxy beam (0.5"W x 0.08"D x 15"L) subjected to impact of a steel ball at 100 in./sec.

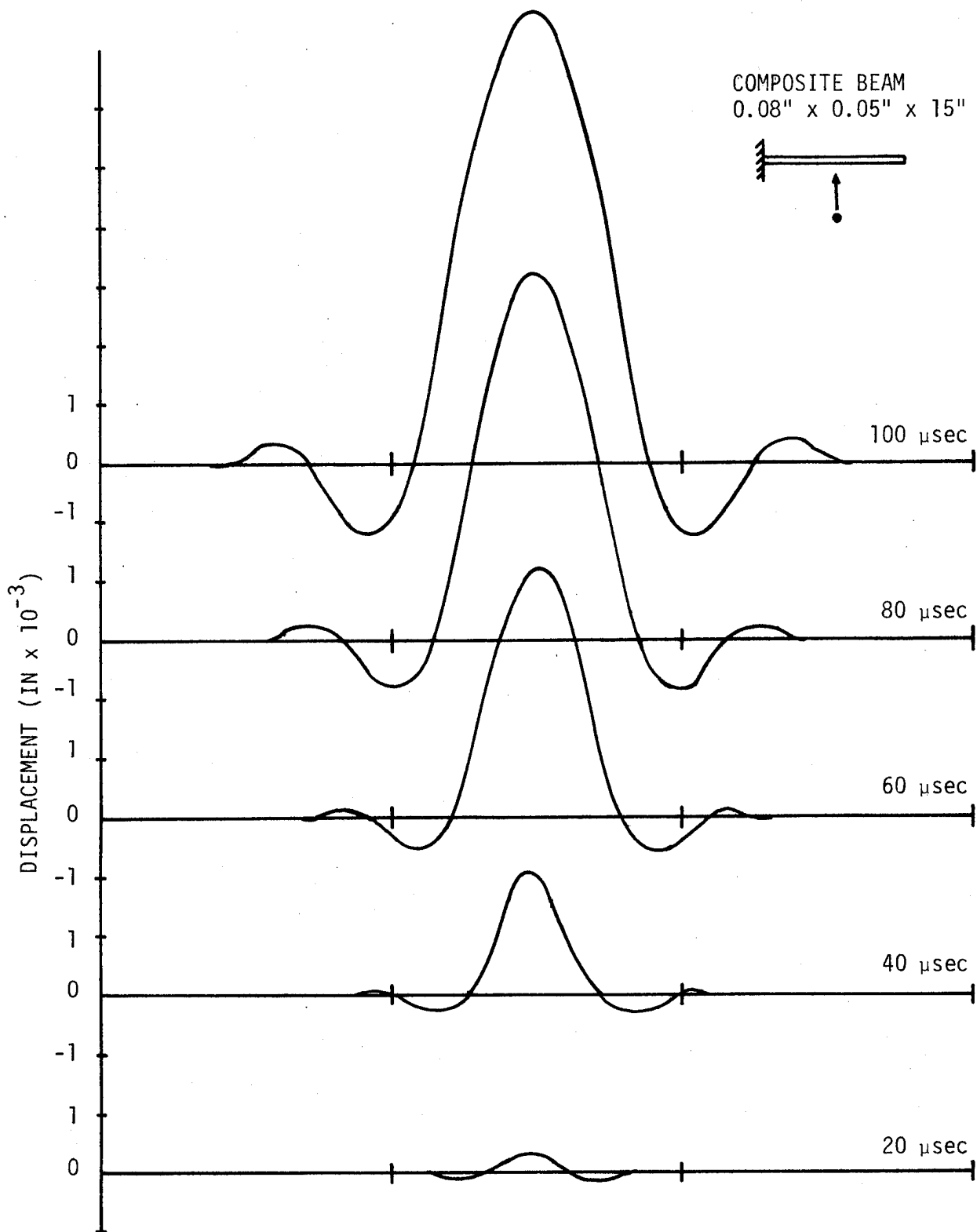


Fig. A-5 Displacement profiles at various times after impact of the composite beam.

Listing of Program

```

PROGRAM MAIN (INPUT,OUTPUT,PLOT,TAPES=INPUT,TAPES=OUTPUT,TAPE11,TA
1PE8)
C
C
C
CONTROL MAIN PROGRAM
C
COMMON /CONTR/ TITLE(7),NP,NE,NB,NDF,NCN,NLD,NMAT,NSZF,LI,NT4,NDIN
1,MATP,NPROB
COMMON /TIME/ T,DT,DDT,TAU,KCON,KCNT
COMMON /DISP/ Q1,Q2,Q3,Q10,Q20,Q30
COMMON /DIMB/ TB,WB,PB,NQ,D11
COMMON /SPHERE/ STF,R,CABU(10),QKONST(10)
COMMON /PLASTIC/ DISPEM,NDISPEM,FORSPM,DISPM,QP
COMMON CORD(100,2),NDP(200,4),IMAT(200),ORT(25,5),NBC(25),NFIX(25)
1,R1(200),R2(200),R3(200),R10(200),R20(200),R30(200),FORS(200),SM(2
200,15),SK(200,15),ISP(200,15),SMPEM(200,15),ESTIF(12,12),EMASS(12,
312),NFIKK(25)
COMMON /COMP/ QBR(3,3,25),ABD(6,6),TH(25),ZK(25),MLAYER
COMMON /PLOT/ NN,TT(25),FF(25),W(25),V(25)
C
C
C
INITIALIZE TAPE NO.
AND NUMBER OF CORNER NODE MAX.
C
C
C
NT4=11
NCN=2
NN=1
C
C
C
PROBLEM IDENTIFICATION
C
CALL PLOTS
101 READ (5,108) NPROB,(TITLE(I),I=1,7)
IF (NPROB.EQ.0) GO TO 105
DO 102 KG=1,200
R10(KG)=0.
R20(KG)=0.
R30(KG)=0.
102 R3(KG)=0.
C
C
C
READ INPUT GEOMETRY AND PROPERTIES
C
CALL GDATA
NDISPEM=0
T=0.
TAU=2.
KCON=0
DDT=DT*DT
C
C
C
LOOP ON NO OF PROBLEMS
C
REWIND NT4
NSZF=NP*NDF
CALL FORMK
CALL FORMM
DO 103 LI=1,NLD
KCNT=1
C
C
C
READ LOADS
C
CALL LOAD
C
C
C
FORM THEN SOLVE SIMULTANEOUS EQUATIONS
C
CALL HMTQ
CALL SOLVE
CALL INTEGTR
C
C
C
ITERATION 2
C
KCNT=2
CALL LOAD
CALL HMTQ

```

	CALL SOLVE	A	72
	CALL INTEGTR	A	73
	T=T+DT	A	74
	IF (T.GT.100.E-6) GO TO 104	A	75
	IF (LI.EQ.10000) GO TO 104	A	76
103	CONTINUE	A	77
104	WRITE (6,106)	A	78
	WRITE (6,107) ((TT(I),FF(I),W(I),U(I)),I=1,NN)	A	79
	WRITE (8,107) ((TT(I),FF(I),W(I),U(I)),I=1,NN)	A	80
	CALL FACTOR (0.8)	A	81
	CALL PLOT (0.0,2.0,3)	A	82
	CALL SCALE (TT,6.0,21,1)	A	83
	CALL SCALE (FF,9.0,21,1)	A	84
	CALL SCALES (9.0,W,21,1,U,21,1)	A	85
C		A	86
C	W(22)=U(22)=TT(22)=FF(22)=0.0	A	87
C	TT(23)=20.	A	88
C	FF(23)=20.	A	89
C	W(23)=U(23)=0.001	A	90
C		A	91
	CALL AXIS (0.0,0.0,10HTIME(SEC),-10,6.0,0.0,TT(22),TT(23),0)	A	92
	CALL AXIS (0.0,0.0,9HFORCE(LB),9,9.0,90.0,FF(22),FF(23),-1)	A	93
	CALL AXIS (6.0,0.0,14HDISP(0.001 IN),14,9.0,90.0,W(22),W(23),-1)	A	94
	CALL LINE (TT,FF,21,1,1,3)	A	95
	CALL DSHLINE (TT,W,21,0.1,0.1,1)	A	96
	CALL DSHLINE (TT,U,21,0.05,0.05,1)	A	97
	CALL PLOT (6.0,9.0,3)	A	98
	CALL PLOT (0.0,9.0,2)	A	99
	CALL SYMBOL (1.0,9.3,0.1,TITLE,0.0,70)	A	100
	CALL SYMBOL (3.5,8.5,0.1,17HBALL DIA.=1/2 IN.,0.0,17)	A	101
	GO TO 101	A	102
105	CALL PLOT (0.0,999)	A	103
	STOP	A	104
C		A	105
106	FORMAT (1H1,4X,10HTIME(MSEC),6X,9HFORCE(LB),2X,13HBALL DISP(IN),2X	A	106
	1,13HBEAM DISP(IN))	A	107
107	FORMAT (4E15.3)	A	108
108	FORMAT (I2,7A10)	A	109
C		A	110
	END	A	111
	SUBROUTINE GDATA	B	2
	COMMON /CONTR/ TITLE(7),NP,NE,NB,NDF,NCN,NLD,NMAT,NSZF,LI,NT4,NDIN	B	3
	1,MATP,NPROB	B	4
	COMMON /TIME/ T,DT,DDT,TAU,KCON,KCNT	B	5
	COMMON /DISP/ Q1,Q2,Q3,Q10,Q20,Q30	B	6
	COMMON /DIMB/ TB,WB,PB,NG,D11	B	7
	COMMON /SPHERE/ STF,R,CABU(10),QKONST(10)	B	8
	COMMON /PLASTIC/ DISPEM,NDISPEM,FORSPM,DISPM,QP	B	9
	COMMON CORD(100,2),NOP(200,4),IMAT(200),ORT(25,5),NBC(25),NFIK(25)	B	10
	1,R1(200),R2(200),R3(200),R10(200),R20(200),R30(200),FORS(200),SM(2	B	11
	200,15),SK(200,15),ISP(200,15),SMPEM(200,15),ESTIF(12,12),EMASS(12,	B	12
	312),NFIK(25)	B	13
	COMMON /COMP/ QBR(3,3,25),ABD(6,6),TH(25),ZK(25),MLAYER	B	14
	COMMON /PLOT/ NN,TT(25),FF(25),W(25),U(25)	B	15
C		B	16
C	READ AND PRINT TITLE AND CONTROL	B	17
C		B	18
	WRITE (6,116) NPROB,(TITLE(I),I=1,7)	B	19
	WRITE (8,116) NPROB,(TITLE(I),I=1,7)	B	20
	READ (5,106) NP,NE,NB,NTM,NMAT,NDIN,MATP,NDC,I1	B	21
	NDF=3	B	22
	NLD=NDIN*NTM	B	23
	FLD=FLOAT(NLD)/10.	B	24
	FDIN=FLOAT(NDIN)/10.	B	25
	READ (5,113) TB,WB,R,NG,Q2,DT	B	26
	WRITE (6,107) NP,NE,NB,NLD,NDF,NMAT	B	27
	NLD=NLD+1	B	28
C		B	29
C	READ AND PRINT MATERIAL DATA	B	30
C	SPHERE DATA: L=NMAT (LAST MAT. CARD)	B	31

C	READ (5,112) (L,(ORT(L,I),I=1,5),N=1,NMAT)	B	32
	PB=ORT(NMAT,5)	B	33
	WRITE (6,122) TB,WB,PB,R,NQ,Q2,DT	B	34
	NQ=(NQ-1)*3+1	B	35
	WRITE (6,121)	B	36
	WRITE (6,115) (N,(ORT(N,I),I=1,5),N=1,NMAT)	B	37
C		B	38
C	READ INDENTATION DATA	B	39
C		B	40
	READ (5,111) STF,DISPEM,QP	B	41
	WRITE (6,123) DISPEM	B	42
	IF (DISPEM.NE.0.0) WRITE (6,124) QP	B	43
		B	44
C	READ NODAL POINT DATA	B	45
C	AND	B	46
C	READ ELEMENT DATA	B	47
C		B	48
	DO 102 I=1,NDC	B	49
	READ (5,114) ND1,ND2,X1,X2,IMT	B	50
	EL=(X2-X1)/FLOAT(ND2-ND1)	B	51
	CORD(ND1,1)=X1	B	52
	CORD(ND2,1)=X2	B	53
	CORD(ND2,2)=0.0	B	54
	CORD(ND1,2)=CORD(ND2,2)	B	55
	NDD=ND2-1	B	56
	DO 101 J=ND1,NDD	B	57
	CORD(J+1,1)=CORD(J,1)+EL	B	58
	CORD(J+1,2)=0.0	B	59
	NOP(J,1)=J	B	60
	NOP(J,2)=J+1	B	61
	NOP(J,4)=0	B	62
	NOP(J,3)=NOP(J,4)	B	63
	IMAT(J)=IMT	B	64
		B	65
101	CONTINUE	B	66
102	CONTINUE	B	67
C		B	68
C	READ BOUNDARY DATA	B	69
C		B	70
	READ (5,110) (NBC(I),NFIX(I),I=1,NB)	B	71
	IF (MATP.EQ.1) CALL CMPD	B	72
		B	73
C	ISOTROPIC MATP=0.0	B	74
C	COMPOSITE MATP=1.0	B	75
C		B	76
	IF (I1.NE.0) GO TO 103	B	77
		B	78
C	PRINT INPUT DATA	B	79
C		B	80
	WRITE (6,117)	B	81
	WRITE (6,108) (N,(CORD(N,M),M=1,2),N=1,NP)	B	82
	WRITE (6,118)	B	83
	WRITE (6,109) (N,(NOP(N,M),M=1,4),IMAT(N),N=1,NE)	B	84
	WRITE (6,119)	B	85
	WRITE (6,110) (NBC(I),NFIX(I),I=1,NB)	B	86
	WRITE (6,120) FDIN,FLD	B	87
103	CONTINUE	B	88
	DO 104 IJ=1,200	B	89
	R10(IJ)=0.	B	90
	R20(IJ)=0.	B	91
	R30(IJ)=0.	B	92
104	FORS(IJ)=0.	B	93
	DO 105 IJ=1,25	B	94
105	NFIXK(IJ)=NFIX(IJ)	B	95
	RETURN	B	96
C		B	97
	106 FORMAT (9I5)	B	98
	107 FORMAT (13HONODAL POINTS,9X,I5/1X,8HELEMENTS,13X,I5/1X,19HBOUNDARY	B	99
	1 CONDITIONS,2X,I5/1X,12HOUTPUT LIMIT,10X,I5/1X,18HDEGREES OF FREED	B	100
	20M,3X,I5/1X,9HMATERIALS,12X,I5)	B	101

108	FORMAT (I10,2F10.3)	B	102
109	FORMAT (6I5)	B	103
110	FORMAT (2I5)	B	104
111	FORMAT (E10.3,2F10.0)	B	105
112	FORMAT (I5,5F10.0)	B	106
113	FORMAT (3F10.0/I5,2F10.0)	B	107
114	FORMAT (2I5,2F10.0,I5)	B	108
115	FORMAT (I5,7X,3(F10.1,4X);F5.3,7X,F8.6//)	B	109
116	FORMAT (1H1,I2,7A10)	B	110
117	FORMAT (14H0 NDDAL POINTS/17X,1HX,10X,1HY)	B	111
118	FORMAT (10H0 ELEMENTS/9X,1HI,4X,1HJ,4X,1HK,8X,3HMAT)	B	112
119	FORMAT (21H0 BOUNDARY CONDITIONS)	B	113
120	FORMAT (16H0PRINTING SCHEME/5X,22H1. REPORT OUTPUT EVERY,F6.2,2X,4 1HMSEC/5X,22H2. TERMINATE OUTPUT AT,F6.2,2X,4HMSEC)	B	114
121	FORMAT (1H0,20H MATERIAL PROPERTIES/1X,8HMAT. NO.,7X,2HE1,12X,2HE2 1,11X,3HG12,10X,3HU12,10X,3HRHO/)	B	115
122	FORMAT (15H0BEAM THICKNESS,11X,F6.3/1X,10HBEAM WIDTH,15X,F6.3/1X,1 14HSPHERE DENSITY,12X,F8.6/1X,13HSPHERE RADIUS,12X,F6.3//1X,11HIMPA 2CT NODE,14X,I2/1X,15HIMPACT VELOCITY,10X,F6.1/1X, 39HINTEGRATION T 3IME INCREMENT(X E-06 SEC),E10.3)	B	116
123	FORMAT (//,1X, 21HPERMANENT DEFORMATION,9X,F8.6)	B	117
124	FORMAT (/ ,1X, 15HUNLOADING POWER,15X,F6.3)	B	118

C

END		B	119
SUBROUTINE ESTIFM (N)		B	120
REAL IB, LB		B	121
COMMON /CONTR/ TITLE(7), NP, NE, NB, NDF, NCN, NLD, NMAT, NSZF, LI, NT4, NDIN		B	122
1, MATP, NPROB		B	123
COMMON /TIME/ T, DT, DDT, TAU, KCON, KCNT		B	124
COMMON /DISP/ Q1, Q2, Q3, Q10, Q20, Q30		B	125
COMMON /DIMB/ TB, WB, PB, NG, D11		C	2
COMMON CORD(100, 2), NOP(200, 4), IMAT(200), ORT(25, 5), NBC(25), NFIX(25)		C	3
1, R1(200), R2(200), R3(200), R10(200), R20(200), R30(200), FORS(200), SM(2		C	4
200, 15), SK(200, 15), ISP(200, 15), SMPEM(200, 15), ESTIF(12, 12), EMASS(12,		C	5
312), NFIXK(25)		C	6
COMMON /COMP/ QBR(3, 3, 25), ABD(6, 6), TH(25), ZK(25), MLAYER		C	7
IB=WB*TB**3/12.		C	8
LB=CORD(N+1, 1)-CORD(N, 1)		C	9
SQLB=LB*LB		C	10
TPLB=LB*LB*LB		C	11
IMN=IMAT(N)		C	12
PARA1=ORT(IMN, 1)*IB/70.		C	13
IF (MATP.EQ.1) PARA1=ABD(4, 4)/70.		C	14
ESTIF(1, 1)=1200./TPLB*PARA1		C	15
ESTIF(1, 2)=600./SQLB*PARA1		C	16
ESTIF(1, 3)=30./LB*PARA1		C	17
ESTIF(1, 4)=-1200./TPLB*PARA1		C	18
ESTIF(1, 5)=600./SQLB*PARA1		C	19
ESTIF(1, 6)=-30./LB*PARA1		C	20
ESTIF(2, 1)=ESTIF(1, 2)		C	21
ESTIF(2, 2)=384./LB*PARA1		C	22
ESTIF(2, 3)=22.*PARA1		C	23
ESTIF(2, 4)=-600./SQLB*PARA1		C	24
ESTIF(2, 5)=216./LB*PARA1		C	25
ESTIF(2, 6)=-8.*PARA1		C	26
ESTIF(3, 1)=ESTIF(1, 3)		C	27
ESTIF(3, 2)=ESTIF(2, 3)		C	28
ESTIF(3, 3)=6.*LB*PARA1		C	29
ESTIF(3, 4)=-30./LB*PARA1		C	30
ESTIF(3, 5)=8.*PARA1		C	31
ESTIF(3, 6)=LB*PARA1		C	32
ESTIF(4, 1)=ESTIF(1, 4)		C	33
ESTIF(4, 2)=ESTIF(2, 4)		C	34
ESTIF(4, 3)=ESTIF(3, 4)		C	35
ESTIF(4, 4)=1200./TPLB*PARA1		C	36
ESTIF(4, 5)=-600./SQLB*PARA1		C	37
ESTIF(4, 6)=30./LB*PARA1		C	38
ESTIF(5, 1)=ESTIF(1, 5)		C	39
ESTIF(5, 2)=ESTIF(2, 5)		C	40
ESTIF(5, 3)=ESTIF(3, 5)		C	41

	ESTIF(5,4)=ESTIF(4,5)	C	48
	ESTIF(5,5)=384./LB*PARA1	C	49
	ESTIF(5,6)=-22.*PARA1	C	50
	ESTIF(6,1)=ESTIF(1,6)	C	51
	ESTIF(6,2)=ESTIF(2,6)	C	52
	ESTIF(6,3)=ESTIF(3,6)	C	53
	ESTIF(6,4)=ESTIF(4,6)	C	54
	ESTIF(6,5)=ESTIF(5,6)	C	55
	ESTIF(6,6)=6.*LB*PARA1	C	56
	IF (N.NE.1) GO TO 101	C	57
	WRITE (6,103)	C	58
	WRITE (6,102) ((ESTIF(I,J),J=1,6),I=1,6)	C	59
101	CONTINUE	C	60
	RETURN	C	61
C		C	62
	102 FORMAT (1X,6E11.3)	C	63
	103 FORMAT (1H0,38H TYPICAL STIFFNESS MATRIX OF AN ELEMENT)	C	64
C		C	65
	END	C	66
	SUBROUTINE EMASSM (N)	D	2
	REAL LB	D	3
	COMMON /CONTR/ TITLE(7),NP,NE,NB,NDF,NCN,NLD,NMAT,NSZF,LI,NT4,NDIN	D	4
	1,MATP,NPROB	D	5
	COMMON /TIME/ T,DT,DDT,TAU,KCON,KCNT	D	6
	COMMON /DISP/ Q1,Q2,Q3,Q10,Q20,Q30	D	7
	COMMON /DIMB/ TB,WB,PB,NQ,D11	D	8
	COMMON CORD(100,2),NOP(200,4),IMAT(200),ORT(25,5),NBC(25),NFIK(25)	D	9
	1,R1(200),R2(200),R3(200),R10(200),R20(200),R30(200),FORS(200),SM(2	D	10
	200,15),SK(200,15),ISP(200,15),SMPM(200,15),ESTIF(12,12),EMASS(12,	D	11
	312),NFIK(25)	D	12
	COMMON /COMP/ QBR(3,3,25),ABD(6,6),TH(25),ZK(25),MLAYER	D	13
	LB=CORD(N+1,1)-CORD(N,1)	D	14
	AB=TB*WB	D	15
	SQLB=LB*LB	D	16
	TPLB=LB*LB*LB	D	17
	QDLB=LB*LB*LB*LB	D	18
	IMN=IMAT(N)	D	19
	PARA2=ORT(IMN,5)*AB*LB/55440.	D	20
	EMASS(1,1)=21720.*PARA2	D	21
	EMASS(1,2)=3732.*LB*PARA2	D	22
	EMASS(1,3)=281.*SQLB*PARA2	D	23
	EMASS(1,4)=6000.*PARA2	D	24
	EMASS(1,5)=-1812.*LB*PARA2	D	25
	EMASS(1,6)=181.*SQLB*PARA2	D	26
	EMASS(2,1)=EMASS(1,2)	D	27
	EMASS(2,2)=832.*SQLB*PARA2	D	28
	EMASS(2,3)=69.*TPLB*PARA2	D	29
	EMASS(2,4)=1812.*LB*PARA2	D	30
	EMASS(2,5)=-532.*SQLB*PARA2	D	31
	EMASS(2,6)=52.*TPLB*PARA2	D	32
	EMASS(3,1)=EMASS(1,3)	D	33
	EMASS(3,2)=EMASS(2,3)	D	34
	EMASS(3,3)=6.*QDLB*PARA2	D	35
	EMASS(3,4)=181.*SQLB*PARA2	D	36
	EMASS(3,5)=-52.*TPLB*PARA2	D	37
	EMASS(3,6)=5.*QDLB*PARA2	D	38
	EMASS(4,1)=EMASS(1,4)	D	39
	EMASS(4,2)=EMASS(2,4)	D	40
	EMASS(4,3)=EMASS(3,4)	D	41
	EMASS(4,4)=21720.*PARA2	D	42
	EMASS(4,5)=-3732.*LB*PARA2	D	43
	EMASS(4,6)=281.*SQLB*PARA2	D	44
	EMASS(5,1)=EMASS(1,5)	D	45
	EMASS(5,2)=EMASS(2,5)	D	46
	EMASS(5,3)=EMASS(3,5)	D	47
	EMASS(5,4)=EMASS(4,5)	D	48
	EMASS(5,5)=832.*SQLB*PARA2	D	49
	EMASS(5,6)=-69.*TPLB*PARA2	D	50
	EMASS(6,1)=EMASS(1,6)	D	51
	EMASS(6,2)=EMASS(2,6)	D	52

```

EMASS(6,3)=EMASS(3,6)
EMASS(6,4)=EMASS(4,6)
EMASS(6,5)=EMASS(5,6)
EMASS(6,6)=6.*QDLB*PARA2
IF (N.NE.1) GO TO 101
WRITE (6,103)
WRITE (6,102) ((EMASS(I,J),J=1,6),I=1,6)
101 CONTINUE
RETURN
C
102 FORMAT (1X,6E11.3)
103 FORMAT (1H0,34H TYPICAL MASS MATRIX OF AN ELEMENT)
C
END
SUBROUTINE FORMM
C
C     FORMS MASS MATRIX
C     IN UPPER TRIANGULAR FORM
C
COMMON /CONTR/ TITLE(7), NP, NE, NB, NDF, NCN, NLD, NMAT, NSZF, LI, NT4, NDIN
1, MATP, NPROB
COMMON /TIME/ T, DT, DDT, TAU, KCON, KCNT
COMMON /DISP/ Q1, Q2, Q3, Q10, Q20, Q30
COMMON /DIMB/ TB, WB, PB, NQ, D11
COMMON CORD(100,2), NOP(200,4), IMAT(200), ORT(25,5), NBC(25), NFIX(25)
1, R1(200), R2(200), R3(200), R10(200), R20(200), R30(200), FORS(200), SM(2
200,15), SK(200,15), ISP(200,15), SMPEM(200,15), ESTIF(12,12), EMASS(12,
312), NFIXK(25)
COMMON /COMP/ QBR(3,3,25), ABD(6,6), TH(25), ZK(25), MLAYER
C
C     SET BANDMAX AND NO. OF EQUATIONS
C
NBAND=9
C
C     ZERO MASS MATRIX
C
DO 101 N=1, NSZF
DO 101 M=1, NBAND
101 SM(N,M)=0.
C
C     SCAN ELEMENTS
C
DO 106 N=1, NE
CALL EMASSM (N)
C
C     RETURNS EMASS AS MASS MATRIX
C
C     STORE EMASS IN SM
C
C     FIRST ROWS
DO 105 JJ=1, NCN
NROWB=(NOP(N, JJ)-1)*NDF
DO 105 J=1, NDF
NROWB=NROWB+1
I=(JJ-1)*NDF+J
C
C     THEN COLUMNS
DO 104 KK=1, NCN
NCOLB=(NOP(N, KK)-1)*NDF
DO 103 K=1, NDF
L=(KK-1)*NDF+K
NCOL=NCOLB+K+1-NROWB
C
C     SKIP STORING IF BELOW BAND
IF (NCOL) 103, 103, 102
102 SM(NROWB, NCOL)=SM(NROWB, NCOL)+EMASS(I, L)
103 CONTINUE

```

```

D 53
D 54
D 55
D 56
D 57
D 58
D 59
D 60
D 61
D 62
D 63
D 64
D 65
D 66
E 2
E 3
E 4
E 5
E 6
E 7
E 8
E 9
E 10
E 11
E 12
E 13
E 14
E 15
E 16
E 17
E 18
E 19
E 20
E 21
E 22
E 23
E 24
E 25
E 26
E 27
E 28
E 29
E 30
E 31
E 32
E 33
E 34
E 35
E 36
E 37
E 38
E 39
E 40
E 41
E 42
E 43
E 44
E 45
E 46
E 47
E 48
E 49
E 50
E 51
E 52
E 53
E 54
E 55
E 56
E 57

```

	104	CONTINUE	E	58
	105	CONTINUE	E	59
	106	CONTINUE	E	60
C			E	61
C		INSERT BOUNDARY CONDITIONS	E	62
C			E	63
	DO 112	N=1,NB	E	64
		NX=10** (NDF-1)	E	65
		I=NBC(N)	E	66
		NROWB=(I-1)*NDF	E	67
C			E	68
C		EXAMINE EACH DEGREE OF FREEDOM	E	69
C			E	70
	DO 111	M=1,NDF	E	71
		NROWB=NROWB+1	E	72
		ICON=NFIX(N)/NX	E	73
		IF (ICON) 110,110,107	E	74
107		SM(NROWB,1)=1.	E	75
	DO 109	J=2,NBAND	E	76
		SM(NROWB,J)=0.	E	77
		NR=NROWB+1-J	E	78
		IF (NR) 109,109,108	E	79
108		SM(NR,J)=0.	E	80
109		CONTINUE	E	81
		NFIX(N)=NFIX(N)-NX*ICON	E	82
110		NX=NX/10	E	83
111		CONTINUE	E	84
112		CONTINUE	E	85
	DO 115	N=1,NSZF	E	86
		K=0	E	87
	DO 114	M=1,NBAND	E	88
		MP=M-K	E	89
		IF (ISP(N,M).LT.ISP(N,1)) GO TO 113	E	90
		SM(N,MP)=SM(N,MP)+(DDT/6.)*SK(N,M)	E	91
		GO TO 114	E	92
113		K=K+1	E	93
114		CONTINUE	E	94
115		CONTINUE	E	95
	DO 116	I=1,NSZF	E	96
	DO 116	J=1,NBAND	E	97
116		SMPER(I,J)=SM(I,J)	E	98
C			E	99
C		WRITE(6,1) ((SM(I,J),J=1,NBAND),I=1,NSZF)	E	100
C		1 FORMAT(2X,9E10.3)	E	101
C			E	102
		RETURN	E	103
C			E	104
	END		E	105
	SUBROUTINE FORMK		F	2
	COMMON /CONTR/ TITLE(7),NP,NE,NB,NDF,NCN,NLD,NMAT,NSZF,LI,NT4,NDIN		F	3
	1,MATP,NPROB		F	4
	COMMON /TIME/ T,DT,DDT,TAU,KCON,KCNT		F	5
	COMMON /DISP/ Q1,Q2,Q3,Q10,Q20,Q30		F	6
	COMMON /DIMB/ TB,WB,PB,NQ,D11		F	7
	COMMON CORD(100,2),NOP(200,4),IMAT(200),ORT(25,5),NBC(25),NFIX(25)		F	8
	1,R1(200),R2(200),R3(200),R10(200),R20(200),R30(200),FORS(200),SM(2		F	9
	200,15),SK(200,15),ISP(200,15),SMPER(200,15),ESTIF(12,12),EMASS(12,		F	10
	312),NFIXK(25)		F	11
	COMMON /COMP/ QBR(3,3,25),ABD(6,6),TH(25),ZK(25),MLAYER		F	12
C			F	13
C		SET MAX. NO. OF TERMS	F	14
C			F	15
	NMAX=9		F	16
	NOFF=9		F	17
C			F	18
C		ZERO ARRAYS	F	19
C			F	20
	DO 103	N=1,NSZF	F	21
	DO 101	M=1,NMAX	F	22
101		SK(N,M)=0.	F	23

	DO 102 M=2,NOFF	F	24
102	ISP(N,M)=0	F	25
103	ISP(N,1)=N	F	26
C		F	27
C	SCAN ELEMENTS	F	28
C		F	29
	DO 110 N=1,NE	F	30
	CALL ESTIFM (N)	F	31
C		F	32
C	RETURNS ESTIF AS STIFFNESS MATRIX	F	33
C		F	34
C	STORE ESTIF IN SK WITH A TERM IN ISP AS A POINTER	F	35
C		F	36
C	FIRST THE ROWS	F	37
C		F	38
	I=0	F	39
	DO 109 JJ=1,NCN	F	40
	NROWB=(NOP(N, JJ)-1)*NDF	F	41
	DO 109 J=1,NDF	F	42
	NROWB=NROWB+1	F	43
	I=I+1	F	44
C		F	45
C	THEN COLUMNS OF ESTIF	F	46
C		F	47
	II=0	F	48
	DO 108 KK=1,NCN	F	49
	NCOLB=(NOP(N, KK)-1)*NDF	F	50
	DO 108 K=1,NDF	F	51
	NCOLB=NCOLB+1	F	52
	II=II+1	F	53
C		F	54
C	SEARCH ISP FOR COLUMN NO.	F	55
C		F	56
	DO 105 M=1,NOFF	F	57
	IF (ISP(NROWB,M)-NCOLB) 104,107,104	F	58
104	IF (ISP(NROWB,M)) 106,106,105	F	59
105	CONTINUE	F	60
C		F	61
C	FOUND A BLANK NOW STORE NCOLB	F	62
C		F	63
106	ISP(NROWB,M)=NCOLB	F	64
C		F	65
C	NOW STORE ESTIF	F	66
C		F	67
107	SK(NROWB,M)=ESTIF(I, II)+SK(NROWB,M)	F	68
C		F	69
C	END LOOP ON COLUMNS	F	70
C		F	71
108	CONTINUE	F	72
C		F	73
C	END LOOP ON ROWS	F	74
C		F	75
109	CONTINUE	F	76
C		F	77
C	END LOOP ON ELEMENTS	F	78
C		F	79
110	CONTINUE	F	80
C		F	81
C	INSERT BOUNDARY CONDITIONS	F	82
C		F	83
	DO 114 N=1,NB	F	84
	NX=10**((NDF-1)	F	85
	I=NBC(N)	F	86
	NROWB=(I-1)*NDF	F	87
C		F	88
C	EXAMINE EACH DEGREE OF FREEDOM	F	89
C		F	90
	DO 113 M=1,NDF	F	91
	NROWB=NROWB+1	F	92
		F	93

```

          ICON=NFIXK(N)/NX
          IF (ICON) 112,112,111
C
C
C      STORE ZERO ON DIAGONAL
111      SK(NROWB,1)=0.0
          NFIXK(N)=NFIXK(N)-NX*ICON
112      NX=NX/10
113      CONTINUE
114 CONTINUE
          RETURN
C
          END
          SUBROUTINE LOAD
          COMMON /CONTR/ TITLE(?),NP,NE,NB,NDF,NCN,NLD,NMAT,NSZF,LI,NT4,NDIN
1, MATP,NPROB
          COMMON /TIME/ T,DT,DDT,TAU,KCON,KCNT
          COMMON /DISP/ Q1,Q2,Q3,Q10,Q20,Q30
          COMMON /DIMB/ TB,WB,PB,NQ,D11
          COMMON /SPHERE/ STF,R,CABU(10),QKONST(10)
          COMMON /PLASTIC/ DISPEM,NDISPEM,FORSPEM,DISPM,QP
          COMMON CORD(100,2),NOP(200,4),IMAT(200),ORT(25,5),NBC(25),NFIK(25)
1,R1(200),R2(200),R3(200),R10(200),R20(200),R30(200),FORS(200),SM(2
200,15),SK(200,15),ISP(200,15),SMPEM(200,15),ESTIF(12,12),EMASS(12,
312),NFIK(25)
          COMMON /COMP/ QBR(3,3,25),ABD(6,6),TH(25),ZK(25),MLAYER
          IF (STF.NE.0.0) GO TO 101
          STFI=(4./3.)*SQRT(R)/((1.-ORT(NMAT,4)**2)/ORT(NMAT,1)+(1.-ORT(1,4)
1**2)/ORT(1,1))
          STFA=(4./3.)*SQRT(R)/((1.-ORT(NMAT,4)**2)/ORT(NMAT,1)+1./ORT(1,2))
          STFI=STFI
          IF (MATP.EQ.1) STFI=STFA
101 PAI=4.*ATAN(1.)
          BALLM=(4./3.)*PAI*(R**3)*PB
C
C
C      SIMPLY SUPPORTED SYMMETRY CST1=0.5
C      CLAMPED CANTILEVER CST1=1.
C
C
C      CST1=1.0
C
C      IF(NBC(1) .EQ. 1) CST1=0.5
C
C
C      Q1=ACCEL. OF THE MASS
C      Q2=VELO. OF THE MASS
C      Q3=DISP. OF THE MASS
C
C
C      IF (LI.GT.1.AND.KCNT.EQ.1) GO TO 102
C      IF (LI.GT.1.AND.KCNT.EQ.2) GO TO 103
C      Q1=0.
C      Q3=0.
C      GO TO 112
102 Q10=Q1
          Q20=Q2
          Q30=Q3
          Q3=Q30+DT*Q20+0.5*DDT*Q10
          R3(NQ)=R30(NQ)+DT*R20(NQ)+0.5*DDT*R10(NQ)
          DIFDO=Q30-R30(NQ)
          DIFDISP=Q3-R3(NQ)
C
C
C      WRITE(6,400) DIFDO,DIFDISP
C
C
C      IF (DIFDISP) 110,104,104
103 Q3=Q30+DT*Q20+DDT*Q10/3.+DDT*Q1/6.
          DIFDO=Q30-R30(NQ)
          DIFDISP=Q3-R3(NQ)
C
C
C      WRITE(6,400) DIFDO,DIFDISP
C      400 FORMAT(/,5X, #DIFDO=#,E15.3,5X, #DIFDISP=#,E15.3)

```

```

F 94
F 95
F 96
F 97
F 98
F 99
F 100
F 101
F 102
F 103
F 104
F 105
F 106
G 2
G 3
G 4
G 5
G 6
G 7
G 8
G 9
G 10
G 11
G 12
G 13
G 14
G 15
G 16
G 17
G 18
G 19
G 20
G 21
G 22
G 23
G 24
G 25
G 26
G 27
G 28
G 29
G 30
G 31
G 32
G 33
G 34
G 35
G 36
G 37
G 38
G 39
G 40
G 41
G 42
G 43
G 44
G 45
G 46
G 47
G 48
G 49
G 50
G 51
G 52
G 53
G 54
G 55
G 56
G 57
G 58

```

```

IF (DIFDISP.LT.0) GO TO 110
104 IF (DISPEM.EQ.0.0) GO TO 105
IF ((DIFDISP.LT.DIFDO).AND.(NDISPEM.EQ.0)) GO TO 107
IF ((DIFDISP.LT.DIFDO).AND.(NDISPEM.GT.0)) GO TO 108
105 DO 106 J=1,NSZF
106 FORS(J)=0.
FORS(NQ)=STF*(DIFDISP)**1.5*CST1
Q1=-FORS(NQ)/BALLM/CST1
IF (KCNT.EQ.1) GO TO 113
IF (KCNT.EQ.2) GO TO 109
107 NDISPEM=1
FORSPM=FORS(NQ)
DISPM=DIFDO
WRITE (6,114) DISPEM,DISPM,DIFDISP,FORSPM
IF ((DIFDISP.LT.DISPEM).OR.(DISPM.LE.DISPEM)) GO TO 111
108 FORS(NQ)=FORSPM*((DIFDISP-DISPEM)/(DISPM-DISPEM))*QP*CST1
Q1=-FORS(NQ)/BALLM/CST1
IF (KCNT.EQ.1) GO TO 113
109 Q2=Q20+0.5*DT*Q10+0.5*DT*Q1
Q3=Q30+DT*Q20+DDT*Q10/3.+DDT*Q1/6.
GO TO 113
110 FORS(NQ)=0.
Q1=0.
GO TO 109
111 LI=10000
GO TO 113
112 FORS(NQ)=0.
113 RETURN
C
114 FORMAT (///,5X, 7HDISPEM=,E10.3,5X, 6HDISPM=,E10.3,5X, 8HDIFDIS
1P=,E10.3,5X, 7HFORSPM=,E10.3)
C
END
SUBROUTINE HMTQ
C
C
C SUBROUTINE FOR FINDING (F)-(K)(U)
C
COMMON /CONTR/ TITLE(7),NP,NE,NB,NDF,NCN,NLD,NMAT,NSZF,LI,NT4,NDIN
1,MATP,NPROB
COMMON /TIME/ T,DT,DDT,TAU,KCON,KCNT
COMMON /DISP/ Q1,Q2,Q3,Q10,Q20,Q30
COMMON /DIMB/ TB,WB,PB,NQ,D11
COMMON CORD(100,2),NOP(200,4),IMAT(200),ORT(25,5),NBC(25),NFIK(25)
1,R1(200),R2(200),R3(200),R10(200),R20(200),R30(200),FORS(200),SM(2
200,15),SK(200,15),ISP(200,15),SMPEM(200,15),ESTIF(12,12),EMASS(12,
312),NFIKK(25)
COMMON /COMP/ QBR(3,3,25),ABD(6,6),TH(25),ZK(25),MLAYER
NT=9
DO 101 IJ=1,NSZF
R1(IJ)=0.
R2(IJ)=0.
101 R3(IJ)=0.
C
C
DO 105 N=1,NSZF
FX=FORS(N)
DO 102 M=1,NT
L=ISP(N,M)
102 FX=FX-SK(N,M)*(R30(L)+DT*R20(L)+(DDT/3.)*R10(L))
IF (SK(N,1)) 104,103,104
103 FX=0.
104 R1(N)=FX
105 CONTINUE
RETURN
C
END
SUBROUTINE SOLVE
C
C
C SPECIFICATION STATEMENTS
C

```

```

G 59
G 60
G 61
G 62
G 63
G 64
G 65
G 66
G 67
G 68
G 69
G 70
G 71
G 72
G 73
G 74
G 75
G 76
G 77
G 78
G 79
G 80
G 81
G 82
G 83
G 84
G 85
G 86
G 87
G 88
G 89
G 90
G 91
H 2
H 3
H 4
H 5
H 6
H 7
H 8
H 9
H 10
H 11
H 12
H 13
H 14
H 15
H 16
H 17
H 18
H 19
H 20
H 21
H 22
H 23
H 24
H 25
H 26
H 27
H 28
H 29
H 30
H 31
H 32
H 33
H 34
I 2
I 3
I 4
I 5

```

```

COMMON /CONTR/ TITLE(7), NP, NE, NB, NDF, NCN, NLD, NMAT, NSZF, LI, NT4, NDIN I 6
1, MATP, NPROB I 7
COMMON /TIME/ T, DT, DDT, TAU, KCON, KCNT I 8
COMMON /DISP/ Q1, Q2, Q3, Q10, Q20, Q30 I 9
COMMON /DIMB/ TB, WB, PB, NQ, D11 I 10
COMMON CORD(100,2), NOP(200,4), IMAT(200), ORT(25,5), NBC(25), NFIX(25) I 11
1, R1(200), R2(200), R3(200), R10(200), R20(200), R30(200), FORS(200), SM(2 I 12
200, 15), SK(200, 15), ISP(200, 15), SMPPEM(200, 15), ESTIF(12, 12), EMASS(12, I 13
312), NFIXK(25) I 14
COMMON /COMP/ QBR(3,3,25), ABD(6,6), TH(25), ZK(25), MLAYER I 15
NBAND=9 I 16
DO 101 I=1, NSZF I 17
DO 101 J=1, NBAND I 18
101 SM(I, J)=SMPPEM(I, J) I 19
C I 20
C I 21
C I 22
REDUCE MATRIX I 23
DO 106 N=1, NSZF I 24
I=N I 25
DO 105 L=2, NBAND I 26
I=I+1 I 27
IF (SM(N, L)) 102, 105, 102 I 28
102 C=SM(N, L)/SM(N, 1) I 29
J=0 I 30
DO 104 K=L, NBAND I 31
J=J+1 I 32
IF (SM(N, K)) 103, 104, 103 I 33
103 SM(I, J)=SM(I, J)-C*SM(N, K) I 34
104 CONTINUE I 35
SM(N, L)=C I 36
C I 37
C I 38
C I 39
C I 40
R1(I)=R1(I)-C*R1(N) I 41
105 CONTINUE I 42
106 R1(N)=R1(N)/SM(N, 1) I 43
C I 44
C I 45
C I 46
BACK-SUBSTITUTION I 47
N=NSZF I 48
107 N=N-1 I 49
IF (N) 111, 111, 108 I 50
108 L=N I 51
DO 110 K=2, NBAND I 52
L=L+1 I 53
IF (SM(N, K)) 109, 110, 109 I 54
109 R1(N)=R1(N)-SM(N, K)*R1(L) I 55
110 CONTINUE I 56
GO TO 107 I 57
111 RETURN I 58
C I 59
END I 60
SUBROUTINE INTEGTN J 2
COMMON /CONTR/ TITLE(7), NP, NE, NB, NDF, NCN, NLD, NMAT, NSZF, LI, NT4, NDIN J 3
1, MATP, NPROB J 4
COMMON /TIME/ T, DT, DDT, TAU, KCON, KCNT J 5
COMMON /DISP/ Q1, Q2, Q3, Q10, Q20, Q30 J 6
COMMON /DIMB/ TB, WB, PB, NQ, D11 J 7
COMMON CORD(100,2), NOP(200,4), IMAT(200), ORT(25,5), NBC(25), NFIX(25) J 8
1, R1(200), R2(200), R3(200), R10(200), R20(200), R30(200), FORS(200), SM(2 J 9
200, 15), SK(200, 15), ISP(200, 15), SMPPEM(200, 15), ESTIF(12, 12), EMASS(12, J 10
312), NFIXK(25) J 11
COMMON /COMP/ QBR(3,3,25), ABD(6,6), TH(25), ZK(25), MLAYER J 12
COMMON /PLOT/ NN, TT(25), FF(25), W(25), U(25) J 13
C J 14
C J 15
C J 16
C J 17
C J 18
R1=ACCEL. OF BEAM J 15
R2=VELO. OF BEAM J 16
R3=DISPL. OF BEAM J 17

```

```

DO 101 IJ=1,NSZF
  R2(IJ)=R20(IJ)+0.5*DT*R10(IJ)+0.5*DT*R1(IJ)
  R3(IJ)=R30(IJ)+DT*R20(IJ)+(DDT/3.)*R10(IJ)+(DDT/6.)*R1(IJ)
101 CONTINUE
  IF (KCNT.EQ.1) GO TO 107
  DO 102 IK=1,NP
    IK4=(IK-1)*3+1
    R30(IK)=R3(IK4)
102 CONTINUE
  IF ((LI/10000).EQ.1) GO TO 103
C
C
C   PRINT CONTROL
C
  NTON=(LI-1)/NDIN
  IF (NTON.NE.KCON) GO TO 105
103 CONTINUE
C
C   SIMPLY SUPPORTED BEAM CST2=2.
C   CANTILEVER CST2=1.
C
  CST2=1.
C
C   IF(NBC(1).EQ.1)CST2=2.
C
  F=CST2*FORS(NQ)
  APHA=Q3-R30(NQ)
  FF(NN)=F
  W(NN)=Q3*1000.
  U(NN)=R30(NQ)*1000.
  WRITE (6,108) (TITLE(I),I=1,7)
  T1=T*1.E6
  TT(NN)=T1
  NN=NN+1
  WRITE (6,109) T1,F,Q3,Q2,Q1,APHA
  DO 104 IK=1,NP
    IK3=IK*3
    STXX=R3(IK3)*TB/2.
    SIGX=ORT(1,1)*STXX
    STYY=-ORT(1,4)*STXX
    WRITE (6,110) IK,R30(IK),STXX,STYY,SIGX
104 CONTINUE
  KCON=KCON+1
105 CONTINUE
  DO 106 IJ=1,NSZF
    R10(IJ)=R1(IJ)
    R20(IJ)=R2(IJ)
106 R30(IJ)=R3(IJ)
107 RETURN
C
108 FORMAT (1H1,7A10///)
109 FORMAT (10X,18HTIME ELAPSED(MSEC),13X,F7.3/10X,9HFORCE(LB),21X,E11
1.3/10X,21HMASS DISPLACEMENT(IN),9X,E11.3/10X,21HMASS VELOCITY(IN/S
2EC),9X,E11.3/10X,20HMASS ACCEL.(IN/SEC2),10X,E11.3/10X,15HINDENTAT
3ION(IN),15X,E11.3///10X,4HNODE,9X,4HDISP,13X,9HSTRAIN-XX,9X,9HSTRA
4IN-YY,9X,9HSTRESS-XX/)
110 FORMAT (9X,I3,7X,E12.3,7X,E12.3,7X,E12.3)
C
  END
  SUBROUTINE CMPD
  COMMON /CONTR/ TITLE(7),NP,NE,NB,NDF,NCN,NLD,NMAT,NSZF,LI,NT4,NDIN
1, MATP,NPROB
  COMMON /TIME/ T,DT,DDT,TAU,KCON,KCNT
  COMMON /DISP/ Q1,Q2,Q3,Q10,Q20,Q30
  COMMON /DIMB/ TB,WB,PB,NQ,D11
  COMMON CORD(100,2),NOP(200,4),IMAT(200),ORT(25,5),NBC(25),NFIX(25)
1,R1(200),R2(200),R3(200),R10(200),R20(200),R30(200),FORS(200),SM(2
200,15),SK(200,15),ISP(200,15),SMPFM(200,15),ESTIF(12,12),EMASS(12,
312),NFIKK(25)
  COMMON /COMP/ QBR(3,3,25),ABD(6,6),TH(25),ZK(25),MLAYER
  DIMENSION Q(3,3), TK(25)

```

```

J 19
J 20
J 21
J 22
J 23
J 24
J 25
J 26
J 27
J 28
J 29
J 30
J 31
J 32
J 33
J 34
J 35
J 36
J 37
J 38
J 39
J 40
J 41
J 42
J 43
J 44
J 45
J 46
J 47
J 48
J 49
J 50
J 51
J 52
J 53
J 54
J 55
J 56
J 57
J 58
J 59
J 60
J 61
J 62
J 63
J 64
J 65
J 66
J 67
J 68
J 69
J 70
J 71
J 72
J 73
J 74
J 75
J 76
K 2
K 3
K 4
K 5
K 6
K 7
K 8
K 9
K 10
K 11
K 12
K 13

```

```

DO 102 J=1,3
DO 102 K=1,3
  ABD(J+3,K+3)=0.0
  ABD(J+3,K)=ABD(J+3,K+3)
  ABD(J,K+3)=ABD(J+3,K)
  ABD(J,K)=ABD(J,K+3)
  DO 101 I=1,25
    QBR(J,K,I)=0.
101  CONTINUE
102  CONTINUE
    READ (5,108) MLAYER
    M=MLAYER
    READ (5,109) (L,TH(L),TK(L),I=1,M)
    TTK=0.0
    ZK(1)=TTK
    DO 103 I=1,M
      TTK=TTK+TK(I)
      ZK(I+1)=TK(I)+ZK(I)
103  CONTINUE
    MM=M+1
    DO 104 I=1,MM
      ZK(I)=ZK(I)-TTK/2.
104  CONTINUE
    DEL=4.*ATAN(1.)/180.
    DEN=1.-ORT(1,2)*ORT(1,4)**2/ORT(1,1)
    Q(1,1)=ORT(1,1)/DEN
    Q(2,2)=ORT(1,2)/DEN
    Q(2,1)=ORT(1,4)*Q(2,2)
    Q(1,2)=Q(2,1)
    Q(3,3)=ORT(1,3)
    Q(3,2)=0.0
    Q(3,1)=Q(3,2)
    Q(2,3)=Q(3,1)
    Q(1,3)=Q(2,3)
    DO 105 I=1,M
      ANGL=TH(I)*DEL
      C=COS(ANGL)
      W=SIN(ANGL)
      QBR(1,1,I)=Q(1,1)*C**4+2.*(Q(1,2)+2.*Q(3,3))*(C*W)**2+Q(2,2)*W*
1      *4
      QBR(2,1,I)=(Q(1,1)+Q(2,2)-4.*Q(3,3))*(C*W)**2+Q(1,2)*(W**4+C**4
1      )
      QBR(1,2,I)=QBR(2,1,I)
      QBR(2,2,I)=Q(1,1)*W**4+2.*(Q(1,2)+2.*Q(3,3))*(C*W)**2+Q(2,2)*C*
1      *4
      QBR(3,1,I)=(Q(1,1)-Q(1,2)-2.*Q(3,3))*W*C**3+(Q(1,2)-Q(2,2)+(2.)
1      *Q(3,3))*(W)*(C**3)
      QBR(1,3,I)=QBR(3,1,I)
      QBR(3,2,I)=(Q(1,1)-Q(1,2)-2.*Q(3,3))*W**3*C+(Q(1,2)-Q(2,2)+2.*Q
1      (3,3))*W*C**3
      QBR(2,3,I)=QBR(3,2,I)
      QBR(3,3,I)=(Q(1,1)+Q(2,2)-2.*Q(1,2)-2.*Q(3,3))*(W*C)**2+Q(3,3)*
1      (W**4+C**4)
      QBR(3,3,I)=QBR(3,3,I)
C
C  WRITE(6,500) I,TH(I),TK(I)
C  WRITE(6,510)
C  WRITE(6,520) ((QBR(J,K,I),K=1,3),J=1,3)
C
105  CONTINUE
    DO 107 J=1,3
    DO 107 K=1,3
      DO 106 I=1,M
        ABD(J,K)=ABD(J,K)+QBR(J,K,I)*(ZK(I+1)-ZK(I))
        ABD(J,K+3)=ABD(J+3,K)+QBR(J,K,I)*(ZK(I+1)**2-ZK(I)**2)/2.
        ABD(J+3,K)=ABD(J,K+3)
        ABD(J+3,K+3)=ABD(J+3,K+3)+QBR(J,K,I)*(ZK(I+1)**3-ZK(I)**3)/3
1      .
106  CONTINUE
107  CONTINUE
    WRITE (6,110)

```

K 14
K 15
K 16
K 17
K 18
K 19
K 20
K 21
K 22
K 23
K 24
K 25
K 26
K 27
K 28
K 29
K 30
K 31
K 32
K 33
K 34
K 35
K 36
K 37
K 38
K 39
K 40
K 41
K 42
K 43
K 44
K 45
K 46
K 47
K 48
K 49
K 50
K 51
K 52
K 53
K 54
K 55
K 56
K 57
K 58
K 59
K 60
K 61
K 62
K 63
K 64
K 65
K 66
K 67
K 68
K 69
K 70
K 71
K 72
K 73
K 74
K 75
K 76
K 77
K 78
K 79
K 80
K 81
K 82
K 83

C	WRITE (6,111) ((ABD(I,J),J=1,6),I=1,6)	K	84
C		K	85
C	500 FORMAT(2X,*LAYER=*,I2,5X,*ANGLE=*,F5.2,5X,*THICKNESS=*,F7.3)	K	86
C	510 FORMAT(2X,*QBAR-MATRIX*)	K	87
C	520 FORMAT(5X,3E12.3/)	K	88
C		K	89
C	RETURN	K	90
C		K	91
C	108 FORMAT (I5)	K	92
C	109 FORMAT (I5,F5.0,F10.0)	K	93
C	110 FORMAT (///,1X,10HABD MATRIX)	K	94
C	111 FORMAT (1X,6E11.3)	K	95
C		K	96
C	END	K	97

APPENDIX B

A COMPUTER PROGRAM FOR ESTIMATING THE CONTACT FORCE HISTORY BY USING THE EQUIVALENT MASS MODEL

This program has been written for simply-supported beams only. Cantilever beams and simply-supported plates will be added in the near future.

This program will be a subprogram in a large finite element program capable of analyzing impact responses of beams and plates. This subprogram will be used to provide an estimate of the contact time so that one may select a proper time increment for the finite difference used in the program. For this reason, the input cards for this subprogram were written to be identical to that for the program presented in Appendix A.

C	ISOTROPIC	MATP=0.0	A	72
C	COMPOSITE	MATP=1.0	A	73
C			A	74
C	IF (I1.NE.0) GO TO 104		A	75
C	PRINT INPUT DATA		A	76
C			A	77
C	WRITE (6,119)		A	78
C	WRITE (6,110) (N,(CORD(N,M),M=1,2),N=1,NP)		A	79
C			A	80
C	WRITE(6,103)		A	81
C	WRITE(6,3)(N,(NOP(N,M),M=1,4),IMAT(N),N=1,NE)		A	82
C			A	83
C	WRITE (6,120)		A	84
C	WRITE (6,111) (NBC(I),NFIX(I),I=1,NB)		A	85
C	WRITE (6,121) FDIN,FLD		A	86
C	104 CONTINUE		A	87
C	DO 105 IJ=1,200		A	88
C	R10(IJ)=0.		A	89
C	R20(IJ)=0.		A	90
C	R30(IJ)=0.		A	91
C	105 FORS(IJ)=0.		A	92
C	DO 106 IJ=1,25		A	93
C	106 NFIXK(IJ)=NFIX(IJ)		A	94
C	CALL TMX		A	95
C			A	96
C	3 FORMAT(6I5)		A	97
C			A	98
C	103 FORMAT(10H0 ELEMENTS/9X,1HI,4X,1HJ,4X,1HK,8X,3HMAT)		A	99
C			A	100
C	GO TO 101		A	101
C	107 STOP		A	102
C			A	103
C	108 FORMAT (9I5)		A	104
C	109 FORMAT (13HONODAL POINTS,9X,I5/1X,8HELEMENTS,13X,I5/1X,19HBOUNDARY		A	105
C	1 CONDITIONS,2X,I5/1X,12HOUTPUT LIMIT,10X,I5/1X,18HDEGREES OF FREED		A	106
C	20M,3X,I5/1X,9HMATERIALS,12X,I5)		A	107
C	110 FORMAT (I10,2F10.3)		A	108
C	111 FORMAT (2I5)		A	109
C	112 FORMAT (E10.3)		A	110
C	113 FORMAT (I5,5F10.0)		A	111
C	114 FORMAT (3F10.0/15,2F10.0)		A	112
C	115 FORMAT (2I5,2F10.0,I5)		A	113
C	116 FORMAT (I5,7X,3(F10.1,4X),F5.3,7X,F8.6//)		A	114
C	117 FORMAT (I2,10A7)		A	115
C	118 FORMAT (1H1,I2,10A7)		A	116
C	119 FORMAT (14H0 NODAL POINTS/17X,1HX,10X,1HY)		A	117
C	120 FORMAT (21H0 BOUNDARY CONDITIONS)		A	118
C	121 FORMAT (16H0PRINTING SCHEME/5X,22H1. REPORT OUTPUT EVERY,F6.2,2X,4		A	119
C	1HMSEC/5X,22H2. TERMINATE OUTPUT AT,F6.2,2X,4HMSEC)		A	120
C	122 FORMAT (1H0,20H MATERIAL PROPERTIES/1X,8HMAT. NO.,7X,2HE1,12X,2HE2		A	121
C	1,11X,3HG12,10X,3HV12,10X,3HRHO/)		A	122
C	123 FORMAT (19H0BEAM THICKNESS(IN),7X,F6.3/1X,14HBEAM WIDTH(IN),11X,F6		A	123
C	1.3/1X,22HSPHERE DENSITY(SL/IN3),4X,F8.6/1X,17HSPHERE RADIUS(IN),8X		A	124
C	2,F6.3//1X,11HIMPACT NODE,14X,I2/1X,23HIMPACT VELOCITY(IN/SEC),2X,F		A	125
C	36.1/1X, 39HINTEGRATION TIME INCREMENT(X E-06 SEC),E10.3)		A	126
C			A	127
C	END		A	128
C	SUBROUTINE CMPD		B	2
C	COMMON /CONTR/ TITLE(10),NP,NE,NB,NDF,NCN,NLD,NMAT,NSZF,LI,NT4,NDI		B	3
C	1N,MATP,NPROB		B	4
C	COMMON /TIME/ T,DT,DDT,TAU,KCON,KCNT		B	5
C	COMMON /DISP/ Q1,Q2,Q3,Q10,Q20,Q30		B	6
C	COMMON /DIMB/ TB,WB,PB,NG,D11		B	7
C	COMMON CORD(100,2),NOP(200,4),IMAT(200),ORT(25,5),NBC(25),NFIX(25)		B	8
C	1,R1(200),R2(200),R3(200),R10(200),R20(200),R30(200),FORS(200),SM(2		B	9
C	200,15),SK(200,15),ISP(200,15),SMPEM(200,15),ESTIF(12,12),EMASS(12,		B	10
C	312),NFIXK(25)		B	11
C	COMMON /COMP/ QBR(3,3,25),ABD(6,6),TH(25),ZK(25),MLAYER		B	12
C	COMMON X1,X2,ND1,ND2		B	13

REAL IB	B	14
DIMENSION Q(3,3), TK(25)	B	15
DO 102 J=1,3	B	16
DO 102 K=1,3	B	17
ABD(J+3,K+3)=0.0	B	18
ABD(J+3,K)=ABD(J+3,K+3)	B	19
ABD(J,K+3)=ABD(J+3,K)	B	20
ABD(J,K)=ABD(J,K+3)	B	21
DO 101 I=1,25	B	22
QBR(J,K,I)=0.	B	23
101 CONTINUE	B	24
102 CONTINUE	B	25
READ (5,108) MAYER	B	26
M=MAYER	B	27
READ (5,109) (L,TH(L),TK(L),I=1,M)	B	28
TTK=0.0	B	29
ZK(1)=TTK	B	30
DO 103 I=1,M	B	31
TTK=TTK+TK(I)	B	32
ZK(I+1)=TK(I)+ZK(I)	B	33
103 CONTINUE	B	34
MM=M+1	B	35
DO 104 I=1,MM	B	36
ZK(I)=ZK(I)-TTK/2.	B	37
104 CONTINUE	B	38
DEL=4.*ATAN(1.)/180.	B	39
DEN=1.-ORT(1,2)*ORT(1,4)**2/ORT(1,1)	B	40
Q(1,1)=ORT(1,1)/DEN	B	41
Q(2,2)=ORT(1,2)/DEN	B	42
Q(2,1)=ORT(1,4)*Q(2,2)	B	43
Q(1,2)=Q(2,1)	B	44
Q(3,3)=ORT(1,3)	B	45
Q(3,2)=0.0	B	46
Q(3,1)=Q(3,2)	B	47
Q(2,3)=Q(3,1)	B	48
Q(1,3)=Q(2,3)	B	49
DO 105 I=1,M	B	50
ANGL=TH(I)*DEL	B	51
C=COS(ANGL)	B	52
W=SIN(ANGL)	B	53
QBR(1,1,I)=Q(1,1)*C**4+2.*(Q(1,2)+2.*Q(3,3))*(C*W)**2+Q(2,2)*W*	B	54
1 *4	B	55
QBR(2,1,I)=(Q(1,1)+Q(2,2)-4.*Q(3,3))*(C*W)**2+Q(1,2)*(W**4+C**4	B	56
1)	B	57
QBR(1,2,I)=QBR(2,1,I)	B	58
QBR(2,2,I)=Q(1,1)*W**4+2.*(Q(1,2)+2.*Q(3,3))*(C*W)**2+Q(2,2)*C*	B	59
1 *4	B	60
QBR(3,1,I)=(Q(1,1)-Q(1,2)-2.*Q(3,3))*W*C**3+(Q(1,2)-Q(2,2)+(2.)	B	61
1 *Q(3,3))*W*(C**3)	B	62
QBR(1,3,I)=QBR(3,1,I)	B	63
QBR(3,2,I)=(Q(1,1)-Q(1,2)-2.*Q(3,3))*W**3*C+(Q(1,2)-Q(2,2)+2.*Q	B	64
1 (3,3))*W*C**3	B	65
QBR(2,3,I)=QBR(3,2,I)	B	66
QBR(3,3,I)=(Q(1,1)+Q(2,2)-2.*Q(1,2)-2.*Q(3,3))*(W*C)**2+Q(3,3)*	B	67
1 (W**4+C**4)	B	68
C	B	69
WRITE(6,500) I,TH(I),TK(I)	B	70
C	B	71
WRITE(6,510)	B	72
C	B	73
WRITE(6,520) ((QBR(J,K,I),K=1,3),J=1,3)	B	74
105 CONTINUE	B	75
DO 107 J=1,3	B	76
DO 107 K=1,3	B	77
DO 106 I=1,M	B	78
ABD(J,K)=ABD(J,K)+QBR(J,K,I)*(ZK(I+1)-ZK(I))	B	79
ABD(J,K+3)=ABD(J+3,K)+QBR(J,K,I)*(ZK(I+1)**2-ZK(I)**2)/2.	B	80
ABD(J+3,K)=ABD(J,K+3)	B	81
ABD(J+3,K+3)=ABD(J+3,K+3)+QBR(J,K,I)*(ZK(I+1)**3-ZK(I)**3)/3	B	82
1	B	83
106 CONTINUE	B	84

	107 CONTINUE	B	84
	WRITE (6,111) ((ABD(I,J),J=1,6),I=1,6)	B	86
	WRITE (6,110)	B	85
C		B	87
C	500 FORMAT(2X,*LAYER=*,I2,5X,*ANGLE=*,F5.2,5X,*THICKNESS=*,F7.3)	B	88
C	510 FORMAT(2X,*QBAR-MATRIX*)	B	89
C	520 FORMAT(5X,3E12.3/)	B	90
C		B	91
	RETURN	B	92
C		B	93
	108 FORMAT (I5)	B	94
	109 FORMAT (I5,F5.0,F10.0)	B	95
	110 FORMAT (///,1X,10HABD MATRIX)	B	96
	111 FORMAT (1X,6E11.3)	B	97
C		B	98
	END	B	99
	SUBROUTINE TMX	C	2
	COMMON /CONTR/ TITLE(10),NP,NE,NB,NDF,NCN,NLD,NMAT,NSZF,LI,NT4,NDI	C	3
	IN,MATP,NPROB	C	4
	COMMON /TIME/ T,DT,DDT,TAU,KCON,KCNT	C	5
	COMMON /DISP/ Q1,Q2,Q3,Q10,Q20,Q30	C	6
	COMMON /DIMB/ TB,WB,PB,NQ,D11	C	7
	COMMON /SPHERE/ STF,R,CABU(10),QKONST(10)	C	8
	COMMON /PLASTIC/ DISPEM,NDISPEM,FORSPEM,DISPM	C	9
	COMMON CORD(100,2),NOP(200,4),IMAT(200),ORT(25,5),NBC(25),NFIK(25)	C	10
	1,R1(200),R2(200),R3(200),R10(200),R20(200),R30(200),FORS(200),SM(2	C	11
	200,15),SK(200,15),ISP(200,15),SMPEM(200,15),ESTIF(12,12),EMASS(12,	C	12
	312),NFIKK(25)	C	13
	COMMON /COMP/ QBR(3,3,25),ABD(6,6),TH(25),ZK(25),MLAYER	C	14
	COMMON X1,X2,ND1,ND2	C	15
	REAL IB	C	16
C		C	17
C		C	18
C		C	19
	EQUIVALENT MODEL FOR ESTIMATING TIME INTERVAL	C	20
	IF (STF.NE.0.0) GO TO 101	C	21
	STFI=(4./3.)*SQRT(R)/((1.-ORT(NMAT,4)**2)/ORT(NMAT,1)+(1.-ORT(1,4)	C	22
	1**2)/ORT(1,1))	C	23
	STFA=(4./3.)*SQRT(R)/((1.-ORT(NMAT,4)**2)/ORT(NMAT,1)+1./ORT(1,2))	C	24
	STF=STFI	C	25
	IF (MATP.EQ.1) STF=STFA	C	26
101	PAI=4.*ATAN(1.)	C	27
	BALLM=(4./3.)*PAI*(R**3)*PB	C	28
	BL=X2-X1	C	29
	AB=WB*TB	C	30
	IB=WB*TB**3/12.	C	31
	WATP=FLOAT(MATP)	C	32
	D11=ORT(1,1)*IB	C	33
	IF (MATP.EQ.1) D11=ABD(4,4)	C	34
	WRITE (6,105) BL,STF,WATP,D11,ABD(4,4)	C	35
	WN1=((D11*(PAI/BL)**4)/(AB*ORT(1,5))**0.5	C	36
	TN1=2.*PAI/WN1	C	37
	TD=0.0	C	38
	DO 103 I=1,1000	C	39
	N=0	C	40
	TD=TD+1.0E-7	C	41
	F1=0.0	C	42
	G1=0.0	C	43
	DO 102 J=1,100	C	44
	N=N+1	C	45
	C=FLOAT(NQ-1)/FLOAT(ND2-ND1)	C	46
	WX=SIN(N*PAI*C)	C	47
	PP=1./(4.*N**4*TD**2-TN1**2)	C	48
	QQ=TN1/(2.*N**2*TD)	C	49
	SS=WN1*N**2*TD/2.	C	50
	SUMF=(PP*N**2*(1-QQ*SIN(SS))*WX)**2	C	51
	SUMG=(PP*COS(SS)*WX)**2	C	52
	F1=F1+SUMF	C	53
	G1=G1+SUMG	C	54
102	CONTINUE	C	55
	SUM1=2.*F1*16.*BL**3*TD**2/(D11*PAI**2)	C	

```
SUM2=2.*G1*16.*ORT(1,5)*AB*BL**7/(D11**2*PAI**4)
EMT=1./(SUM1+SUM2)
STFE=1./EMT+1./BALLM
STFT=STF*STFE
APHAMAX=(1.25*Q2**2/STFT)**0.4
TOTALT=2.94*APHAMAX/Q2
FMAX=STF*APHAMAX**1.5
EPS=TOTALT-TD
IF (ABS(EPS).LE.1.E-7) GO TO 104
103 CONTINUE
104 WRITE (6,106) TOTALT,TD,FMAX,APHAMAX,EMT
   RETURN
C
105 FORMAT (//,5X, 5HBEAM=,E10.3,5X, 4HSTF=,E10.3,5X, 5HMATP=,E10.3
   1,5X, 4HD11=,E10.3,5X, 9HABD(4,4)=,E10.3)
106 FORMAT (//,5X, 7HTOTALT=,E10.3,5X, 3HTD=,E10.3,5X, 5HFMAX=,E10.
   13,5X, 8HAPHAMAX=,E10.3,5X, 4HEMT=,E10.3)
C
   END
C 56
C 57
C 58
C 59
C 60
C 61
C 62
C 63
C 64
C 65
C 66
C 67
C 68
C 69
C 70
C 71
C 72
C 73
C 74
```

INTERIM REPORT DISTRIBUTION LIST

NSG3185

CONTACT LAW AND IMPACT RESPONSES OF LAMINATED COMPOSITES

Advanced Research Projects Agency
Washington DC 20525
Attn: Library

Advanced Technology Center, Inc.
LTV Aerospace Corporation
P.O. Box 6144
Dallas, TX 75222
Attn: D. H. Petersen
W. J. Renton

Air Force Flight Dynamics Laboratory
Wright-Patterson Air Force Base, OH 45433
Attn: E. E. Baily
G. P. Sendekyj (FBC)
R. S. Sandhu

Air Force Materials Laboratory
Wright-Patterson Air Force Base, OH 45433
Attn: H. S. Schwartz (LN)
T. J. Reinhart (MBC)
G. P. Peterson (LC)
E. J. Morrissey (LAE)
S. W. Tsai (MBM)
N. J. Pagano
J. M. Whitney (MBM)

Air Force Office of Scientific Research
Washington DC 20333
Attn: J. F. Masi (SREP)

Air Force Office of Scientific Research
1400 Wilson Blvd.
Arlington, VA 22209

AFOSR/NA
Bolling AFB, DC 20332
Attn: J. Morgan

Air Force Rocket Propulsion Laboratory
Edwards, CA 93523
Attn: Library

Babcock & Wilcox Company
Advanced Composites Department
P.O. Box 419
Alliance, Ohio 44601
Attn: P. M. Leopold

Bell Helicopter Company
P.O. Box 482
Ft. Worth, TX 76101
Attn: H. Zinberg

The Boeing Company
P. O. Box 3999
Seattle, WA 98124
Attn: J. T. Hoggatt, MS. 88-33
T. R. Porter

The Boeing Company
Vertol Division
Morton, PA 19070
Attn: E. C. Durchlaub

Battelle Memorial Institute
Columbus Laboratories
505 King Avenue
Columbus, OH 43201
Attn: L. E. Hulbert

Brunswick Corporation
Defense Products Division
P. O. Box 4594
43000 Industrial Avenue
Lincoln, NE 68504
Attn: R. Morse

Celanese Research Company
86 Morris Ave.
Summit, NJ 07901
Attn: H. S. Kliger

Chemical Propulsion Information Agency
Applied Physics Laboratory
8621 Georgia Avenue
Silver Spring, MD 20910
Attn: Library

Commander
Natick Laboratories
U. S. Army
Natick, MA 01762
Attn: Library

Commander
Naval Air Systems Command
U. S. Navy Department
Washington DC 20360
Attn: M. Stander, AIR-43032D

Commander
Naval Ordnance Systems Command
U.S. Navy Department
Washington DC 20360
Attn: B. Drimmer, ORD-033
M. Kinna, ORD-033A

Cornell University
Dept. Theoretical & Applied Mech.
Thurston Hall
Ithaca, NY 14853
Attn: S. L. Phoenix

Defense Metals Information Center
Battelle Memorial Institute
Columbus Laboratories
505 King Avenue
Columbus, OH 43201

Department of the Army
U.S. Army Aviation Materials Laboratory
Ft. Eustis, VA 23604
Attn: I. E. Figge, Sr.
Library

Department of the Army
U.S. Army Aviation Systems Command
P.O. Box 209
St. Louis, MO 63166
Attn: R. Vollmer, AMSAV-A-UE

Department of the Army
Plastics Technical Evaluation Center
Picatinny Arsenal
Dover, NJ 07801
Attn: H. E. Pebly, Jr.

Department of the Army
Watervliet Arsenal
Watervliet, NY 12189
Attn: G. D'Andrea

Department of the Army
Watertown Arsenal
Watertown, MA 02172
Attn: A. Thomas

Department of the Army
Redstone Arsenal
Huntsville, AL 35809
Attn: R. J. Thompson, AMSMI-RSS

Department of the Navy
Naval Ordnance Laboratory
White Oak
Silver Spring, MD 20910
Attn: R. Simon

Department of the Navy
U.S. Naval Ship R&D Laboratory
Annapolis, MD 21402
Attn: C. Hersner, Code 2724

Director
Deep Submergence Systems Project
6900 Wisconsin Avenue
Washington DC 20015
Attn: H. Bernstein, DSSP-221

Director
Naval Research Laboratory
Washington DC 20390
Attn: Code 8430
I. Wolock, Code 8433

Drexel University
32nd and Chestnut Streets
Philadelphia, PA 19104
Attn: P. C. Chou

E. I. DuPont DeNemours & Co.
DuPont Experimental Station
Wilmington, DE 19898
Attn: D. L. G. Sturgeon

Fiber Science, Inc.
245 East 157 Street
Gardena, CA 90248
Attn: E. Dunahoo

General Dynamics
P.O. Box 748
Ft. Worth, TX 76100
Attn: D. J. Wilkins
Library

General Dynamics/Convair
P.O. Box 1128
San Diego, CA 92112
Attn: J. L. Christian

General Electric Co.
Evendale, OH 45215
Attn: C. Stotler
R. Ravenhall
R. Stabrylla

General Motors Corporation
Detroit Diesel-Allison Division
Indianapolis, IN 46244
Attn: M. Herman

Georgia Institute of Technology
School of Aerospace Engineering
Atlanta, GA 30332
Attn: L. W. Rehfield

Grumman Aerospace Corporation
Bethpage, Long Island, NY 11714
Attn: S. Dastin
J. B. Whiteside

Hamilton Standard Division
United Aircraft Corporation
Windsor Locks, CT 06096
Attn: W. A. Percival

Hercules, Inc.
Allegheny Ballistics Laboratory
P. O. Box 210
Cumberland, MD 21053
Attn: A. A. Vicario

Hughes Aircraft Company
Culver City, CA 90230
Attn: A. Knoell

Illinois Institute of Technology
10 West 32 Street
Chicago, IL 60616
Attn: L. J. Broutman

IIT Research Institute
10 West 35 Street
Chicago, IL 60616
Attn: I. M. Daniel

Jet Propulsion Laboratory
4800 Oak Grove Drive
Pasadena, CA 91103
Attn: Library

Lawrence Livermore Laboratory
P.O. Box 808, L-421
Livermore, CA 94550
Attn: T. T. Chiao
E. M. Wu

Lehigh University
Institute of Fracture &
Solid Mechanics
Bethlehem, PA 18015
Attn: G. C. Sih

Lockheed-Georgia Co.
Advanced Composites Information Center
Dept. 72-14, Zone 402
Marietta, GA 30060
Attn: T. M. Hsu

Lockheed Missiles and Space Co.
P.O. Box 504
Sunnyvale, CA 94087
Attn: R. W. Fenn

Lockheed-California
Burbank, CA 91503
Attn: J. T. Ryder
K. N. Lauraitis
J. C. Ekvall

McDonnell Douglas Aircraft Corporation
P.O. Box 516
Lambert Field, MS 63166
Attn: J. C. Watson

McDonnell Douglas Aircraft Corporation
3855 Lakewood Blvd.
Long Beach, CA 90810
Attn: L. B. Greszczuk

Material Sciences Corporation
1777 Walton Road
Blue Bell, PA 19422
Attn: B. W. Rosen

Massachusetts Institute of Technology
Cambridge, MA 02139
Attn: F. J. McGarry
J. F. Mandell
J. W. Mar

NASA-Ames Research Center
Moffett Field, CA 94035
Attn: Dr. J. Parker
Library

NASA-Flight Research Center
P.O. Box 273
Edwards, CA 93523
Attn: Library

NASA-George C. Marshall Space Flight Center
Huntsville, AL 35812
Attn: C. E. Cataldo, S&E-ASTN-MX
Library

NASA-Goddard Space Flight Center
Greenbelt, MD 20771
Attn: Library

NASA-Langley Research Center
Hampton, VA 23365
Attn: J. H. Starnes
R. A. Pride, MS 188a
M. C. Card
J. R. Davidson

NASA-Lewis Research Center
21000 Brookpark Road
Cleveland, Ohio 44135
Attn: Administration & Technical Service Section
Tech. Report Control, MS. 5-5
Tech. Utilization, MS 3-19
AFSC Liaison, MS. 501-3
Rel. and Quality Assur., MS 500-211
L. Berke, MS 49-3
C. P. Blankenship, MS 105-1
R. F. Lark, MS 49-3
J. C. Freche, MS 49-1
R. H. Johns, MS 49-3
C. C. Chamis, MS 49-3 (10 copies)
T. T. Serafini, MS 49-1
Library, MS 60-3 (2 copies)

NASA-Lyndon B. Johnson Space Center
Houston, TX 77001
Attn: S. Glorioso, SMD-ES52
Library

NASA Scientific and Tech. Information Facility
P.O. Box 8757
Balt/Wash International Airport, MD 21240
Attn: Acquisitions Branch (10 copies)

National Aeronautics & Space Administration
Office of Advanced Research & Technology
Washington DC 20546
Attn: L. Harris, Code RWS
M. Greenfield, Code RWS

National Aeronautics & Space Administration
Office of Technology Utilization
Washington DC 20546

National Bureau of Standards
Eng. Mech. Section
Washington DC 20234
Attn: R. Mitchell

National Technology Information Service
Springfield, VA 22161 (6 copies)

National Science Foundation
Engineering Division
1800 G. Street, NW
Washington DC 20540
Attn: Library

Northrop Corporation Aircraft Group
3901 West Broadway
Hawthorne, CA 90250
Attn: R. M. Verette
G. C. Grimes

Pratt & Whitney Aircraft
East Hartford, CT 06108
Attn: J. M. Woodward

Rockwell International
Los Angeles Division
International Airport
Los Angeles, CA 90009
Attn: L. M. Lackman
D. Y. Konishi

Sikorsky Aircraft Division
United Aircraft Corporation
Stratford, CT 06602
Attn: Library

Southern Methodist University
Dallas, TX 75275
Attn: R. M. Jones

Southwest Research Institute
8500 Culebra Road
San Antonio, TX 78284
Attn: P. H. Francis

Space & Missile Systems Organization
Air Force Unit Post Office
Los Angeles, CA 90045
Attn: Technical Data Center

Structural Composites Industries, Inc.
6344 N. Irwindale Avenue
Azusa, CA 91702
Attn: R. Gordon

Texas A&M
Mechanics & Materials Research Center
College Station, TX 77843
Attn: R. A. Schapery

TRW, Inc.
23555 Euclid Avenue
Cleveland, OH 44117
Attn: I. J. Toth

Union Carbide Corporation
P. O. Box 6116
Cleveland, OH 44101
Attn: J. C. Bowman

United Technologies Research Center
East Hartford, CT 06108
Attn: R. C. Novak
Dr. A. Dennis

University of Dayton Research Institute
Dayton, OH 45409
Attn: R. W. Kim

University of Delaware
Mechanical & Aerospace Engineering
Newark, DE 19711
Attn: B. R. Pipes

University of Illinois
Department of Theoretical & Applied Mechanics
Urbana, IL 61801
Attn: S. S. Wang

University of Oklahoma
School of Aerospace Mechanical & Nuclear Engineering
Norman, OK 73069
Attn: C. W. Bert

University of Wyoming
College of Engineering
University Station Box 3295
Laramie, WY 82071
Attn: D. F. Adams

U. S. Army Materials & Mechanics Research Center
Watertown Arsenal
Watertown, MA 02172
Attn: E. M. Leno
D. W. Oplinger

V.P. I. and S. U.
Dept. of Eng. Mech.
Blacksburg, VA 24061
Attn: R. H. Heller
 H. J. Brinson
 C. T. Herakovich